A SEARCH FOR GRAVITATIONAL WAVES FROM COALESCING BINARY STARS USING THE CALTECH 40 METER GRAVITY WAVE DETECTOR

Thesis by

Sheryl L. Smith

In Partial Fulfillment of the Requirements

for the Degree of

Doctor of Philosophy

California Institute of Technology

Pasadena, California

1988

(Submitted May 16, 1988)

To *MY* Mom and Dad

Acknowledgements

I am deeply indebted to the entire gravity wave group, both past and present. I would like to thank my advisor—Ron Drever, whose enthusiasm seems unbounded and whose insight has helped solve many difficulties. I am especially grateful to both Mike Zucker and Bob Spero, both of whom could always be relied upon. I would like to thank Stan Whitcomb for suggesting that I work on a filter for coalescing binary stars. I would also like to thank Kip Thorne, whose encouragement I have always valued.

My family has been very supportive, and I could never have maintained my sanity without their help. I'd also like to thank Elizabeth; she has always been there.

And finally, I have to thank Ted, who has made the past five years the most memorable and joyous of my life.

Abstract

A search for gravitational radiation from coalescing compact binary stars was conducted. This is the first time that the Caltech gravity wave detector has been used to search for burst sources. This detector is made of two 40 meter Fabry-Perot interferometers. The mirrors of the Fabry-Perot cavities are suspended, so that they are free to move in response to a gravity wave. The Caltech detector is a prototype for a set of larger detectors (4 km long cavities). The purpose of this search was to develop techniques applicable to the larger detectors.

An algorithm was developed which searches for the distinctive waveform of a coalescing binary, regardless of the masses of the stars in that binary. Thirty-six minutes of data were analyzed. These data spanned one hour and were collected when the Glasgow detector was also operating, (the Glasgow and Caltech detectors had comparable sensitivity at the time of this experiment). The limit this search sets varies with the mass parameter, η, which is a function of the stars' masses. For two $1.4M_{\odot}$ stars no coalescences were observed with $h > 5 \times 10^{-17}$; this corresponds to a binary approximately 25 parsecs away.

At the time of this experiment the Caltech detector had a displacement sensitivity of 10^{-17} m/$\sqrt{\text{Hz}}$ at frequencies near 1kHz. Since then the detector has improved so that at frequencies near 1kHz the displacement sensitivity is 4×10^{-18}m/$\sqrt{\text{Hz}}$. At this level of sensitivity there are many conceivable sources of noise which must be considered and, if necessary, eliminated. How fluctuations in the spatial geometry of the input beam and the cavities can cause displacement noise is discussed in Chapter 4. Work which has been done to reduce these fluctuations is also described.

Contents

List of Figures

List of Tables

Chapter 1

Introduction

1.1 What are Gravity Waves?

All geometric theories of gravity, including general relativity, include gravitational radiation. In a manner analogous to accelerating charges emitting electromagnetic waves, gravity waves are created when mass accelerates; but since momentum is conserved, the dipole moment doesn't radiate. The quadrupole moment of an accelerating system of masses is the lowest moment to produce radiation, so spherically symmetric systems do not radiate.

As a gravitational wave goes by, it distorts the curvature of space-time such that the distances between free masses change. Gravity waves are transverse waves, and have two possible polarizations. The easiest way to explain how gravity waves interact with matter is to look at their effect on a ring of test particles; this is illustrated in Figure 1.1. This figure shows how a gravity wave deforms a circular ring of test masses into an ellipse. The wave amplitude is the change in distance between two free masses divided by twice the distance between them, this is called the strain, h.

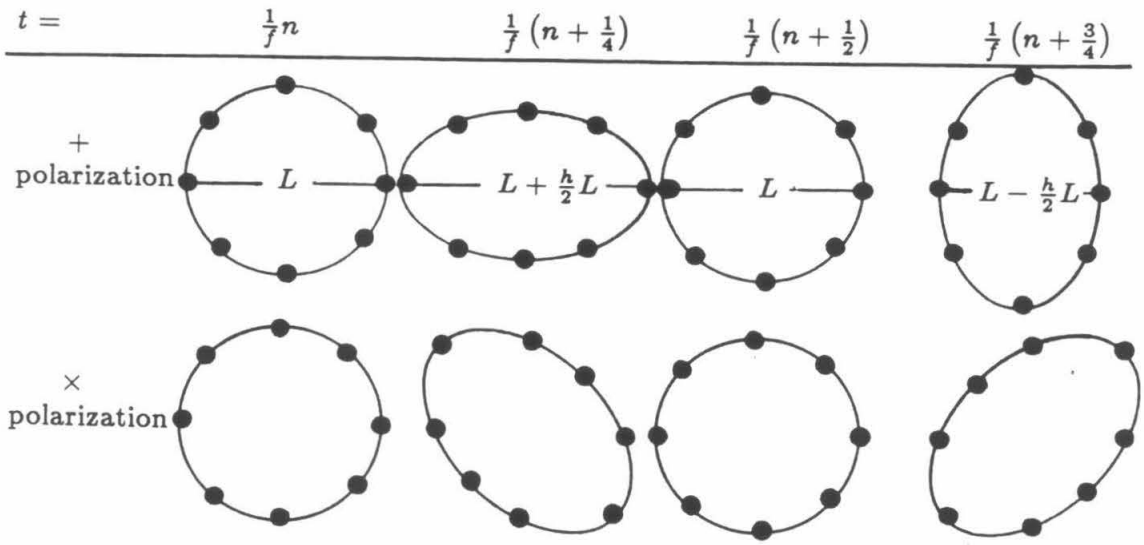

Figure 1.1: The effect of a gravity wave on a ring of test particles.

Gravitational waves have been *indirectly* observed. Two stars rotating about each other have a quadrupole moment; hence they should emit gravitational radiation. The energy lost to gravity waves causes the stars to spiral together, and their orbital frequency will increase. Taylor and Weisberg have made careful measurements of the orbital period of the binary pulsar PSR 1913+16, and have found that the binary pulsar and its companion star are losing orbital energy at precisely the rate predicted by general relativity.[1] It is hard to conceive of another effect which could cause the orbit to behave in this manner, therefore this is strong evidence that gravity waves do exist.

1.2 Attempts to Detect Gravity Waves

The binary pulsar provides strong evidence that Einstein's theory is correct, and that gravity waves exist, but they have yet to be directly observed. The first attempts at detection were made by Weber in the 1960s using a resonant bar detector.[2] As a gravity wave goes by it excites a resonance in the bar, which acts like a big spring connecting two masses. This resonance is detected using a transducer, piezoelectric strain sensors in the original bars. Since then bar detectors have been further developed and used in searches. The most sensitive bar detectors, cooled to liquid helium temperatures with superconducting displacement transducers, have a sensitivity of $h \simeq 10^{-18}$ and a bandwidth of approximately 1Hz around the bar's resonant frequency (usually about 1kHz).[3]

For the past decade, detectors employing laser interferometry have been under development at Caltech, MIT, Glasgow University and the Max Planck Institute, Garching. As a gravity wave goes by, the masses move relative to each other so that one arm of the interferometer becomes longer as the other becomes shorter, this appears as a phase shift in the light in the two arms. The primary advantage this has over bar detectors is that the arms can be made very long, and since the signal strength is proportional to the distance between the masses, the detectors signal-to-noise ratio can be improved.

The first interferometric gravity wave detector was made by Moss, Miller and Forward in 1971.[4] In 1975, work on the Max Planck interferometer began. In 1977, the Glasgow group also started work on an interferometric gravity wave detector. Work on the Caltech and MIT gravity wave detectors began in 1979. The Caltech detector is made of two Fabry-Perot cavities. It is discussed in detail in Chapter 3.

The Caltech detector is a prototype for two larger detectors which would form a national observatory for gravitational astronomy, known as the LIGO, (Laser Interferometer Gravitational Wave Observatory). This facility would be made of two 4km detectors separated by transcontinental distances. Eventually this observatory should be sensitive to events as far away as one giga-parsec.[5]

In 1983, the Caltech prototype was used to search for periodic gravitational radiation from the millisecond pulsar.[6] In 1985, the MIT prototype was used to search for radiation from both periodic and burst sources.[7,8]

1.3 Scientific Benefits of Detection

The scientific benefits of detecting gravity waves can be broken into two classes, those which benefit physics and those which benefit astrophysics; of course, the distinction is not always clear.

The most obvious payoff is the verification that gravitational radiation exists, supplementing the strong, but indirect, evidence from the binary pulsar. Through direct detection of gravitational radiation one can confirm that gravitons have zero rest mass and spin $s = 2$, as predicted by general relativity. Observation of the coalescence of two black holes would provide the first test of general relativity in a highly non-linear, dynamic system. This would be done by comparing theoretical waveforms with those observed.[5,9]

The establishment of gravitational astronomy should provide astrophysicists with information unavailable through traditional astronomy. This is because gravitational waves carry much different information from electromagnetic waves. Observation of supernovae should lead to more information about the physics of neutron stars. Gravitational waves from coalescing binaries can be used as

"standard candles" to determine the Hubble constant; this would be the most direct measure of the Hubble constant to date.[10] Detection of primordial gravity waves would provide information on the earliest moments of the universe. Even if these were not detected, the LIGO could eventually place interesting limits on the strength of this background.

1.4 Outline of this Thesis

The rest of this thesis is organized in the following manner:

1. a description of sources, emphasizing coalescing compact binaries.
2. a description of the Caltech detector.
3. an analysis of a specific noise source in interferometric detectors, and a description of work done to reduce this in the Caltech prototype.
4. a description of the data analysis: the algorithm used, data collection and processing methods.
5. the results of this data analysis, and the conclusions one can draw from those results.
6. the appendices, which contain information that I felt was too detailed for the body of the thesis, *e.g.* the computer codes used in the data analysis.

Chapter 2

Sources of Gravity Waves

2.1 Generation of Gravitational Radiation

Gravity waves are generated when mass accelerates in a non-spherical manner. The amplitude of a gravity wave is called h. A rough estimate of h is:

$$|h| \approx \frac{M}{r}\left(\frac{2\pi L}{\lambda}\right)^2 \frac{G}{c^2} \tag{2.1}$$

where L is the typical length scale of the radiating system, r is the distance from the observer to the source, M is the accelerating mass (the fraction of the mass accelerating in a non-spherical manner) and λ is the wavelength of the gravitational radiation, (the frequency will be c/λ, and depends upon the acceleration); G and c are the gravitational constant and the speed of light respectively.

The theory of gravity wave generation is discussed extensively elsewhere, [9,11,12]. An excellent review of the theory of gravitational radiation and predicted source strengths is given in *300 Years of Gravitation.* [9]

Because gravity is such a weak force, it would be exceedingly difficult to generate detectable gravity waves in a laboratory. The only hope for detection

is to look for astrophysical events involving large amounts of mass undergoing violent motion, such as in a supernova.

2.2 Astrophysical Sources

Astrophysical sources are usually broken into three groups—burst sources, periodic sources and the stochastic background. In the following paragraphs, each of these astrophysical sources is discussed briefly. In Section 2.3, coalescing binaries are described in detail, since it is this source that this thesis concentrates on. Compact binaries do not cleanly fall into any *one* of the above categories. They are quasi-periodic, having a signal which changes frequency quite slowly until the last few moments before the stars collide. However, since the signal would be in the bandwidth of an Earth-bound detector for only a few seconds, from the detector viewpoint these sources resemble bursts.

Periodic gravitational radiation is characterized by having a fixed well-defined frequency. It could be generated by rotating neutron stars, where any lack in axial symmetry would cause the system to radiate. Figure 2.1 [5] shows expected source strengths for gravitational radiation from neutron stars. The data analyzed in this thesis will also be used to look for periodic gravitational radiation [13]. This should set the best limit to date on periodic sources.

Burst sources are those which only last a few brief moments and, hence, tend to cover a wide range of frequencies. Predicted sources of bursts of radiation include collapse of a star to form a black hole, supernovae (collapse to a neutron star), and matter falling into black holes. It is difficult to predict the strength of radiation from supernovae and black hole formation, since it is unknown how aspherical the collapse of a star would be. It is possible to predict the expected

event rate for supernovae, but the event rate for anything involving black holes is a complete mystery. Predicted event strengths for various burst sources are shown in Figure 2.2. [5]

The stochastic background is broad band continuous radiation. The most interesting source of this would be the big bang. Just as there is a 3K background of electromagnetic radiation, one would expect there to be a background of gravitational radiation. The gravitational radiation would probably not be at 3K, since gravitons decoupled from matter at approximately the Planck time (10^{-43} seconds after the big bang; primordial photons did not decouple from matter until approximately one million years after the big bang). The strength of the primordial background is still very speculative, with estimates varying by as much as fourteen orders of magnitude. Other sources of a stochastic background would be radiation from many individual sources which added together to form a continuous background radiation. These individual events could include the deaths (by collapse to a black hole or neutron star) of population III stars. These are hypothesized pre-galactic massive stars that died long ago. Another source of this background would be the decay of nonsuperconducting cosmic strings. A third source would be binary stars (here I am referring to ordinary stars, not necessarily compact stars). There are so many binary stars that together they would produce a strong stochastic background at frequencies less than .03 Hz.[9]

All the astrophysical sources mentioned so far are rather unreliable; either the event rate or the source strength is largely unknown. The most reliable source predicted so far is radiation from compact coalescing binaries.

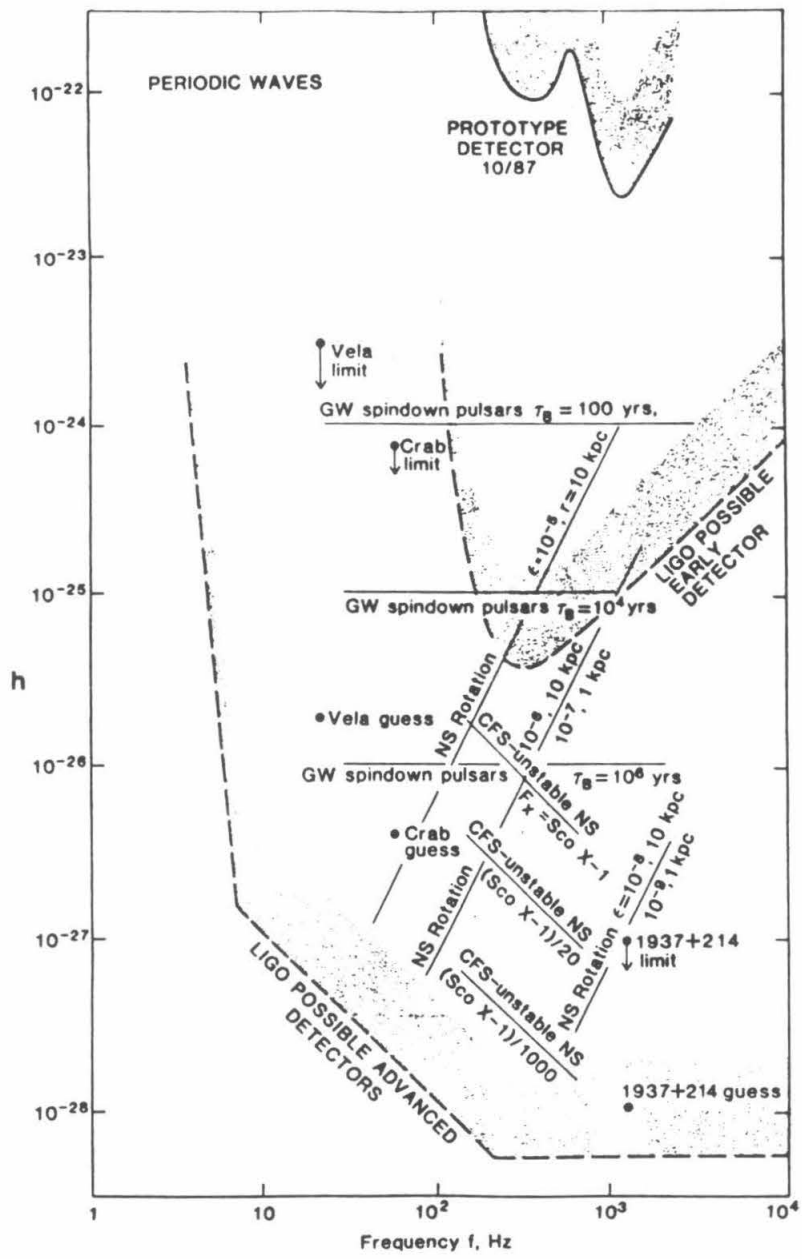

Figure 2.1: The estimated wave strengths for periodic gravitational radiation and the sensitivities for interferometric detectors today and in the proposed LIGO. An integration time of 10^7 seconds is assumed.[5]

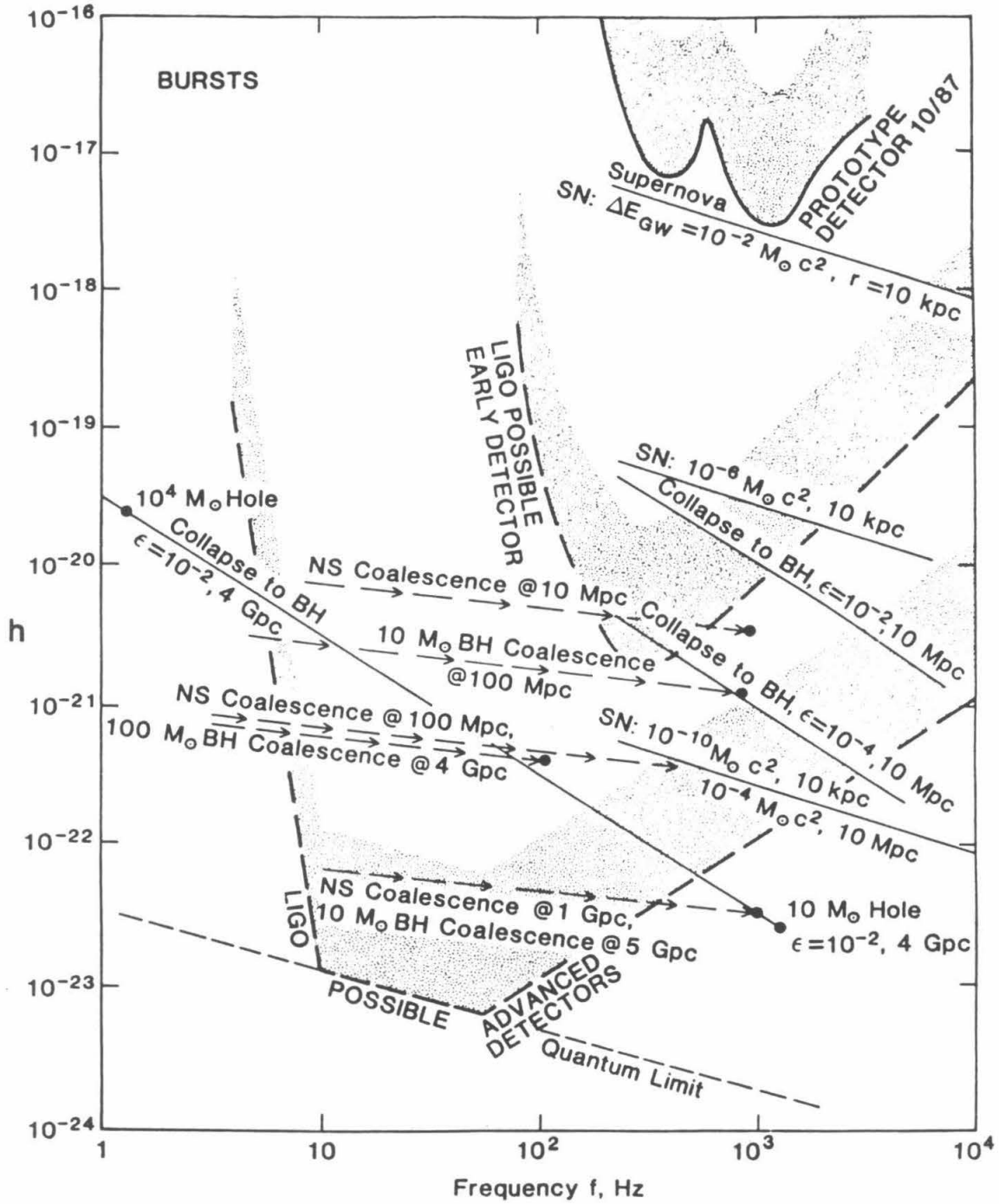

Figure 2.2: The estimated wave strengths for burst sources of gravitational radiation and the sensitivities for interferometric detectors today and in the proposed LIGO.[5]

2.3 Coalescing Compact Binaries

One promising source of gravity waves is coalescing compact binary stars. [11,14,15,16,17] As two stars rotate about each other they emit energy in the form of gravitational radiation, causing the stars to spiral together. As the stars get closer together their angular velocity ω increases; hence, the radiation they emit changes frequency. The frequency of the radiation changes as

$$f_{rad} = f_0 \left(1 - \frac{t}{\tau}\right)^{-3/8} \tag{2.2}$$

where f_0 equals the radiation frequency at $t = 0$, and τ is the time at which the two stars would collide, if no tidal disruption occurs. This calculation assumes nonrelativistic velocities and ignores the eccentricity of the orbit. Since emission of gravity waves tends to circularize the stars' orbit it is reasonable to assume that by the time the stars are about to coalesce their orbits are nearly circular. It also treats the stars as point particles, a good approximation for compact stars such as black holes and neutron stars. The frequency of the stars' orbit is a function of their masses and the time until coalescence:

$$\omega = \left((\eta\tau)\left(1 - \frac{t}{\tau}\right)\right)^{-3/8} \tag{2.3}$$

where

$$\eta = \frac{256}{5} \frac{m_1 m_2}{(m_1 + m_2)^{1/3}} \tag{2.4}$$

(in geometrized units, $G = c = 1, M_\odot = 4.9255\mu\text{sec}$). The gravitational radiation will have twice this frequency:

$$f_{rad} = \frac{2\omega}{2\pi}. \tag{2.5}$$

The amplitude of the radiation is a function of the distance from the detector to the binary, r, the star masses and τ. The strain has amplitude:

$$h = \frac{4}{r}\frac{m_1 m_2}{(m_1+m_2)^{1/3}}\omega^{2/3} \tag{2.6}$$

$$= \frac{5}{64r}\eta^{3/4}(\tau - t)^{-1/4}. \tag{2.7}$$

(See Figures 2.3 and 2.4.) The exact amplitude of the strain measured at the detector depends on the observer's position relative to the binary. The expected signal at the detector would be:

$$S(t) = \alpha h(t)\cos\left[\left(2\pi\int(f_{rad})dt\right) + \phi\right] \tag{2.8}$$

where α depends on the orientation of the binary relative to the detector and ϕ is the signal's phase. The larger the stars' masses the greater h and the slower the frequency. The radiation reaching Earth will be elliptically polarized; since detectors tend to be sensitive to only one linear polarization, this implies the strain measured at the detector will be at most $h/2$. The signal strength will almost certainly be less than this, since it is unlikely that the source and detector will be optimally aligned.

At some time close to τ this calculation will break down and the strain will no longer be accurately described by Equation 2.8. If the two stars are neutron stars then this will occur when tidal disruption occurs, and the gravitational field of the heavier star tears the other neutron star apart. The time at which this is expected to occur depends on the masses of the neutron stars; the lighter the stars the earlier they would tidally disrupt.[18] A binary consisting of a $1.3M_\odot$ neutron star and a $1.5M_\odot$ neutron star would tidally disrupt at $t \approx \tau - .003$ seconds. For black holes one might expect Equation 2.8 to break down when the

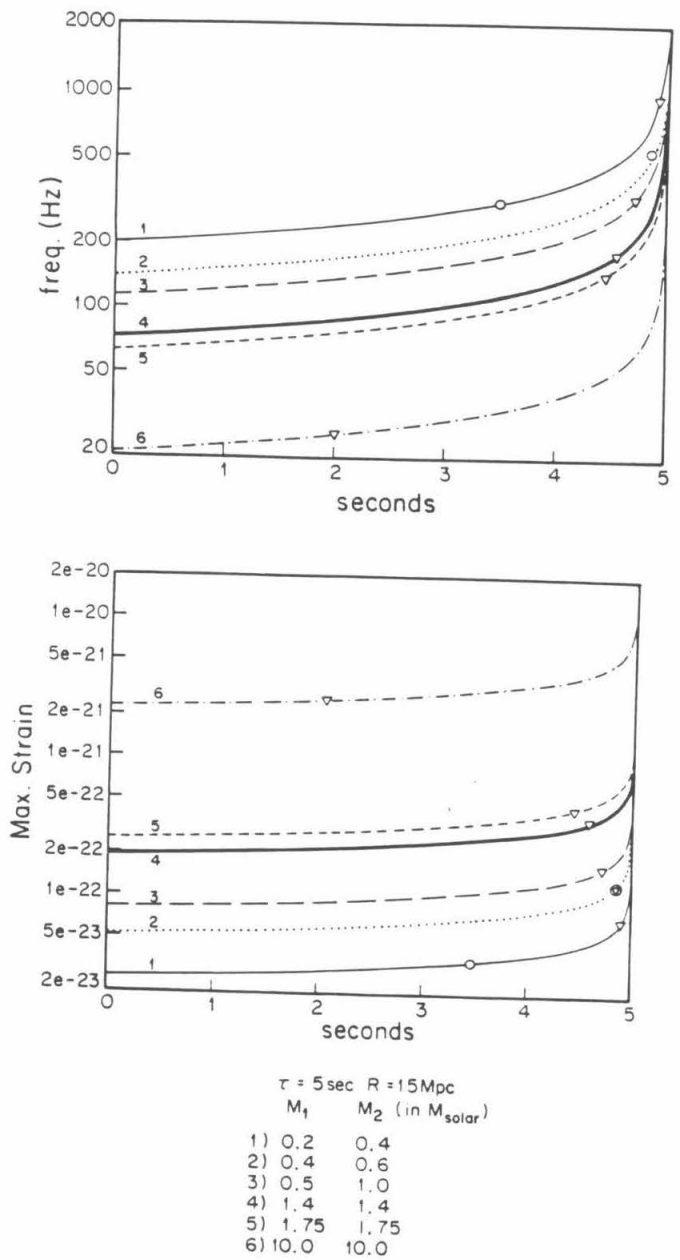

Figure 2.3: The frequency and amplitude of gravitational radiation emitted from coalescing binaries. The circles represent when tidal disruption is expected for a binary made of neutron stars.[18] The triangles represent when the velocity of the stars is $0.1c$. If no tidal disruption occurs, then the stars would coalesce at $t = \tau = 5$ sec.

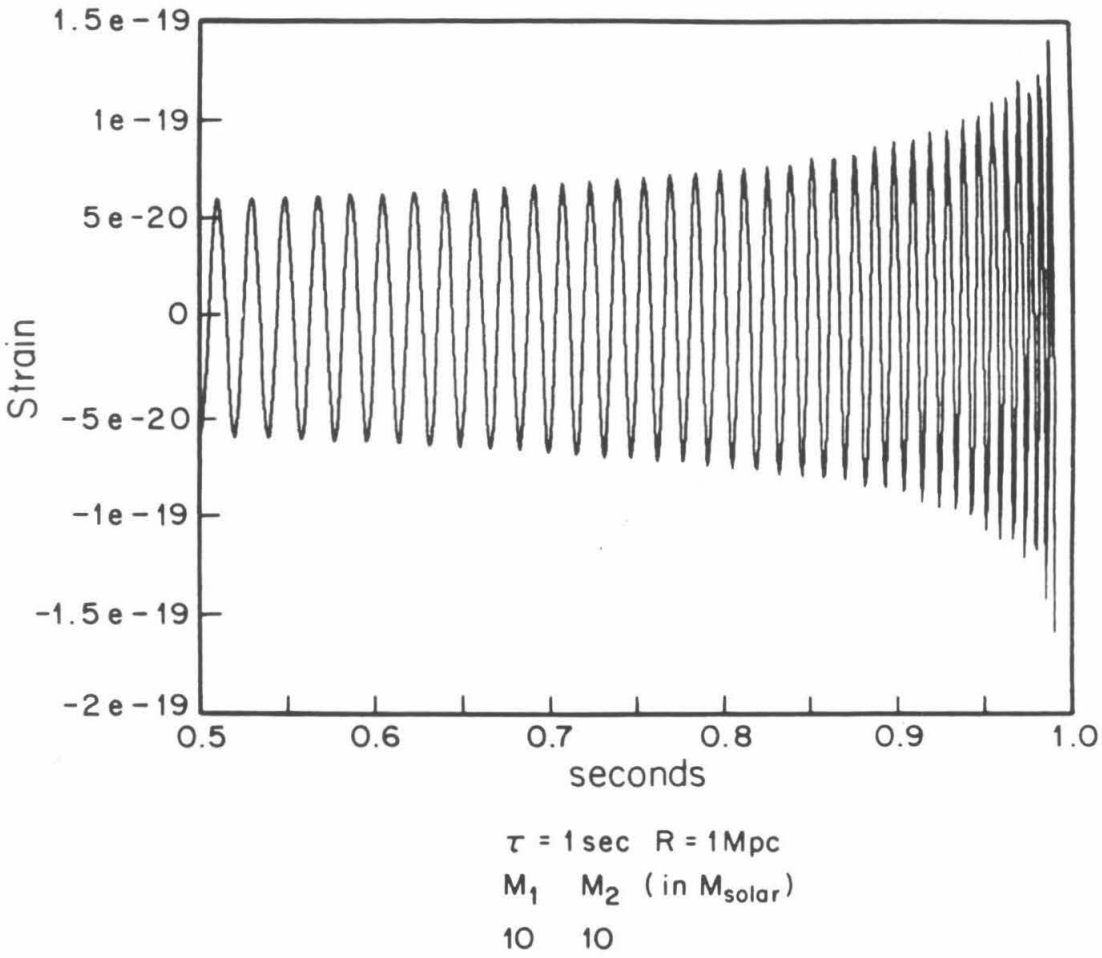

Figure 2.4: The waveform from a binary made of two $10M_{\odot}$ black holes.

velocities become too relativistic. For two $10M_{\odot}$ black holes their velocity would exceed $.5c$ at $t = \tau - 10^{-5}$ seconds.

Work has been done to estimate the event rate of bursts from coalescing compact binaries, but without more observational data it is difficult to reach any firm conclusions. The event rate for radiation from neutron stars has been estimated by Clark, van den Heuvel, and Sutantyo.[19] They make a statistical argument based on the number of observed pulsars, and the fraction of those in a close binary (a binary which would be expected to coalesce within the Hubble time). Assuming that the death rate of neutron stars equals the birth rate, and calculating the birth rate from the number of observed supernovae, they predict an event rate of approximately 3×10^{-4} per year per galaxy. This estimate is based on a very small set of observations (1 binary pulsar out of 315 known pulsars), and hence is probably inaccurate. Even less is known about the event rate of bursts from black hole coalescences. The most optimistic scenario was proposed by Bond and Carr [20,21]. They hypothesize that a large fraction of the "missing mass" may be in black hole remnants of population III stars. This would lead to an event rate of approximately 3 bursts/year at the strain level of $h \approx 10^{-16}$ [9].

As mentioned earlier (in Chapter 1), the detection of any gravitational radiation would be of enormous import. The detection of coalescing binaries would have some unusual benefits, different from the detection of radiation from other sources. If one or both of the stars were neutron stars, then by carefully studying the waveform while tidal disruption occurred, one could learn a great deal about the nature of neutron stars. The fact that tidal disruption occurs after a long precursor, (the chirp waveform described by Equation 2.8), makes it easier to find these events. An additional benefit, which seems to be truly unique to

gravitational radiation from coalescing binaries, is that detection can lead to a direct measure of Hubble's constant. If a coalescence were observed in 3 or 4 detectors, then the location of the binary could be determined within an error box of approximately 36 square degrees. Multiple detection will also allow one to accurately measure the absolute strain h, given in Equation 2.6. By measuring both the amplitude h and the frequency, one can calculate both η and r. If one knows r and where in the sky the binary was, one can associate that binary coalescence with either an optical event or the galaxy in which it was located, leading to a known distance, r, between here and the galaxy. Hubble's constant would then be determined by the Doppler shift of light from that galaxy. This would be the most direct measure of Hubble's constant to date.[10]

Because compact binary stars are known to exist and one can make rough estimates of their coalescence rate, and because the strength of the radiation is well known, compact binary stars offer one of the most reliable potential sources of radiation. It is for this reason that efforts should be made to develop techniques for searching for this radiation.

Chapter 3

The Caltech Detector

3.1 The Detector

3.1.1 Theory of Operation

The Caltech gravity wave detector is made of four "free" masses arranged to form two optical cavities perpendicular to one another. The two Fabry-Perot cavities in the Caltech detector share the same input beam but, unlike a Michelson detector, the output beams are not recombined. In its simplest configuration, which was used when this search was carried out, the laser light is stabilized to one cavity, the first arm of the detector. This light is then an excellent length standard above a few hundred hertz. The second cavity is held in resonance by moving the far mass (see Figure 3.1).

Imagine a gravity wave traveling perpendicularly to the detector. As it goes by it will change the length of the first arm by an amount $hL/2$; the laser light will track this and its wavelength, λ, will change accordingly. The gravity wave will cause the second cavity's length to change by an equal and opposite amount. To remain on resonance the feedback will compensate for both this motion and

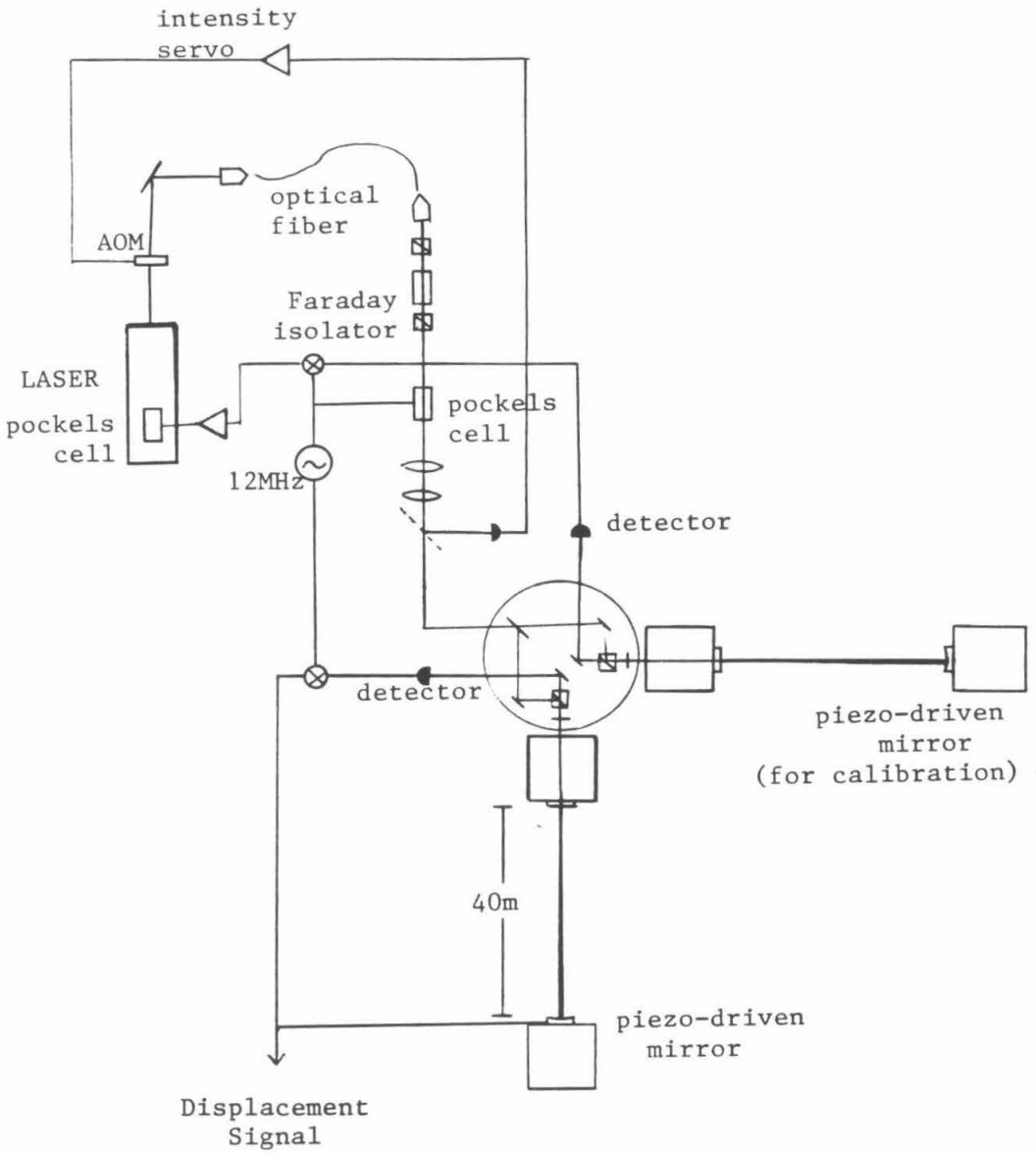

Figure 3.1: A simplified schematic of the Caltech detector.

the change in λ. Hence if a gravity wave goes by it appears in the feedback signal as a relative displacement between the two arms of hL. Gravity waves affect all objects this way. What makes the test masses special is the accuracy with which we monitor their position, and the care we take to isolate them from other forces.

The detector is calibrated by moving the far mirror of the first cavity a set amount. At the time of this experiment this was done by applying a sinusoidal voltage near 1kHz across a piezo mounted between the mirror and the test mass. Currently we calibrate our detector by putting a low current through coils located near magnets mounted on the test mass.

In March, 1987, when this search was conducted, the Caltech detector had a noise level of $h \simeq 5 \times 10^{-19}/\sqrt{\text{Hz}}$, and a bandwidth from 300Hz to 5kHz. This noise level would fluctuate by as much as a factor of two. Its noise spectrum is shown in Figure 3.2. Since then the detector has been improved so that its current noise level is $h \simeq 1 \times 10^{-19}/\sqrt{\text{Hz}}$; see Figure 3.3.

The detector can be thought of as consisting of three parts:

1. the test masses—which are as "inertial" as possible

2. the light—which monitors the distance between the test masses

3. the orientation control system—which keeps the mirrors on the test masses well aligned relative to the light, while not compromising the masses' isolation. I have worked on understanding how spatial fluctuations in the laser beam and the cavity mirrors can couple into the detector's output noise, and how to reduce this noise. This is discussed extensively in Chapter 4 .

In designing this detector, sensitivity, rather than stability, has always been of primary importance. This is because this detector is a prototype for two

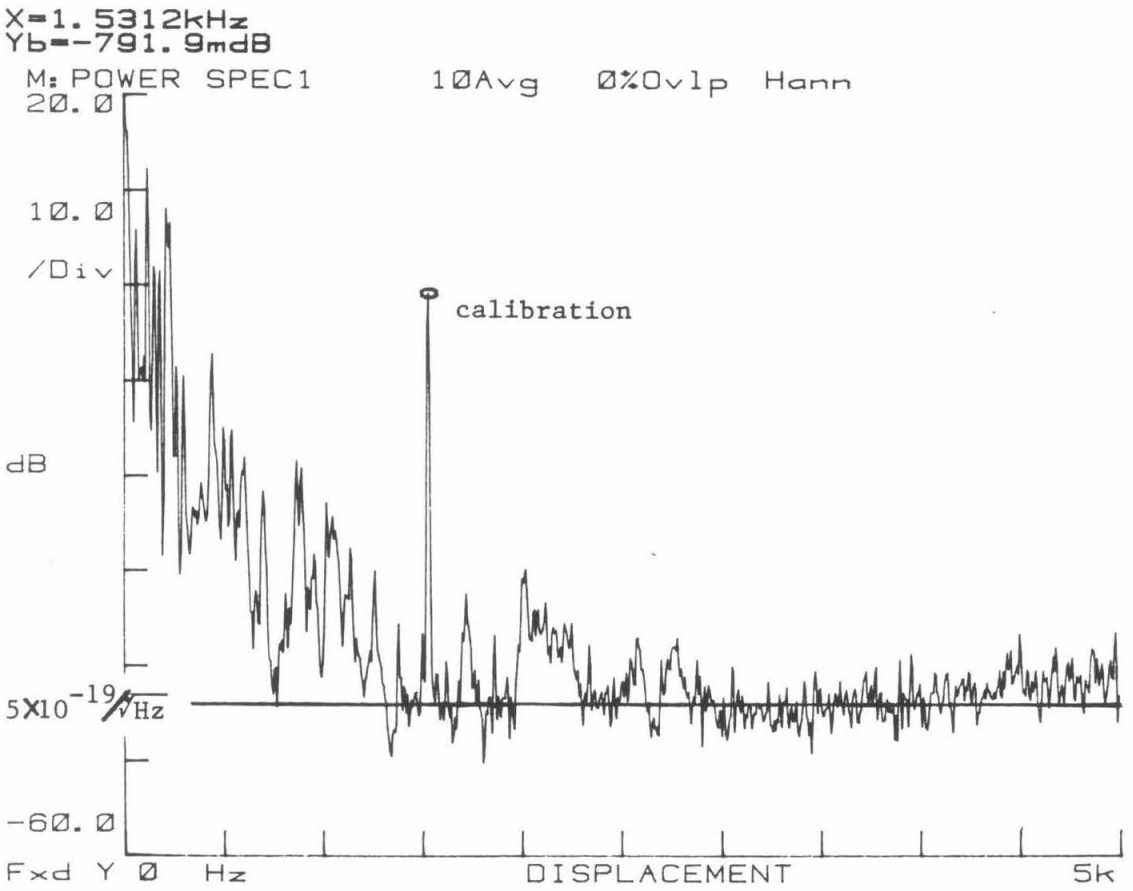

Figure 3.2: The noise spectrum of the Caltech interferometer at the time of this experiment.

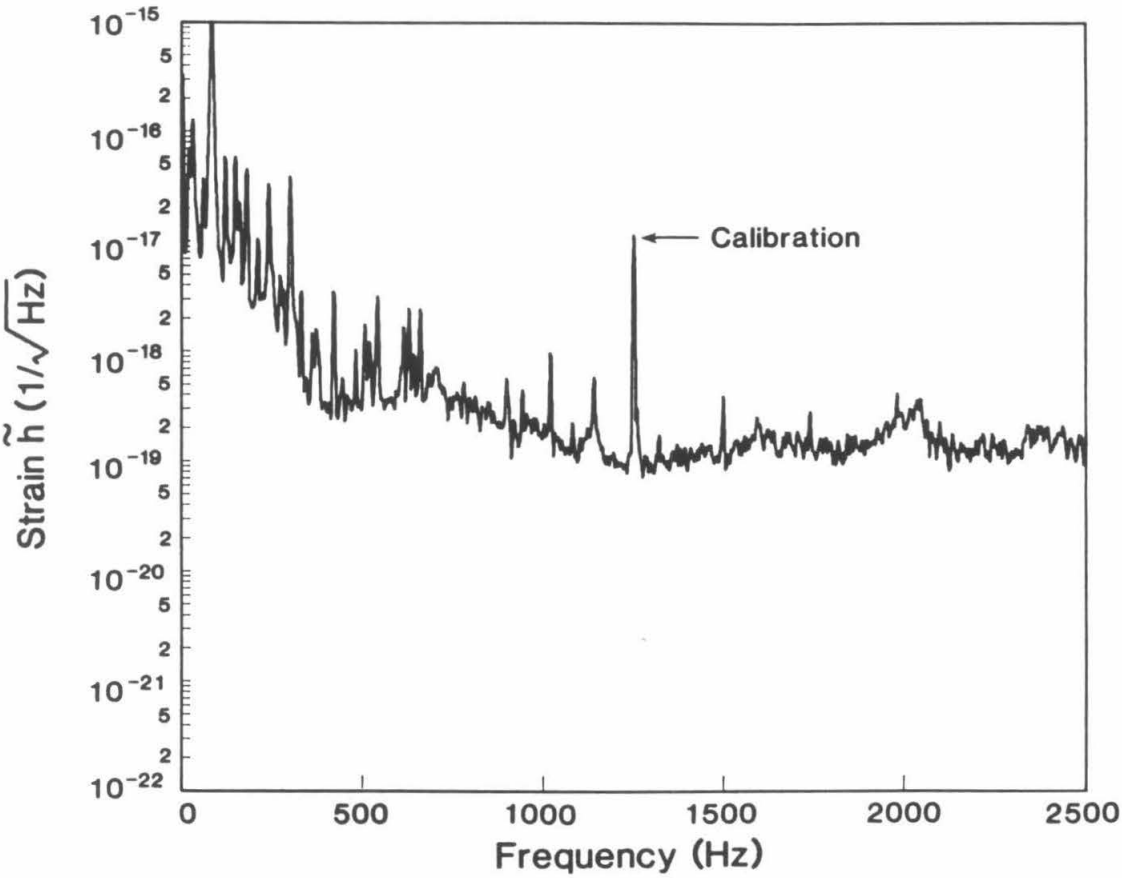

Figure 3.3: The best noise spectrum of the Caltech interferometer, taken in September, 1987

4km detectors (the LIGO). Before that is built, it is important that what will limit its performance is understood. In order to optimize the stability of the detector, we would first have to freeze various components design—this would essentially freeze the detector's performance, which we are not yet willing to do. At the time this experiment was carried out, the detector was "on" 70% of the time. After the data run was over, the chart recorder data was carefully examined and it was discovered that the main limitation on the live time was caused by servos running out of dynamic range due to thermal drift. Since then the piezo-electric transducers in the cavities have been replaced with coils and magnets. Although this was done to improve the detector's sensitivity, it also has the effect of increasing the dynamic range of the servos, and hence should improve the detector's stability.

3.1.2 The Test Masses

The test masses are cylinders with high reflection mirrors attached. These masses are suspended from 1Hz pendula, so that they are essentially free to move along the optical axis at frequencies above 1Hz. This implies that they are approximately inertial along the beam axis. The object is to prevent any forces other than gravity from acting upon these test masses. Since what one wishes to measure is the distance between three inertial reference points, it is important that the masses be as quiet as possible. It is also important that the mirrors do not move relative to the center of mass of the test masses. This can be caused by thermal noise. Four years ago, mechanically complicated test masses were replaced with simple cylinders so that the thermal noise in the test masses would not limit the detector's sensitivity. The joint between the mirror and the test

mass is also critical; this is discussed more in Section 3.2.3. The fact that the test masses are free to move at frequencies above 1Hz implies that the detector can be broad band. Currently the bandwidth of the detector ranges from 300Hz to about 5kHz. The lower limit is probably caused by seismic noise and resonances in the beam splitter mass; the upper limit is caused by shot noise in the light. Both these noise sources and others are discussed more in Section 3.2.

The fact that this detector is broad band implies that it is well suited for a search for gravitational waves from coalescing binaries. This is because the radiation from a coalescing binary sweeps through many frequencies. [14]

3.1.3 The Light

The Caltech detector uses a Coherent Innova 100 argon-ion laser, operating single line, single mode. The light travels through a chain of optics designed to "clean" the beam in various ways; it is then directed into the vacuum tank. There it goes through a beam splitter. At this point the beam is vertically polarized. The two beams are then reflected off of steering mirrors, through polarizing beam splitter cubes and 1/4 wave plates, and then into the cavities. The beam splitter cubes and 1/4 wave plates act as "circulators." Because the light is vertically polarized it is first reflected by the cubes, then the wave plates circularize the light. The light reflected from the input cavity mirror and the light leaking out of the cavity go back through the wave plate, where they become horizontally polarized. This light is transmitted through the beam splitting cube; it then hits another steering mirror, exits the vacuum tank and hits the photodiode. Use of these circulators isolates the laser from the light reflected from the cavity and insures that the photodiodes see as much light as possible.

The input laser beam must be very quiet in all respects. The most important aspect of the light is its frequency, since this is our length standard. Gas lasers have much more frequency noise than is acceptable, but, by servoing the laser frequency to a cavity, one can get to the shot noise limit. At the time of this experiment the laser was stabilized to one arm of the gravity wave detector using a back-reflection locking technique. [22] The light is phase modulated at 12MHz to put sidebands on the light. Since the free spectral range of the cavities is approximately 3.7MHz and these are high finesse cavities, the sidebands do not resonate with the cavity. By looking at the interference of the sidebands with the light leaking from the cavity and demodulating the signal, one gets a measure of the relative phase of the input light to the light from the cavity. The frequency stabilization is discussed extensively in M. E. Zucker's thesis. [13]

The second cavity is held on resonance using a similar method. The phase error is detected in the same way, but rather than feeding this signal back to the laser, the cavity is held on resonance by moving the far mirror. At the time of this experiment that was done using piezoelectric discs between the mass and the mirror. These servos hold the cavity resonance on a dark fringe—so that most of the light is transmitted through the cavities, or lost through absorption and scattering at the cavity mirror surfaces.

Because the light at the photodiode is modulated at 12MHz, the detector is insensitive to low frequency intensity noise to first order. However, because the detector is so sensitive, second order effects cannot be lightly dismissed. An intensity servo has been installed. There is a pick-off window in the beam, not far from the beam splitter mass. This is pointed into a photodiode which measures the incident power to the two cavities of the detector. Any fluctuations can be removed using a servo. The signal from the photodiode is amplified and

filtered and then fed back to an acousto-optic modulator (AOM). By changing the amplitude of the RF drive to the AOM, one can vary the amount of light in the first order spot, and hence the amount of light input into the detector. This servo is discussed more in M. E. Zucker's thesis. [13] One problem with this servo is that varying the amplitude of the drive of the AOM can cause spatial fluctuations in the beam, converting intensity noise into beam fluctuations. For this reason the AOM is placed before a single mode optical fiber (discussed more in Section 4.2.2). The optical fiber converts spatial fluctuations into intensity fluctuations, but by putting the intensity monitor after the fiber one can servo out this effect. This arrangement leads to a light beam which has both low intensity noise and spatial fluctuations. Currently the detector is not limited by intensity noise, so that the intensity servo is usually left off.

It is important to eliminate spurious interferometers in the beam path. Light back-reflected into the laser can cause optical feedback, which will cause the laser to go multimode. Spurious interferometers elsewhere can cause phase noise—so that the laser is stabilized not to the cavity, but to a combination of the cavity and the spurious interferometer. The AOM used in the intensity servo is also used as an optical isolator. We use the first order spot of the acousto, which is frequency shifted from the input light by 40MHz. Any back-reflected light (from the fiber input, for example) is shifted 80MHz from the laser, so that it does not cause any optical feedback problems. Occasionally the AOM's frequency will drift so that the offset equals the free spectral range of the laser (approximately 75MHz), at which point optical feedback becomes a problem again. When this happens one merely needs to adjust the modulation frequency of the AOM slightly. Between the fiber's output and the beam splitter there is a Faraday isolator, preventing the output cleave of the fiber from forming a spurious interferometer with the

cavity mirrors. The fiber itself can act as an interferometer, but by placing the phase modulator after the fiber this problem is made negligible. Since the fiber-interferometer is quiet at frequencies near the modulation frequency, it does not cause problems in the measurement of the phase at the modulation frequency. If the modulator were placed before the fiber, this would not be true; the fiber's noise would be inseparable from the phase fluctuations in the cavities.

3.2 Noise Sources

Potential noise sources in interferometric gravity wave detectors have been discussed extensively elsewhere; [6,23,24,25] below, a brief explanation of many of the more important ones is given. First those sources which move the masses—preventing them from being ideal inertial test masses, are discussed, then those which affect one's ability to measure the distance between the masses accurately are described.

3.2.1 Noise Sources which Affect the Test Masses

There are many effects which can cause a test mass, or a test mass' mirror to move. These include:

- seismic noise
- gravity gradient noise
- thermal noise
- the standard quantum limit.

Seismic noise can directly cause the length of each cavity to change. To prevent this from happening, the suspension point of each pendulum is attached to the top of a stack of lead and rubber. In addition, the pendulum itself gives isolation that improves as $1/f^2$ at frequencies above 1Hz. The seismic isolation has been directly measured [26] and it was found to currently be adequate at frequencies above 300Hz. Seismic noise can also cause noise by causing the masses to twist and turn. How this causes displacement noise is discussed in Chapter 4.

Another way in which seismic noise can now enter in is through the coil/magnet arrangement used to adjust the length of the second cavity. Seismic noise can cause the coils to move, so that the magnetic field of the coils is moving. This is a second order effect because the coils and magnets are spaced such that the coil's force on the magnet is at a maximum. Since the amplitude of this noise is a function of the amount of current through the coils, if the coils are driven hard enough, one can see the seismic motion come through. Figure 3.4 shows how the seismic noise can enter into the interferometer non-linearly via the coils. The coils were driven with a 1.53kHz sine wave, $I = .36$mAmps. This moved the far mass 2.4×10^{-13} meters. There is excess noise on either side of this peak due to the ground motion of the coils, and the 1Hz pendular motion of the mass. This noise completely vanishes when the sine wave is turned off. Eventually the coils will also need to be isolated from ground motion, either by placing them on a stack of lead and rubber, or, for more isolation, by attaching them to another suspended mass. Seismic noise is not a fundamental limitation, since one can conceivably isolate the masses from all seismic noise.

A more fundamental limit to the detector's low frequency performance is due to gravitational gradients. Local fluctuations in the gravitational field will cause

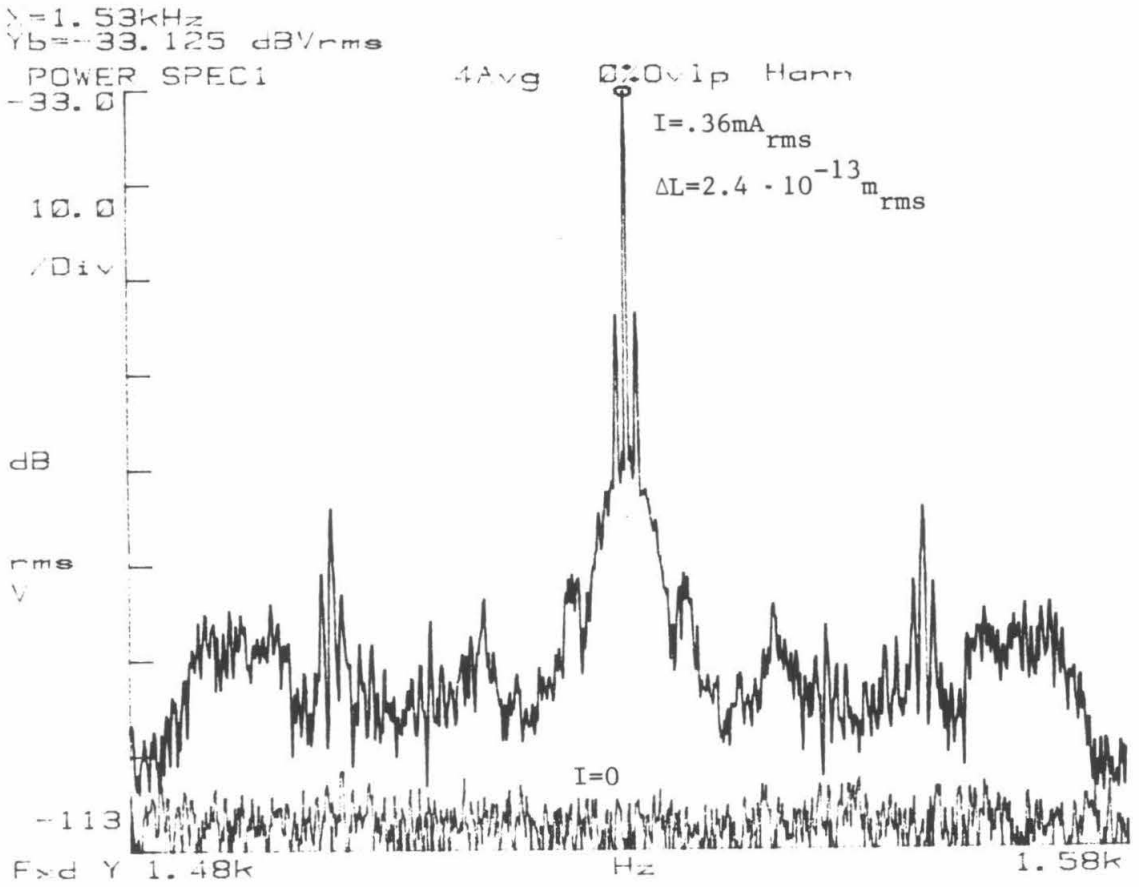

Figure 3.4: A close-up of the noise spectrum of the Caltech interferometer, taken with and without the coils by one mass being driven.

the masses to move. This can be due to planes flying overhead, for example. This is different from low frequency gravitational waves, since it is a purely Newtonian effect. This would prevent the proposed LIGO from ever being sensitive to frequencies below approximately 10Hz.

Thermal noise enters in through driving mechanical resonances in the system. The most important of these is the mechanical resonance of the test mass itself. Currently the test masses are made of fused quartz, and have a mechanical Q of 50,000, and a resonant frequency of 27kHz. At frequencies well below the resonant frequency of the test masses, the displacement noise this causes goes as [6]:

$$\frac{\delta x^2}{\delta f} = \frac{4kT}{mQw_0^3} \tag{3.1}$$

(δx is the displacement noise in a bandwidth δf, ω_0 is the resonant frequency of the test mass, m is its mass and T is the temperature). This implies that the thermal noise would be approximately $10^{-20}\text{meters}/\sqrt{\text{Hz}}$. Because of the Q and high resonant frequency of our test masses, the thermal noise in the test masses is negligible in our prototype detector.

The beam splitter mass is a much more complicated structure than the test masses, and consequently has many more mechanical resonances, at lower frequencies and with lower Q. Though the detector should not be as sensitive to the motion of this mass as it is to the test masses, the beam splitter mass is so noisy that it probably is a contributor to the low frequency noise of the detector.

Another mechanical resonance which causes problems is the suspension wire resonances. These are the resonances corresponding to the "violin" modes of the wires. To minimize the effect of these resonances, the wires used are at approximately half their breaking strength; this causes the resonances to be at high

frequencies (700Hz) so that few harmonics enter into the detector's bandwidth. The wires are probably excited by seismic noise, but eventually (in the LIGO) even the thermal noise in these could become a limitation.

The standard quantum limit is not currently a problem, but it could conceivably become a problem in the future. Heisenberg's uncertainty principle sets a limit on the sensitivity which is a function of frequency.[27]

$$\frac{\delta x}{\sqrt{\text{Hz}}} \approx \sqrt{\frac{2\hbar}{m\omega^2}} \tag{3.2}$$

The detector currently has 1.5kg test masses, yielding a limit of $h \approx 2\times10^{-21}/\sqrt{\text{Hz}}$ at 1kHz; it is still approximately a factor of 50 away from this limit. When this limit is no longer negligible, heavier test masses will be used.

All the noise sources just mentioned are independent of the cavities' length, therefore the signal-to-noise ratio due to these effects would be improved by a factor of 100 by making a detector with 4km cavities.

3.2.2 Noise Sources Limiting the Measurement Accuracy

Many things can mar the measurement of the light's phase. These include:

- shot noise
- frequency noise
- intensity noise.

The term "shot noise" refers to photon counting statistics. One cannot measure the phase of the light better than $\delta\varphi \approx 1/\sqrt{N}$, where N is the number of photons. The displacement sensitivity is a function of the phase sensitivity and the number

of bounces, B, that the light makes in traveling back and forth in the cavity;*

$$\delta L \approx \frac{\lambda}{(2\pi)^2 B}\delta\varphi. \tag{3.3}$$

The actual limit on performance is much more complicated than that, it is a function of the fringe visibility of the cavities, the cavity mirrors' reflectivities and losses, and the light's intensity. [25,28] Currently we avoid this noise source by turning up the laser power whenever shot noise becomes a problem. Shot noise is not a fundamental limitation, it is possible to decrease the shot noise without using more laser power by injecting squeezed light into the unused port of the beam splitter.[29,30] Eventually shot noise will become a technical problem, since both the use of squeezed light and very high laser power are not trivial.

As mentioned in Section 3.1.3, any frequency noise in the light can cause noise in the detector because the light is the length standard. Since this noise is common to both arms, one can tolerate some frequency noise by subtracting the phase error signal of the first cavity from that of the second. This subtraction can gain one a factor of more than 100 attenuation in frequency noise, (this is measured by adding frequency noise at 1kHz to the light and seeing how well the electronic subtraction can remove it). Eventually the light from the two cavities will be recombined, this will optically subtract the common frequency noise.

Intensity noise in the light can also cause noise in the detector. This can come in through at least two distinct mechanisms. First, intensity fluctuations can mimic phase fluctuations. This is usually not a problem. Since the phase is measured at the modulation frequency, where there is not excessive intensity noise in the laser, the detector is insensitive to intensity fluctuations to first order.

*In a Fabry-Perot, B is defined as $c\tau/L$, where τ is the storage time of the light in the cavity. In the Caltech detector, $B \approx 3000$.

The second mechanism is caused by fluctuations in the shape of the mirror surface due to the heating of the mirror. These fluctuations actually cause the length of the cavity to change. This will not be a problem until we are forced to use very high power to eliminate shot noise. In the Caltech interferometer, if one employed enough power to reach the standard quantum limit, then these mirror heating effects would dominate the standard quantum limit at all frequencies above $f = 220\text{Hz}$, even if the intensity of the light were shot noise limited.[31]

3.2.3 Other Noise Sources

In addition to the noise sources mentioned above, there are always the unexpected noise sources which are only discovered through building a detector. These noise sources tend to appear in groups. The detector's sensitivity will reach a plateau at which there are many noise sources of comparable magnitude. All must be eliminated before the detector's sensitivity will improve significantly. Two prime examples of these unexpected noise sources were uncovered within the past two years.

The first of these was discovered by our colleagues in Glasgow. Both the Caltech and Glasgow detectors were limited to a displacement sensitivity of approximately $2 \times 10^{-17}\text{m}/\sqrt{\text{Hz}}$. Both groups had metal test masses with mirrors attached with a thin layer of vacuum grease. Glasgow discovered that by replacing the grease with glue joints their noise level improved. Our group quickly followed suit, and replaced the grease with a thin layer of epoxy resin. This resin is melted between the mirror and the test mass; as the test mass cools, the resin hardens. Our detector's performance improved slightly but, unfortunately, the glue joint distorted the mirrors so that "bad" (non-gaussian) modes would res-

onate. When these modes were resonating, the detector's noise was worse than before. Both the Glasgow group and the Caltech group decided that the best way to join the mirrors to the test masses was to have them made of the same material (fused quartz) and to optically contact them together.† This entailed removing our piezo-electric transducers, replacing them with coils and magnets. At the time of this experiment, the fused quartz test masses had not yet arrived, so that during the data run the mirrors were distorted and occasionally a cavity would jump into a bad mode. When the Glasgow group replaced their test masses with fused quartz, the noise level of their detector improved dramatically; its current sensitivity is 1.2×10^{-18}meters/$\sqrt{\text{Hz}}$. When we made a similar change, our noise level only improved a small amount. We had to continue to search for what was limiting our detector's performance.

This noise source was uncovered last fall, and has led to our most recent improvement in sensitivity. The laser locking servo has a unity gain point of 1 MHz.[13] Excessive frequency noise above a few hundred kilohertz was mixing down to our frequency band.

The only way to be certain that this non-linear frequency noise was the noise source limiting our detector's performance was to eliminate it and see if the detector's performance improved. This was done by placing a short Fabry-Perot cavity in the main beam path. This cavity acts like a narrow band filter—transmitting only light with frequency in a 200kHz band. Installation of this cavity improved the signal-to-noise by a factor of two.

Unfortunately this cavity attenuates the light so that our best spectrum is uncomfortably close to the shot-noise limit. This problem can be alleviated by

†This is done by polishing two surfaces until they are both optically flat, and just putting them together; molecular forces will hold them together.

removing the optical fiber—whose transmission is less than that of the cavity. The optical fiber's purpose is to remove beam jitter—angular fluctuations in the laser beam. The Fabry-Perot cavity will also do this [32], making the fiber extraneous.

In designing any instrument as sensitive as a gravity wave detector, it is important to remember that there will always be the unexpected problems. An instrument like the LIGO cannot just be developed on paper—it is vital that prototype work be done in order to reveal the unexpected.

Chapter 4

Spatial Fluctuations of the Test Masses and Light Source

4.1 Effects on the Detector Sensitivity

Apparent displacement noise can be caused by the fluctuations in the orientation of the mirrors relative to the input beam and to each other. When perfectly aligned, the two cavity mirrors are pointed directly at one another and the input beam is perpendicular to both. The fundamental mode of the cavity (TEM_{00}) matches the input beam exactly, (Figure 4.1). If the alignment is perfect then the fundamental mode is of length L, and no other modes are excited. When operating the gravity wave detector it is always the TEM_{00} mode of the cavity which is resonating. If one of the masses is slightly tilted, the length of the TEM_{00} mode will change from L to $L + \Delta L$, even though the distance between the test masses' center of mass is unchanged. This is one way fluctuations in the cavity geometry can cause displacement noise. Another is caused by the relative motion between the input laser beam and the TEM_{00} mode of the cavity. Spatial fluctuations in the input light will excite small amounts of off-axis modes. Since

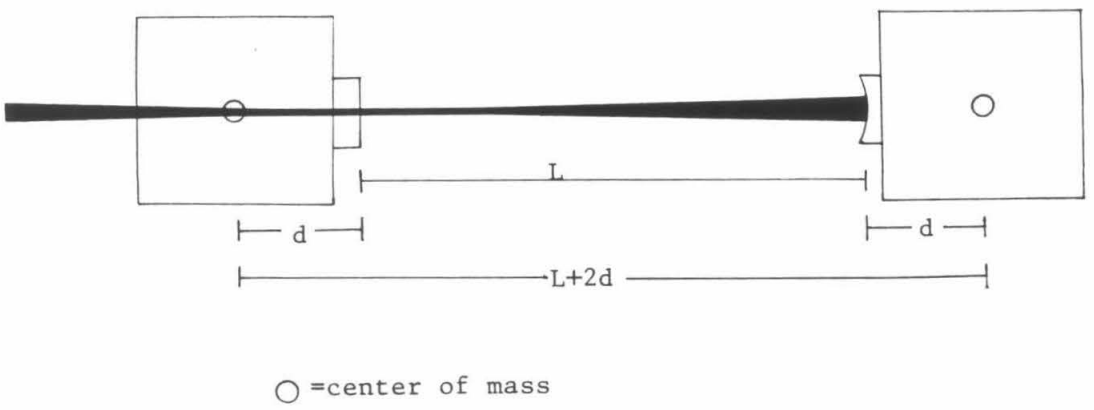

Figure 4.1: Perfect Alignment

these modes have different resonant frequencies than the TEM_{00} mode, they will cause phase noise, which cannot be distinguished from displacement noise. These two effects can be treated separately since only a small amount of an off-axis mode is ever excited.[33] A third spatial fluctuation in the cavity is caused by transverse motion of the test mirrors. In the following sections the contribution to the displacement noise due to each of these effects is presented. Throughout this chapter it is assumed that the mirrors are spatially uniform; any noise which may be caused by scanning an imperfect mirror surface is neglected.

4.1.1 Change in the Length of the TEM_{00} Mode

Consider a cavity made of two mirrors, each mounted to a test mass which is suspended at its center of mass. Assume the input mirror is flat, and the output mirror has a radius of curvature R. On each mass let the distance between the mirror surface and the center of mass be d, and the distance between the mirror

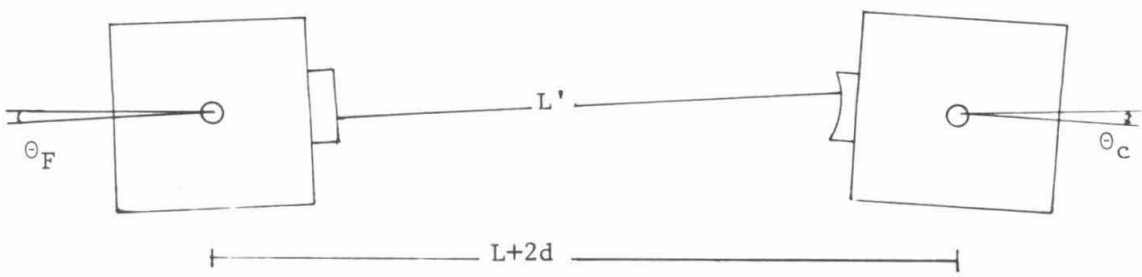

Figure 4.2: Angular motion of the test masses changes the cavity's length.

surfaces be L, (on the Caltech interferometer $R = 62m$, $d \simeq 6cm$ and $L \simeq 40m$; Figure 4.1). The TEM_{00} mode is perpendicular to the mirror surface on both mirrors, hence if either mirror is rotated about its center of mass, the length of the cavity will change, see Figure 4.2. The TEM_{00} mode should coincide with the line connecting the center of mass of each test mass, making the cavity insensitive to the test mass rotating about the optical axis. To second order in θ the length of the TEM_{00} mode is :

$$L' = L + \left[\frac{1}{2}(R - L - d)\theta_F^2 + \frac{1}{2}(R + d)\theta_C^2 + (R + d)\theta_C\theta_F\right]. \qquad (4.1)$$

Since the seismic isolation of the masses should also attenuate any angular excitation of the masses, one might expect the angular noise of the cavity mirrors to be approximately $\delta L/d$. Unfortunately, this is not the case. The cavity mirrors angular position must be servoed in order to keep the cavities aligned. The servo senses the angular position using an optical lever. A HeNe laser beam is reflected off the cavity mirror, and the angle of the cavity mirror is measured using a

position sensitive diode. Any noise in the error signal of the servo is then fed back onto the test mass. This servoloop is discussed more in Section 4.2.1.

The angular noise of the mirrors of the Caltech interferometer has been measured. This was done by measuring the error point of the servoloop. Figure 4.3 shows a fairly typical spectrum. An empirical fit to the spectral density of the angular noise of a typical mirror is:

$$S_\theta(f) = \begin{cases} A & \text{if } 0 \leq f \leq f_0 \\ A(f/f_0)^2 & \text{if } f_0 \leq f \leq 100\text{Hz} \end{cases} \tag{4.2}$$

where f_0 and A are adjusted for the best fit. Above 100Hz it is difficult to accurately measure the angle. In the Caltech detector typical values for A and f_0 are 4×10^{-9}radians/$\sqrt{\text{Hz}}$, and 16Hz respectively. Using this noise spectrum one can calculate the approximate contribution this makes to the noise in the Caltech gravity wave detector. The noise limit this places on the Caltech interferometer for $A = 4 \times 10^{-9}$radians/$\sqrt{\text{Hz}}$ and $f_0 = 16$Hz is shown in Figure 4.4. The solid line shows the noise level when the DC alignment of the cavity is perfect, ($\theta_{0F} = \theta_{0C} = 0$). The dashed line is for when the cavity is poorly aligned, $\theta_{0F} = \theta_{0C} = 50\mu$radians, (this is the maximum misalignment ever tolerated). This assumes that the angular noise has the form given by Equation 4.2. Because this treats the motion of the two masses as perfectly correlated, this plot shows an upper limit to the noise. Above 100Hz the noise certainly falls off faster then f^{-2}, since the seismic noise is known to be smaller at higher frequencies and the isolation has been measured to improve faster then f^{-2}.[26]

It is important to note that this noise source scales with the length of the detector, so that if this were the limiting noise source of a detector, making the detector longer would not improve one's signal-to-noise ratio.

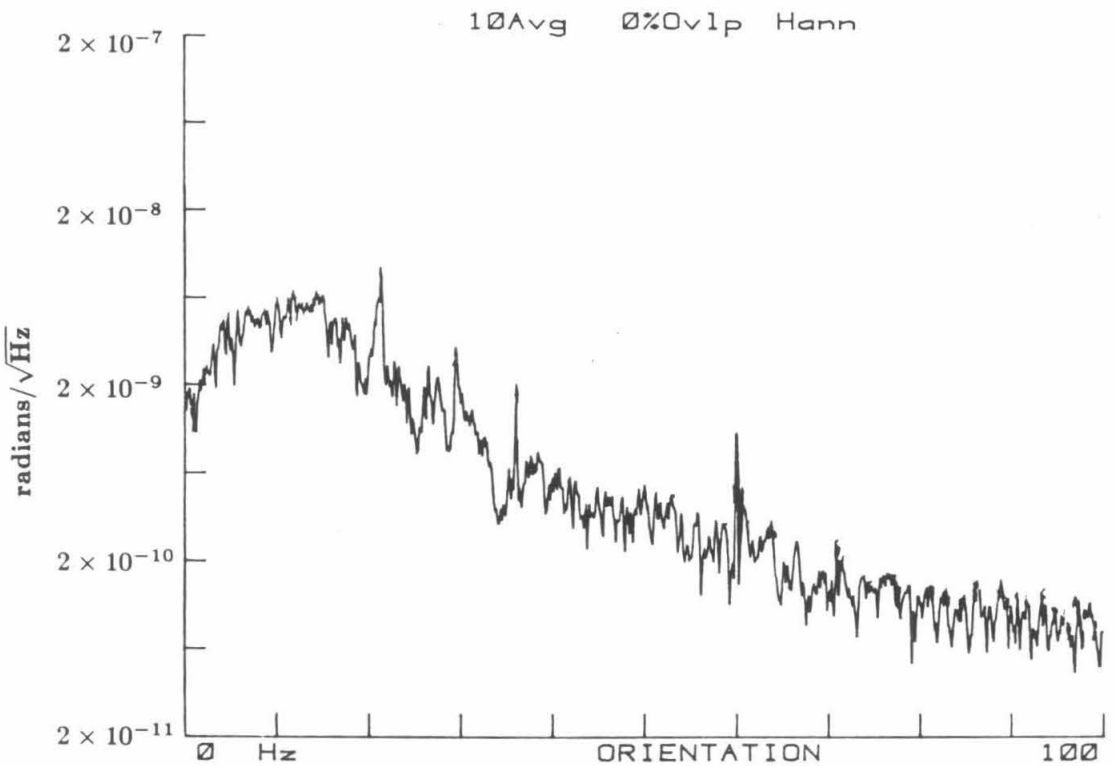

Figure 4.3: Angular motion of one of the test masses as a function of frequency.

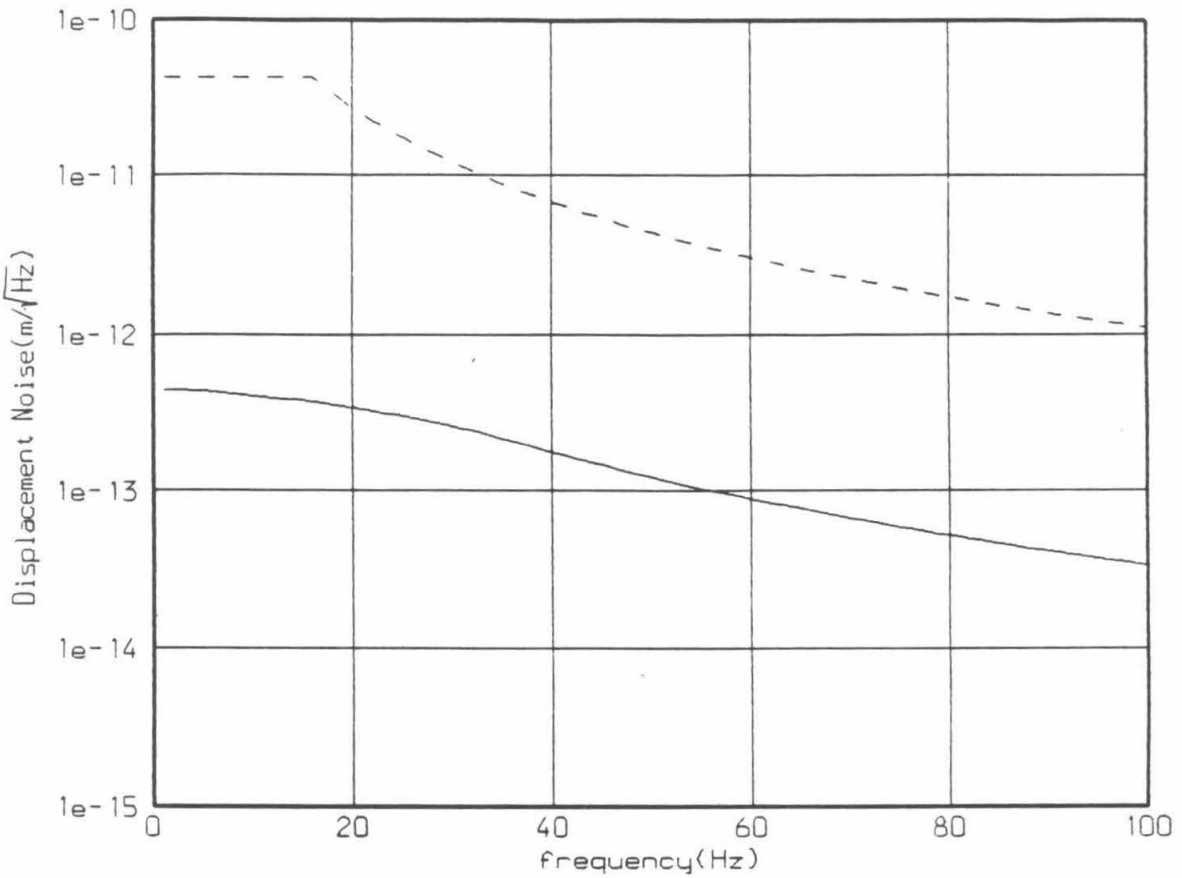

Figure 4.4: The detector noise due to the angular fluctuations of the cavity mirrors. This curve sets an upper limit, assuming that the angular noise has the form given by equation 4.2, with $A = 4 \times 10^{-9}$radians/$\sqrt{\text{Hz}}$ and $f_0 = 16$Hz. The solid curve is for when the cavity is perfectly aligned, $\theta_{0C} = \theta_{0F} = 0\mu$radians. The dashed line is for when the cavity is poorly aligned, $\theta_{0C} = \theta_{0F} = 50\mu$radians.

4.1.2 Excitation of Off-Axis Modes

Excitation of other modes causes "phase noise," which is indistinguishable from a change in length of the cavity. How this causes displacement noise in the detector is shown in detail in Appendix A. In this section a general outline of the calculation is given.

First consider a cavity in which only the TEM_{00} mode has been excited. The phase of the light leaking out of the cavity relative to the incident light is measured using a phase modulation technique.[22] This signal is used to hold the cavity on resonance, $L = n\lambda/2$. If the cavity changes length by a small amount ΔL then the signal measured is:

$$S \propto |A_{inc}|^2 \left(\frac{r_2 |\, t_1 \,|^2}{1 - 2r_1r_2 + (r_1r_2)^2} \right) \left(\frac{4\pi \Delta L}{\lambda} \right) \tag{4.3}$$

where A_{inc} is the amplitude of the input beam, t_1 is the transmissivity of the input mirror, and r_1, r_2 are the mirrors' reflectivities, (in the Caltech detector $r_1 \approx .9997$, $r_2 \approx .99995$).[25,34]

Now consider the case where the incident light does not totally agree with the TEM_{00} mode of the cavity, but is "contaminated" with some light which spatially matches the TEM_{01} mode. $A_{inc} = A_{inc_{00}} + A_{inc_{01}}$, where $A_{inc_{01}} = \epsilon A_{inc}$, $\epsilon \ll 1$. This would cause an error in the measurement of the phase of the TEM_{00} mode, which would cause an apparent displacement signal:

$$\Delta L = \epsilon^2 \frac{\lambda}{4\pi} \sin(\delta_1) \left(\frac{1 - 2r_1r_2 + (r_1r_2)^2}{1 - 2r_1r_2\cos(\delta_1) + (r_1r_2)^2} \right) \tag{4.4}$$

where $\delta_1 = 2\cos^{-1}(\sqrt{1 - L/R})$. The derivation of this formula is given in Appendix A. To calculate how large ΔL is, one must first calculate ϵ. This calculation has been done before, [32,35]; it is also presented in Appendix A. Suppose that the input beam is at small angle, α, to the axis of the TEM_{00} mode and

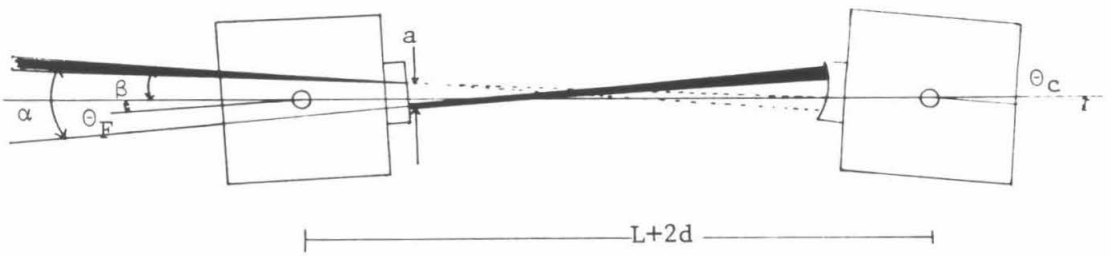

Figure 4.5: Excitation of off-axis modes.

is displaced by a small amount, a, at the waist. To first order in a and α:

$$\epsilon = \left(\frac{a}{y_0} + \frac{\pi i \alpha y_0}{\lambda} \right) \tag{4.5}$$

(y_0 is the waist size of the cavity; in the Caltech detector this is .22cm). Since a and α are the displacement and angle between the input beam and the cavity mode, they are the sum of input beam "jitter" and motion of the TEM_{00} mode caused by the cavity mirrors moving. Using a coordinate system where the $\hat{z}$ axis is defined by the line connecting the two test masses center of mass, let β be the angle between the input beam and the $\hat{z}$ axis, and let b be the distance between the input beam and the $\hat{z}$ axis at the waist of the cavity, (when the input mirror is flat, the waist is at the input mirror). The angle between the input beam and the TEM_{00} mode of the cavity is $\alpha = \beta + \theta_F$. The displacement between the input beam and the TEM_{00} mode of the cavity is $a = b + ((R - L)\,\theta_F + R\theta_C)$, (see Figure 4.5). In the case where the excitation of off-axis modes is due to mass motion, then the resulting error in ΔL is much smaller then that discussed

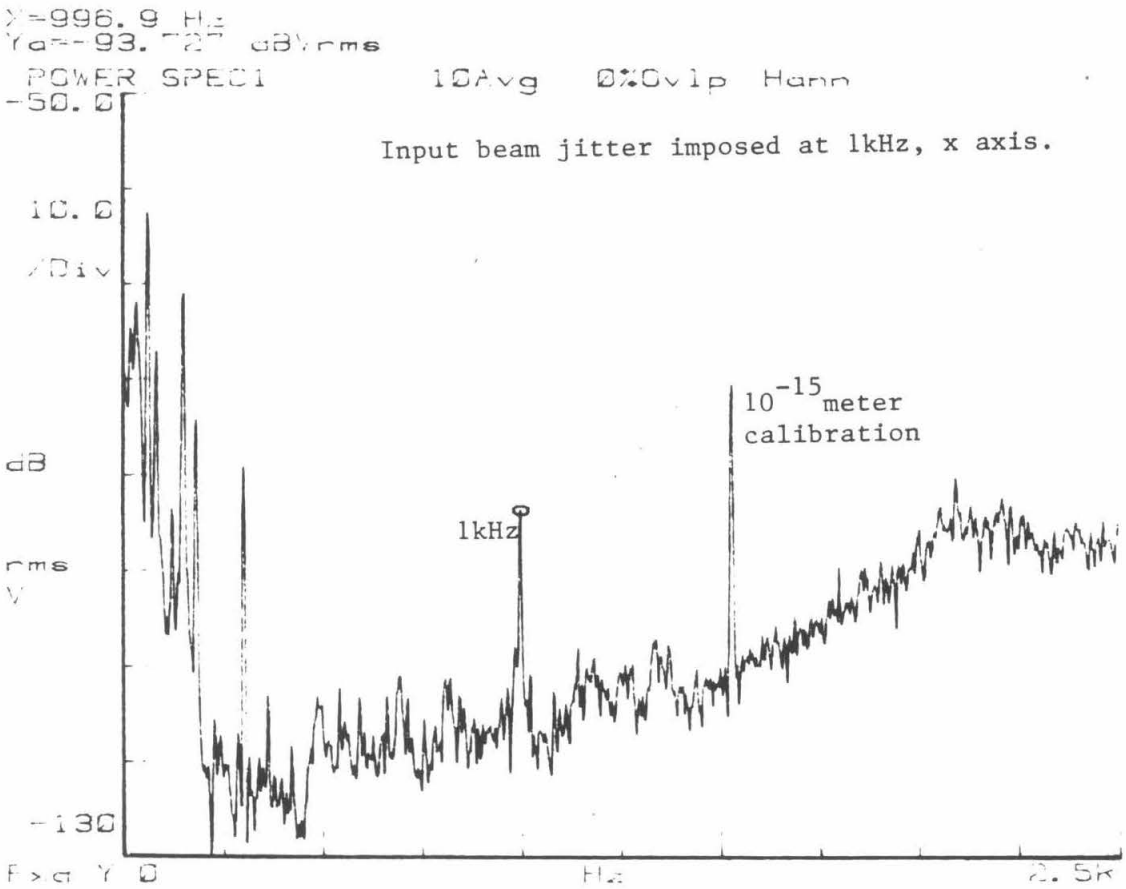

Figure 4.6: The detector's noise spectrum, with imposed beam jitter.

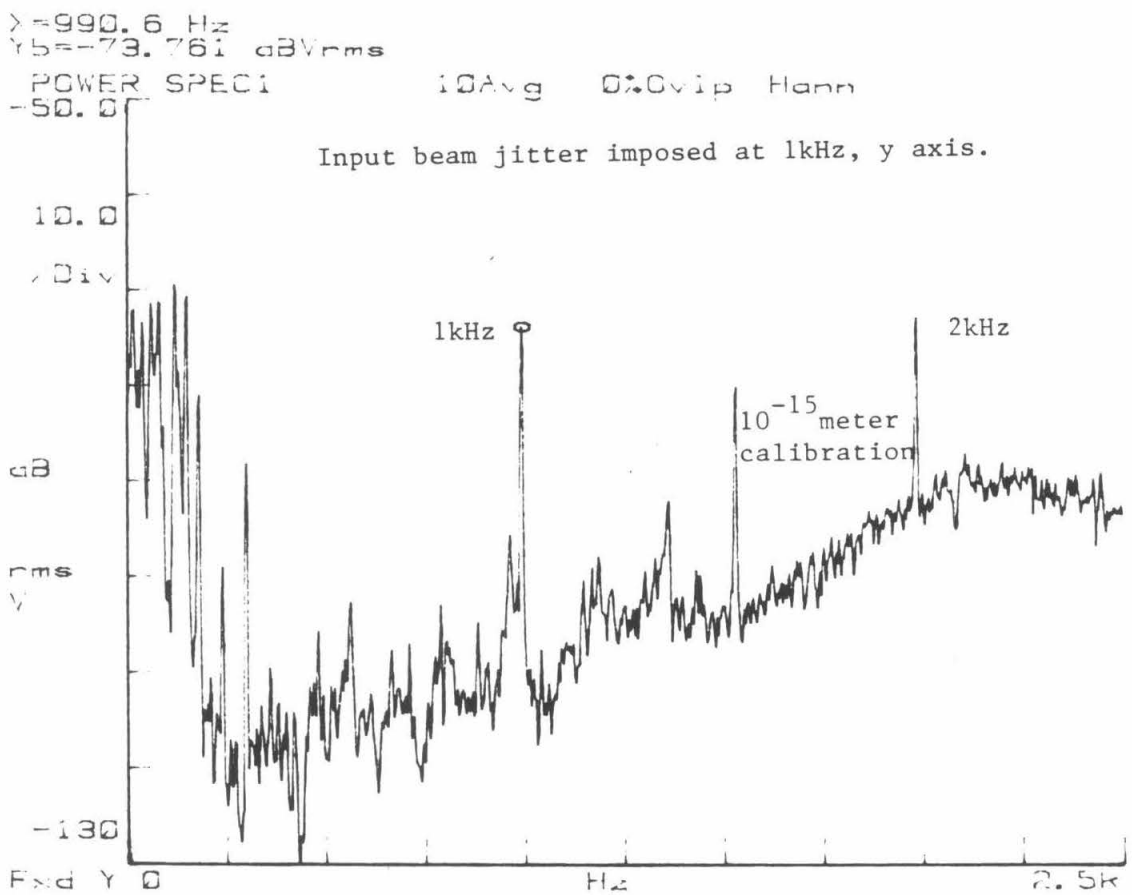

Figure 4.7: The detector's noise spectrum, with imposed beam jitter.

in Section 4.1.1.

Figure 4.6 shows the displacement noise spectrum of the Caltech gravity wave detector with imposed input beam "jitter." A 1 kHz sine wave was imposed on the horizontal axis of the input light using a PZT mirror. The rms amplitude was approximately .3 μradians. The peak at 1 kHz corresponds to a displacement noise level of approximately $10^{-15}\mathrm{m}_{\mathrm{rms}}$. There is no peak at 2kHz, which is not surprising since Equations 4.4 and 4.5 lead one to expect a noise level of approximately $10^{-20}\mathrm{m}_{\mathrm{rms}}$ at 2kHz, which would be well below the noise floor of this spectrum.

Lest one become complacent about beam jitter, Figure 4.7 shows a similar noise spectrum taken while a 1kHz sine wave was imposed on the vertical axis of the same PZT mirror. In this the peak at 2kHz corresponds to a displacement noise level of approximately $10^{-15}\mathrm{m}_{\mathrm{rms}}$. This could be due to a number of effects, such as scanning an imperfection in either the optics or the photodiode. In this instance I suspect that it is due to light falling on and off the active region of the photodiode.

It is interesting to note how this noise source scales with the size of the detector. If the ratio of the cavity length to the mirror's radius of curvature remains fixed, and the storage time of the cavity is held constant then the displacement noise due to this effect increases proportionally to L^2. Assume that $\epsilon \approx 10^{-7}$, and that the storage time of the cavity is 1msec. In a 40 meter cavity this storage time implies that $r_1 r_2 = .9997$. The displacement noise would then be $\Delta L \approx 10^{-29}$ meters. In a 4km detector a 1msec storage time implies that $r_1 r_2 = .97$, leading to an apparent displacement noise $\Delta L \approx 10^{-25}$ meters. Even if one shortens the storage time of the cavities this effect should not limit a detector's performance.

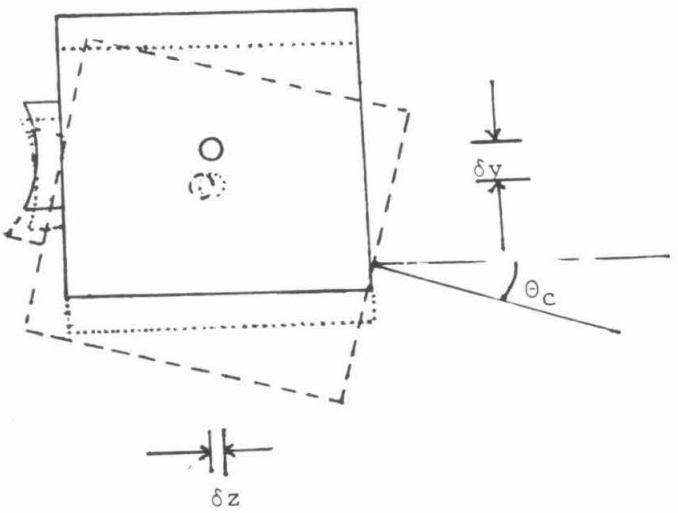

Figure 4.8: Transverse motion of a curved mirror.

4.1.3 Transverse Motion of the Mirrors

Motion of the curved mirrors perpendicular to the beam axis can also mimic displacement noise. Perpendicular motion of a curved mirror can be represented by a combination of a rotation and motion along the beam axis, (Figure 4.8). The equivalent motion would be (to second order):

$$\delta z = (\delta y)^2/2(R+d) \tag{4.6}$$

$$\theta = \delta y/(R+d). \tag{4.7}$$

Since the sideways motion δy of a test mass should be approximately $\delta z = \Delta L$ (it would be impossible to isolate motion along the $\hat{z}$ axis orders of magnitude better than motion along the $\hat{y}$ axis), the term in Equation 4.6 is negligible. θ

will appear as displacement noise in the same manner discussed in Section 4.1.1.

$$\begin{aligned} \Delta L &= \frac{1}{2}(R+d)\theta_C^2 \\ &= \frac{1}{2}(\delta y)^2/(R+d) \end{aligned} \tag{4.8}$$

This too would be much less then ΔL. Perpendicular motion of the flat mirror should have no effect on the displacement noise.

4.2 Reducing Spatial Fluctuations

4.2.1 Reduction of Mass Jitter

In order to keep the cavities aligned, the angle of each mirror must be carefully controlled. This must be done in a way which neither compromises the seismic isolation nor the mechanical Q of the test masses. As mentioned earlier (in Section 3.2.1) each mass is suspended by two wires, which provide some of the seismic isolation. These wires are attached to a control block, which is suspended by a single wire from the top of a lead and rubber stack, (see Figure 4.9). The control block is free to turn and tilt. Its angular position is controlled by the use of magnets and coils. Eight permanent magnets are mounted on the control block, by altering the current through coils located near these magnets, the orientation of the control block, and hence the mass, is controlled.

The angular position of the masses is sensed using optical levers, (see Figure 4.9). A HeNe laser shines light down the 40 meter pipe, where it reflects off of the cavity mirror and comes back to a quadrant diode. By measuring where the light hits the diode one has an accurate measure of the angle of the cavity mirror. The dominant error in this measurement is caused by jitter in the input HeNe laser

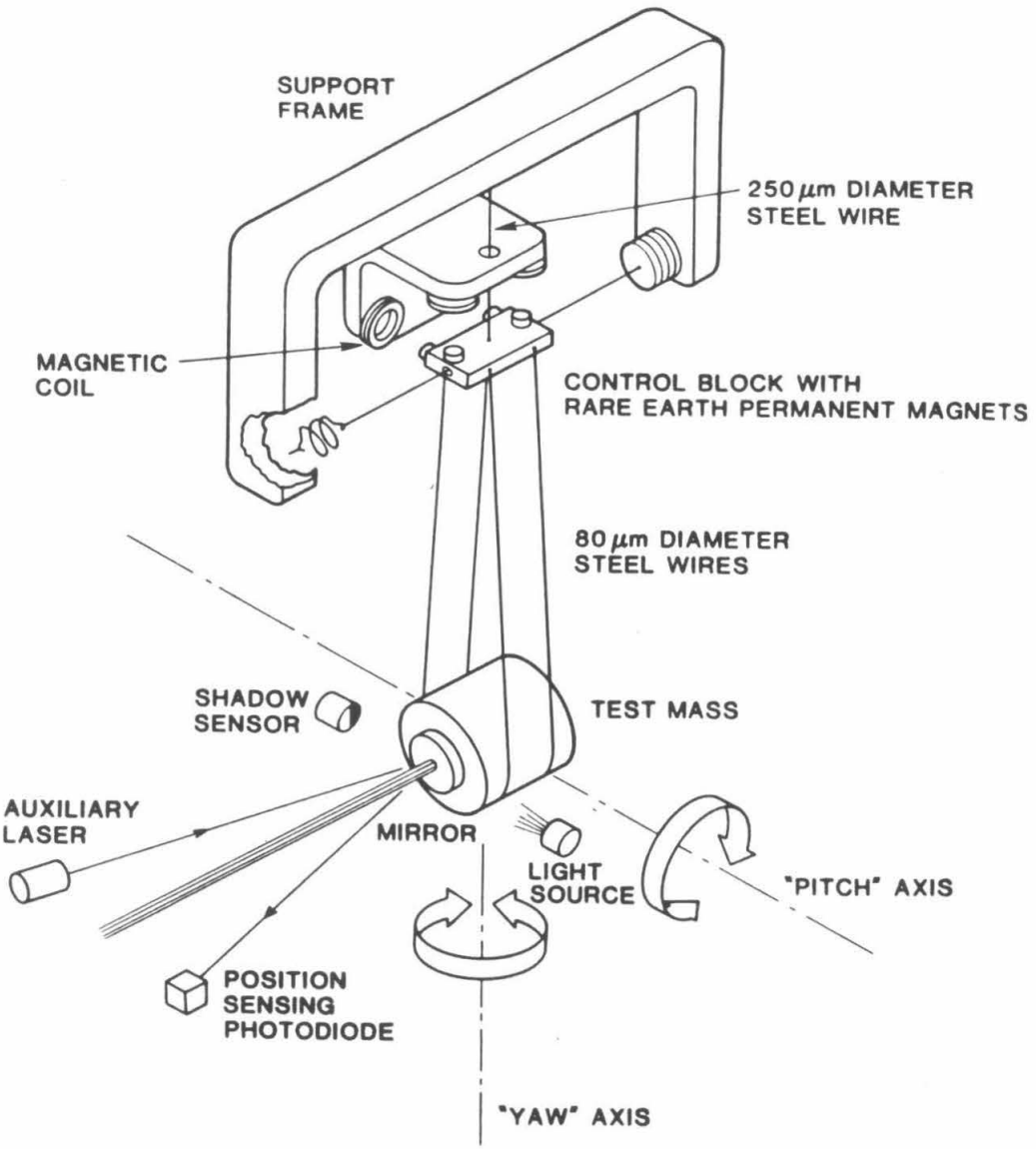

Figure 4.9: The test mass suspension and control.

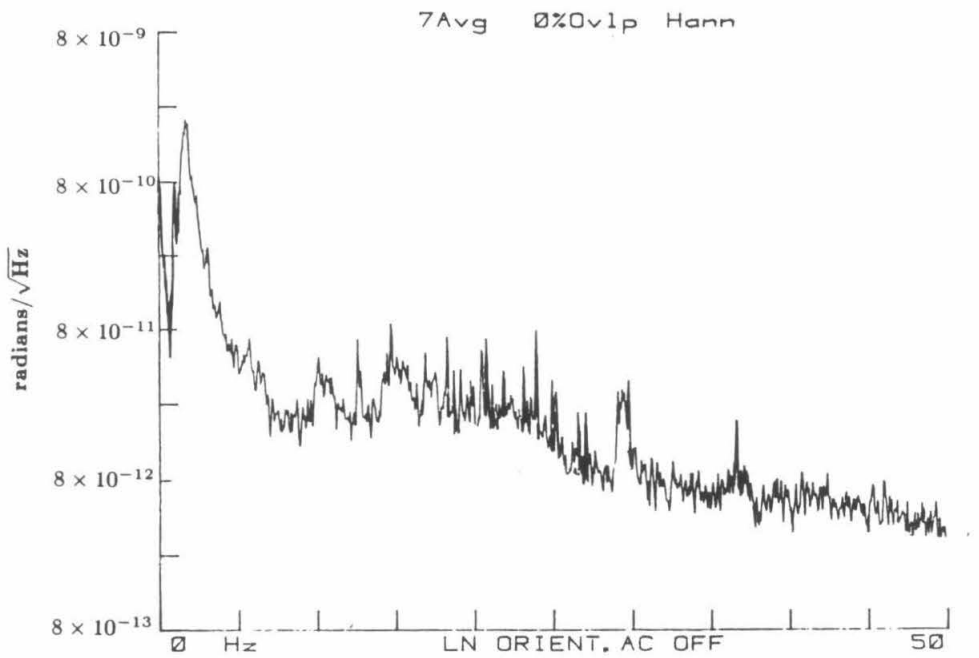

Figure 4.10: Angular motion, measured when the air conditioning was off.

beam. These optical levers could be made insensitive to angular beam jitter if, instead of using the cavity mirrors, the light was reflected off of 40 meter curved mirrors. This would require mounting additional mirrors to the test masses, and it was feared that this would harm the mechanical Q of these masses.

The servoloop which takes the error signal from the quadrant diode and feeds back to the coils is discussed in Mark Hereld's thesis. [6]

The angular fluctuations of one of the test masses are shown in Figures 4.10 and 4.11. These clearly show that air currents and mechanical vibrations caused by the air conditioning impose noise on the test masses error signal, which is then fed back to the masses. Unfortunately, because of thermal drifts, it is necessary to leave the air conditioning on when running the detector for long time periods, otherwise the reliability of the detector is considerably reduced. By installing an optical fiber feed-through from the HeNe laser into the vacuum system, the

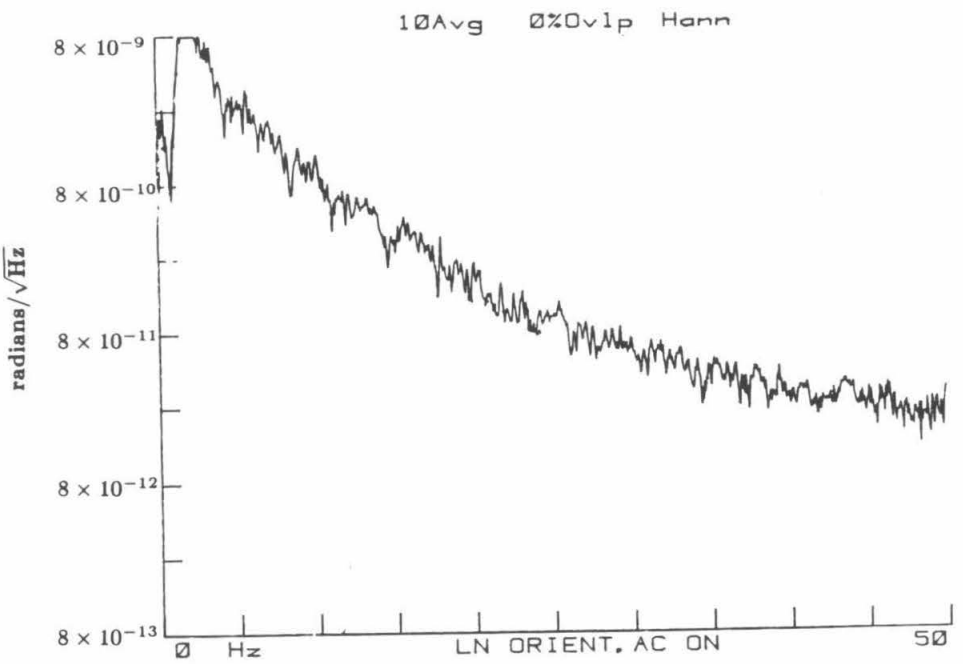

Figure 4.11: Angular motion, measured when the air conditioning was on.

effects of the air conditioning were reduced at very low frequencies, (see Figures 4.12 and 4.13). The fiber is a single mode fiber, it enters the vacuum through a hole drilled in a blank, which has been sealed with epoxy. The fiber's output must be carefully collimated to travel the 80 meters from its output to the mirror and back to the quadrant diode. This is done with two lenses mounted a fixed distance apart in a brass cylinder, the distance from the fiber to the first lens is adjustable. The remaining jitter on the control beam is due to motion of the tower which the fiber output coupler is mounted to. This tower is not isolated from ground noise, and has a resonance at 18Hz. The system could be improved by replacing the tower with one which is sturdier, and perhaps seismically isolated.

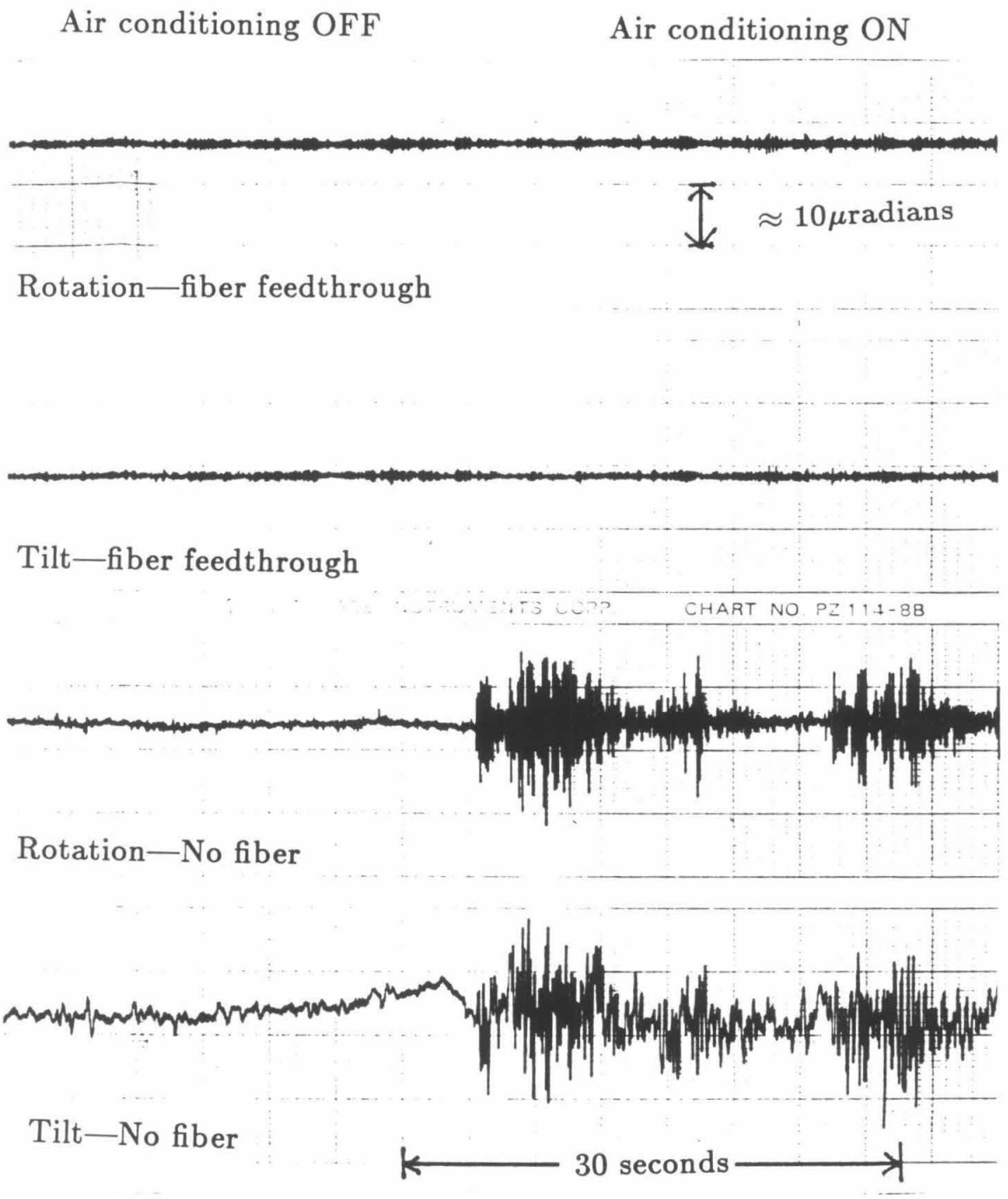

Figure 4.12: Angular motion versus time.

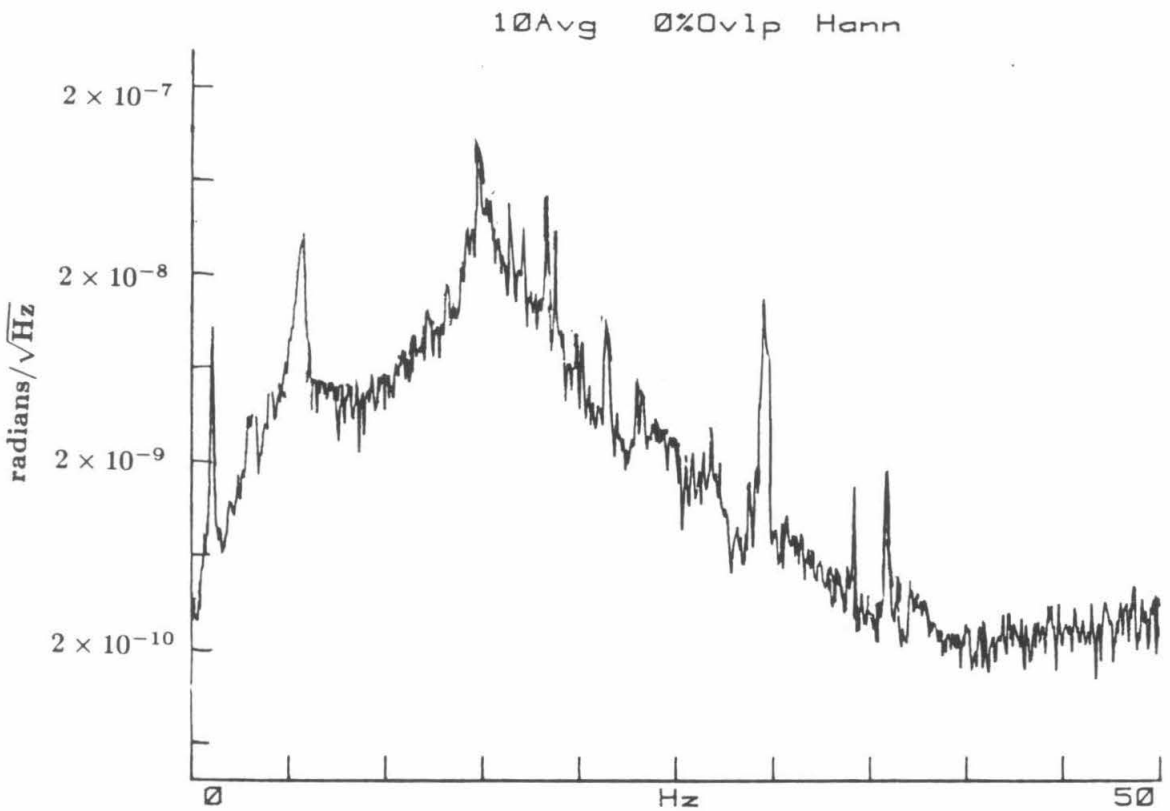

Figure 4.13: Angular noise with fiber feed-through for orientation control.

4.2.2 Reduction of Beam Jitter

A more pressing problem than angular mass motion has been reduction of motion of the input beam. Though the detector is less sensitive to motion of the input beam than it is to motion of the masses, the laser beam tends to be a great deal noisier. The laser is not as well isolated as the masses, so that angular noise on the laser beam tends to become a noise limitation first. The laser beam picks up angular noise from both motion of the mirror mounts and air currents. The laser mirrors are isolated from the argon tube, to reduce motion of the laser cavity mirrors caused by the tubes cooling water.[13] All the mirrors in the main beam path are thermally compensated, so that fluctuations in the temperature of the lab will have a minimal effect on the pointing of the beam. Fluctuations were further reduced by installing a single mode fiber in the beam path. This technique was first employed in gravity wave detectors by MIT. Since the fiber will only transmit one spatial mode, this acts as a spatial filter. A drawback of the fiber is its low power handling ability. It is limited to approximately one watt incident power, and its throughput is roughly 50%. Figure 4.14 shows the angular noise in the input beam both with and without the fiber. Another factor of 10 reduction was achieved by placing the output coupler of the fiber in the vacuum, and mounting the output coupler on top of a lead and rubber isolation stack.

As discussed in Chapter 3, a mode cleaning cavity will also act as a spatial filter.[32] Mode cleaning cavities are more difficult to employ then optical fibers because they must be held on resonance, whereas the fiber makes no demands on the frequency of the light. They do have some definite advantages over fibers in that they also act as temporal filters, and they are capable of handling higher

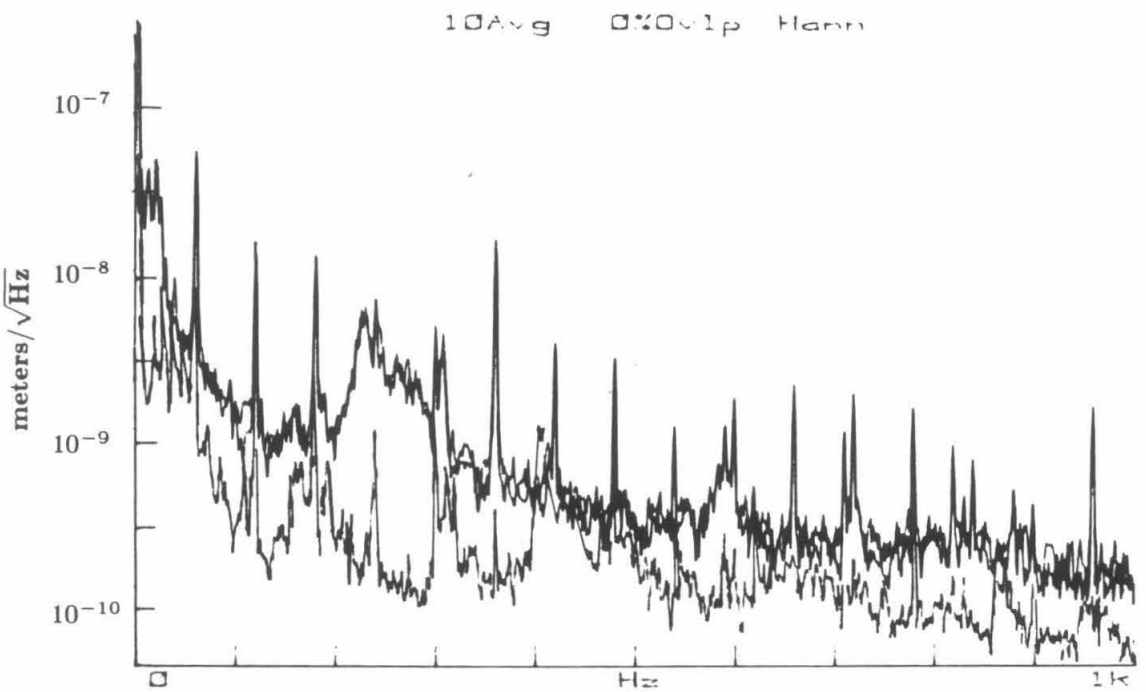

Figure 4.14: Reduction of angular input beam noise by using an optical fiber.

power. Because the Caltech detector needs the temporal filtering of a mode cleaner, the group is currently working on optimizing one's design. After this has been done the fiber will be removed. It will not be removed before then because it is easier to alter the design of the mode cleaner while the fiber is still in the system. The mode cleaner's length and position can be changed without having to readjust the mode-matching lenses (the lenses which match the input beams waist size and position to that of the 40 meter cavities). In addition the optics between the mode cleaner and the cavity do not have to be in vacuum as long as the fiber is present. Once the mode cleaner is installed, it should provide even better isolation from beam wiggle at frequencies ranging from five to a few hundred hertz because it is suspended in much the same manner as the test masses, and is therefore better isolated from ground noise than the fiber's output coupler.

Currently neither beam jitter nor angular motion of the test masses is a limiting noise factor in the detector above 200Hz. Below that the detector's noise is probably limited by seismic noise, which could couple in by directly moving the test masses along the beam axis and by causing angular motion of the masses.

Chapter 5

Data Analysis

Approximately 36 minutes of data from the Caltech detector were thoroughly examined for coalescing binaries. These data spanned over one hour and were collected on the evening of March 8, 1987, when both the Caltech and Glasgow detectors were operating. This search set a limit on the strength of gravitational waves from coalescing binaries which varies with the mass parameter η, (see Equation 2.4). The limits set for various values of η are discussed in chapter 6.

In this chapter the algorithm used to search for coalescing binaries, the data run, and the data analysis are discussed.

5.1 An Algorithm to Search For Coalescing Compact Binaries

5.1.1 Optimal Filters

Detecting gravity waves is difficult because one must search for such small, rare events. Since the signal is so small, it is important not only to build sensitive instruments, but also to analyze the data as carefully as possible. It is illogical

to struggle to improve one's detector by a factor of ten, and to then waste that improvement through sloppy data handling.

The best filter possible is called an "optimal filter." Suppose that one has a detector with a power spectral noise density $N_h(f)$, then it can be proven that the best possible filter will give you a signal-to-noise ratio (in amplitude, not power):

$$\frac{S}{N} = \left[\int_{-\infty}^{+\infty} \frac{\left|\tilde{S}(f)\right|^2}{N_h(f)}\, df \right]^{\frac{1}{2}} \tag{5.1}$$

where $\tilde{S}(f)$ is the Fourier transform of the signal $S(t)$. Such a filter is called an optimal filter.[36] In the case where the noise is white, then Equation 5.1 reduces to:

$$\frac{S}{N} = \left[\frac{\int_{-\infty}^{+\infty} [S(t)]^2\, dt}{N_h} \right]^{\frac{1}{2}}. \tag{5.2}$$

A filter which is optimal for input white noise is called a matched filter.[36]

A major problem in searching for coalescing binaries is that there are three unknowns in the waveform, (see Equation 2.8 or 5.3), the mass parameter, η, the time of coalescence, τ, and the phase, ϕ. My goal was to develop a filter which would be close to optimal for any value of η and τ. Since there is no way to know the phase of the signal prior to detecting it, the filter should make no assumptions about the value of ϕ; this implies that the best signal-to-noise ratio possible will be a factor of $\sqrt{2}$ less than that given by Equations 5.1 and 5.2.

5.1.2 The Signal

As stated in Section 2.3, the expected signal from coalescing compact binary stars would have the form:

$$S(t) \propto (\tau - t)^{-\frac{1}{4}} \cos\left(2\pi f_0 (1 - t/\tau)^{5/8} + \phi\right) \tag{5.3}$$

where $f_0 = (\eta\tau)^{-3/8}/\pi$; η is a function of the stars masses and τ is the time of coalescence, (η is precisely defined in Section 2.3). Although the strain is largest in the binary's last few moments, when the frequency is greatest, the Fourier transform of the strain, $\tilde{S}(f)$, doesn't increase with frequency. Because the frequency is changing more rapidly as the stars get closer to coalescence, the Fourier transform of the strain is larger at lower frequencies. To optimize the signal one should search through low frequencies and integrate the signal for as long as possible. If one searches for binaries long before coalescence then the frequency is nearly constant. Clearly the easiest way to search through many frequencies is to do a Fourier transform of the detector output. This will separate the signal from background noise at other frequencies. Unfortunately, when the frequency of the gravitational radiation is nearly constant, it is below the frequency at which earth-bound detectors would probably be limited by gravity gradient noise.

One's best chance of detection is in the binary's last few moments. At this time the frequency is high enough to be in the detector's frequency range. For two neutron stars, each with mass $1.4M_\odot$, the frequency is above 500Hz for approximately .03 seconds. The frequency remains approximately constant for only n cycles, where:

$$n = \sqrt{\frac{4}{3} f_{min}(\tau - t_{min})} \tag{5.4}$$

(f_{min} equals the minimum frequency of the detector, and $(\tau - t_{min})$ is the length of time from $f = f_{min}$ until coalescence). After n cycles the phase shift is greater than π. No longer can the signal be efficiently separated from background noise by doing a simple Fourier transform. Unless the change in frequency is tracked, only a few cycles can be integrated over. For $m_1 = m_2 = 1.4M_\odot$ and a detector

which is sensitive down to 500 Hz less than five cycles can be integrated over. If one tracks the frequency, then one is only limited by the time the signal is in the detector's frequency range. This means that with the same detector the signal could be integrated over 24 cycles. Consider a detector which is sensitive down to $f = f_{min}$, and has white noise above this frequency. The best signal-to-noise ratio which can be obtained through filtering is calculated by replacing the lower limit of integration in Equation 5.2 with t_{min}, the time at which $f_{rad}(t) = f_{min}$. This yields:

$$\frac{S}{N} = \frac{5\alpha}{64r\sqrt{N_h}}\eta^{\frac{3}{4}}\left[(\tau - t_{min})^{\frac{1}{2}} - (\tau - t_{final})^{\frac{1}{2}}\right]^{\frac{1}{2}} \tag{5.5}$$

where t_{final} is when the waveform ends, (t_{final} might be less than τ due to tidal disruption).

5.1.3 The Algorithm

As stated earlier, a major difficulty in searching for coalescing binaries is that η and τ are unknown. In order to track the changing frequency, both η and τ must be fixed, so one must search through all the possible values of η and τ. If one assumes a value for τ, then ignorance of η is the same as ignorance of the initial frequency f_0, so searching through all values of η is equivalent to searching through many frequencies. If the frequency were constant, this would be simple, one would perform an FFT:

$$F(S, f) = \int S(t)e^{-2\pi i f t}dt. \tag{5.6}$$

But the frequency is not constant, so a normal Fourier transform won't work. The way to get around this is by changing variables. Instead of working with real frequency and real time, characterize the signal with initial frequency, f_0,

and a timelike variable:

$$\chi = -\frac{8}{5}\tau\left(1 - \frac{t}{\tau}\right)^{\frac{5}{8}} \tag{5.7}$$

then the signal will appear periodic when mapped versus χ.

$$S(\chi) \propto \chi^{-\frac{2}{5}} \cos(2\pi f_0 \chi + \phi) \tag{5.8}$$

This timelike variable χ works for all binaries, regardless of the stars' masses. Resampling the data in even steps of χ allows one to perform an FFT.

$$F(S, f_0) = \int S(\chi) e^{-2\pi i f_0 \chi} d\chi \tag{5.9}$$

This transform will track the gravity wave's frequency, and separate it from background noise at other frequencies. (The doppler shift due to the earth's motion has been neglected, but over an integration period of 100 seconds it causes a fractional change in frequency of approximately 10^{-8}, which is negligible.)

This filter assumes that one knows the time of coalescence, so one must search through τ in discrete steps. To use this filter, fix τ, then resample the data in even steps of χ. One can then perform an FFT, which will search through all values of f_0, and hence η, simultaneously. This filter is actually a bank of filters, each frequency channel of the FFT filters for a different value of η. Using an FFT cuts down on computation time, but at the cost of integrating all the signals over the same time period. Since different binaries will emit signals in the detector's frequency range for different time periods, it is impossible to optimize the integration period for all binaries simultaneously, (see Table 5.1). How critical this problem is depends on the frequency range of the detector used, and how well the noise below f_{min} is filtered out.

M_1	M_2	Seconds from $f = f_{min}$ until coalescence			
(in $M_\odot$)		$f_{min} = 500$Hz	$f_{min} = 305$Hz	$f_{min} = 200$Hz	$f_{min} = 50$Hz
0.2	0.4	.43	1.6	5.0	200.
0.4	0.6	.17	.64	2.0	79.
1.0	1.0	.05	.19	.60	24.
1.4	1.4	.03	.11	.34	14.
1.75	1.75	.02	.08	.23	9.4
10.	10.	.001	.004	.013	.52

Table 5.1: The length of time the signal will have $f > f_{min}$ if no tidal disruption occurs.

5.1.4 Numerical Tests

Prior to collecting data with the detector, this algorithm was tested numerically. Figure 5.1 shows the output of this filter when applied to a data set consisting of computer-generated white noise with a gaussian distribution (to simulate noise in a detector) plus a signal. The signal strength was approximately equal to one standard deviation of the noise in the data set (it varied from 1.2σ to 3σ), the filter integrated from $t = .5$sec (when the frequency of the signal was 173Hz) to $t = .99$sec, with $\tau = 1.0$sec. The sampling rate was 10kHz. The peak can clearly be seen above the background noise, its relative height is approximately:

$$\left[\frac{\int_{.5sec}^{.99sec}(S(t))^2 dt}{2N_h}\right]^{\frac{1}{2}} = 30 \tag{5.10}$$

$N_h = 1/5000\text{Hz}; S(t) = (\tau - t)^{-\frac{1}{4}} \cos\left(2\pi f_0 (1 - t/\tau)^{\frac{5}{8}}\right)$.

This filter's output gives astrophysically relevant information immediately. When a signal is detected, f_0 and τ are known. From these η can be immediately

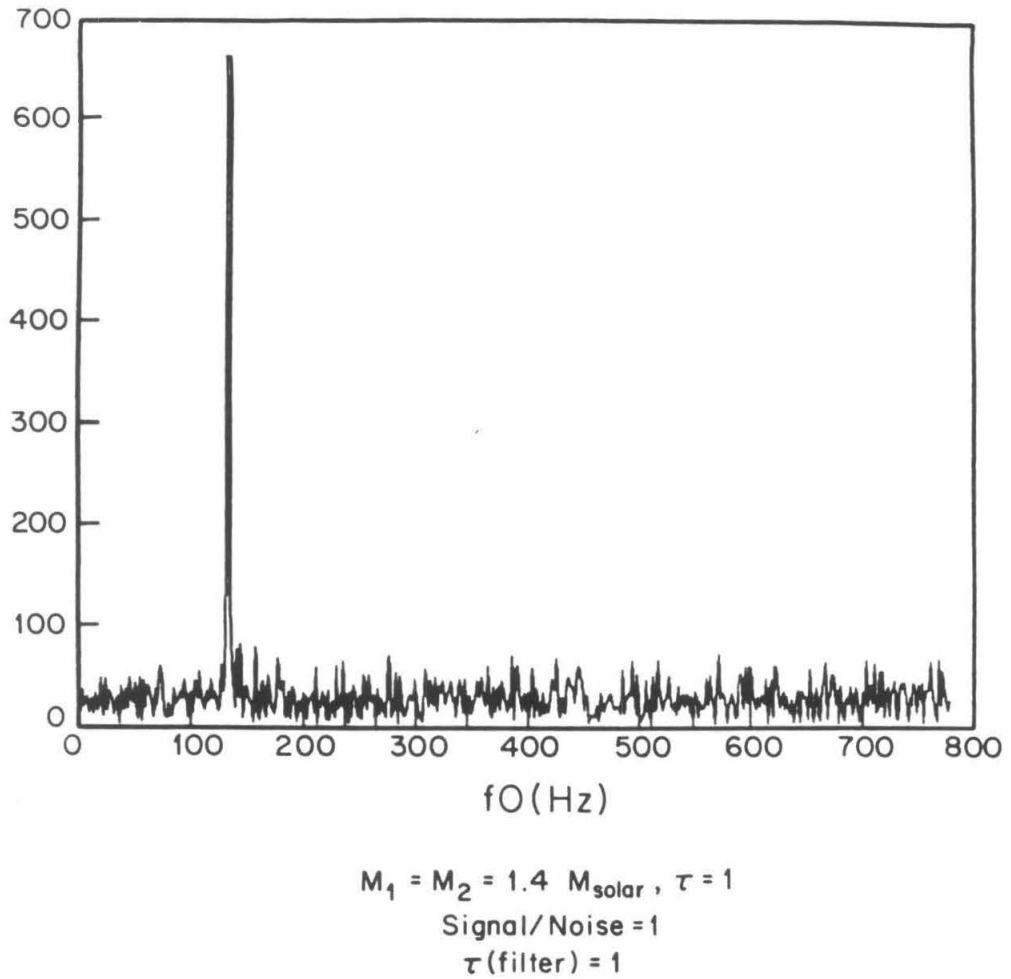

Figure 5.1: The output of this filter when there is no error in τ. The input was computer generated white noise with a Gaussian distribution plus a signal equal to that predicted for a binary made of two $1.4M_{\odot}$ neutron stars. The signal amplitude varied from 1.2σ to 3σ, (σ is the standard deviation of the noise). The filter analyzed from $(\tau - t) = 0.5$ sec until $(\tau - t) = 0.01$ sec. The peak can be seen at $f_0 = 133$Hz which implies that $\eta = 1.0 \times 10^{-7}\text{sec}^{5/3}$, as expected for a binary made of two $1.4M_{\odot}$ stars.

calculated, giving information about the mass of the stars in the binary. The peak in Figure 5.1 is at $f_0 = 133$Hz which implies that $\eta = 1.0 \times 10^{-7}\text{sec}^{\frac{5}{3}}$ as expected for a binary made of $1.4M_\odot$ stars. (It is important to note that there is nothing special about $m_1 = m_2 = 1.4M_\odot$, this filter will work for any mass combination; for example, if $m_1 = m_2 = 10.M_\odot$, a peak would appear at 39Hz.) The filter's performance will deteriorate if there is an error in τ. If there is a .1 second error in τ, then the peak will only be 40% as high.

The speed of this algorithm was checked on a Masscomp 500 computer. A detector frequency range of 200 to 2000 Hz was assumed, and the filter was optimized for two $1.4M_\odot$ stars. The FFT was performed from $(\tau - t) = .34$ seconds (at which time a binary with two $1.4M_\odot$ would have $f = 200$Hz) until $(\tau - t) = .01$ seconds. This was repeated every .1 seconds. The data were sampled at 10 kHz. The algorithm analyzed 10 seconds of data in 8.2 seconds, (5.3 seconds were spent reading in the data and 2.9 seconds were spent performing the calculation). The Masscomp 500 computer has an array processor which is capable of performing a 1024 element FFT in 4.5 msec.

5.2 Analysis of the Data

Numerical simulations are nice because they allow one to simplify a problem and check performance in an ideal case, but ideal situations rarely exist. The data taken from the detector differ from simulated data in that they are *not* white; the spectrum has many features as can be seen in the noise spectrum, Figure 5.2. Another feature of the spectrum is that the detector's response varies with frequency. A white strain signal will not produce a flat response from the detector; this can also be seen in Figure 5.2. The solid line shows the

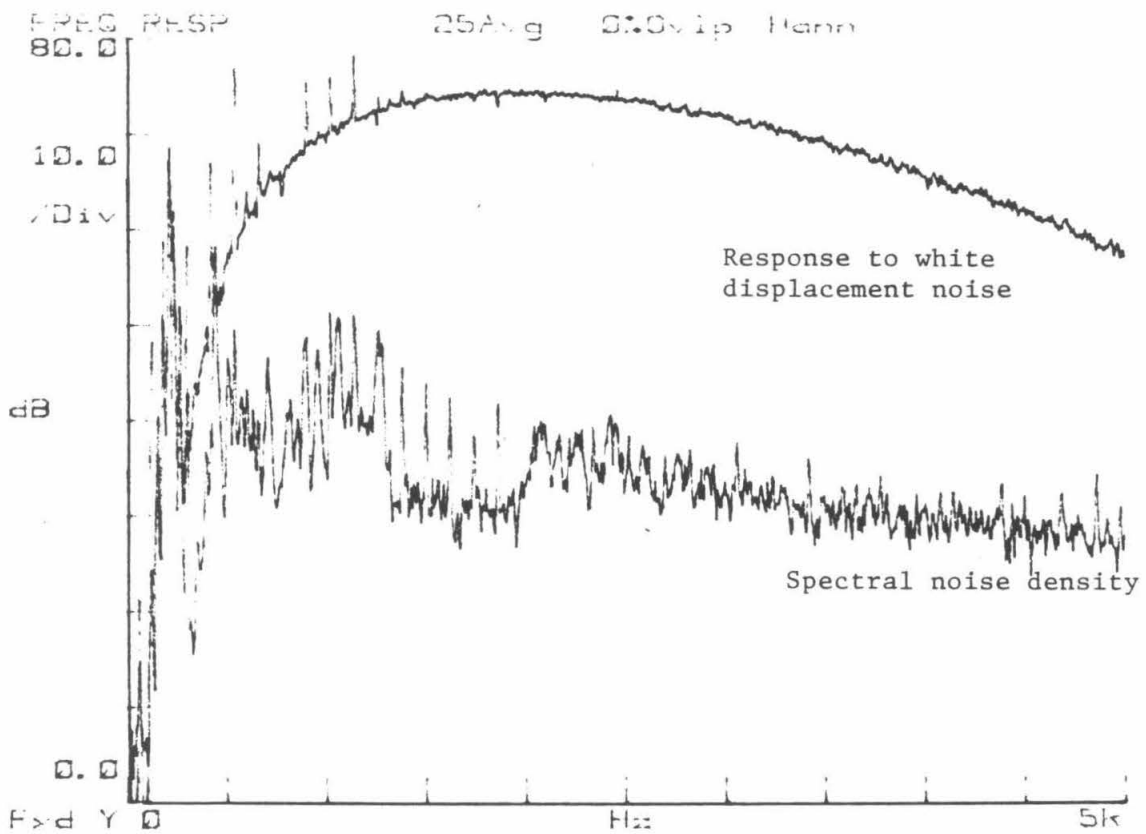

Figure 5.2: The noise spectrum and frequency response of the Caltech detector.

detector's response as a function of frequency. This is primarily due to filters designed to keep the signal within the dynamic range of our analog to digital converter(ADC). The data collected from the detector also contain spans where a cavity fell out of resonance—so that the signal has no correlation with the strain, but is merely representative of a servo trying to acquire lock.

5.2.1 The Coincidence Run

In February and March of 1987, the Caltech detector was run in coincidence with both the Glasgow and MIT detectors. On Feb 23, 1987, a supernova occurred in the large magellanic cloud. This seemed to be an excellent time to collect data. Although the chances of detecting any radiation relating to the supernova were remote, this time was as good as any other to collect data, and there was a slim chance that something unexpected might occur. Examples of the unexpected include gravity waves not traveling at the speed of light, so that the radiation from the supernova would arrive after its optical discovery, the supernova triggering another cataclysmic event, or the supernova leading to a highly non-spherical rapidly rotating pulsar whose rotational energy would be emitted as gravitational radiation. We convinced our colleagues at MIT and Glasgow that it was worthwhile to collect data at this time, not so much because of the supernova, but for the experience we would gain through a coordinated run that could not be gained in any other manner. All three groups struggled to get on the air as quickly as possible, the Caltech group collected its first data two days after the discovery of the supernova. The data acquisition software was written by A. Bostick during those two days; it is presented in Appendix B. Table C.2 shows when the various detectors were "live." I carefully analyzed

the data collected on the evening of March 8 at which time both the Caltech and Glasgow detectors were operating. The exact times the data analyzed were collected is shown in Table C.1.

5.2.2 Data Collection

In order to distinguish between "good" data, data which are reasonably quiet, and "bad" data, those which were collected while a cavity wasn't resonating or was unusually noisy for some other reason, information other than just the gravity wave signal was recorded. Nine signals in all were recorded, five of these on tape, and eight on a chart recorder, (there was some redundancy). The five signals recorded on tape were:

1. The gravity wave signal.
2. The low frequency feedback to the first arm servo.
3. The WWV signal.
4. A seismometer and microphone signal, added together.
5. The light power of the back-reflected light from the second cavity.

For simplicity all five signals which were recorded on tape were sampled at the same frequency, 10kHz. This is not a very efficient method of recording data, but unfortunately the data acquisition software was written in a hurry. Data were recorded on tape in blocks of 10240 points, 2048 from each channel; there were 2100 blocks per tape, so each tape spans 7 minutes, 10 seconds. It took approximately 3 minutes to change tapes, and since there was only one tape

Signals to the ADC

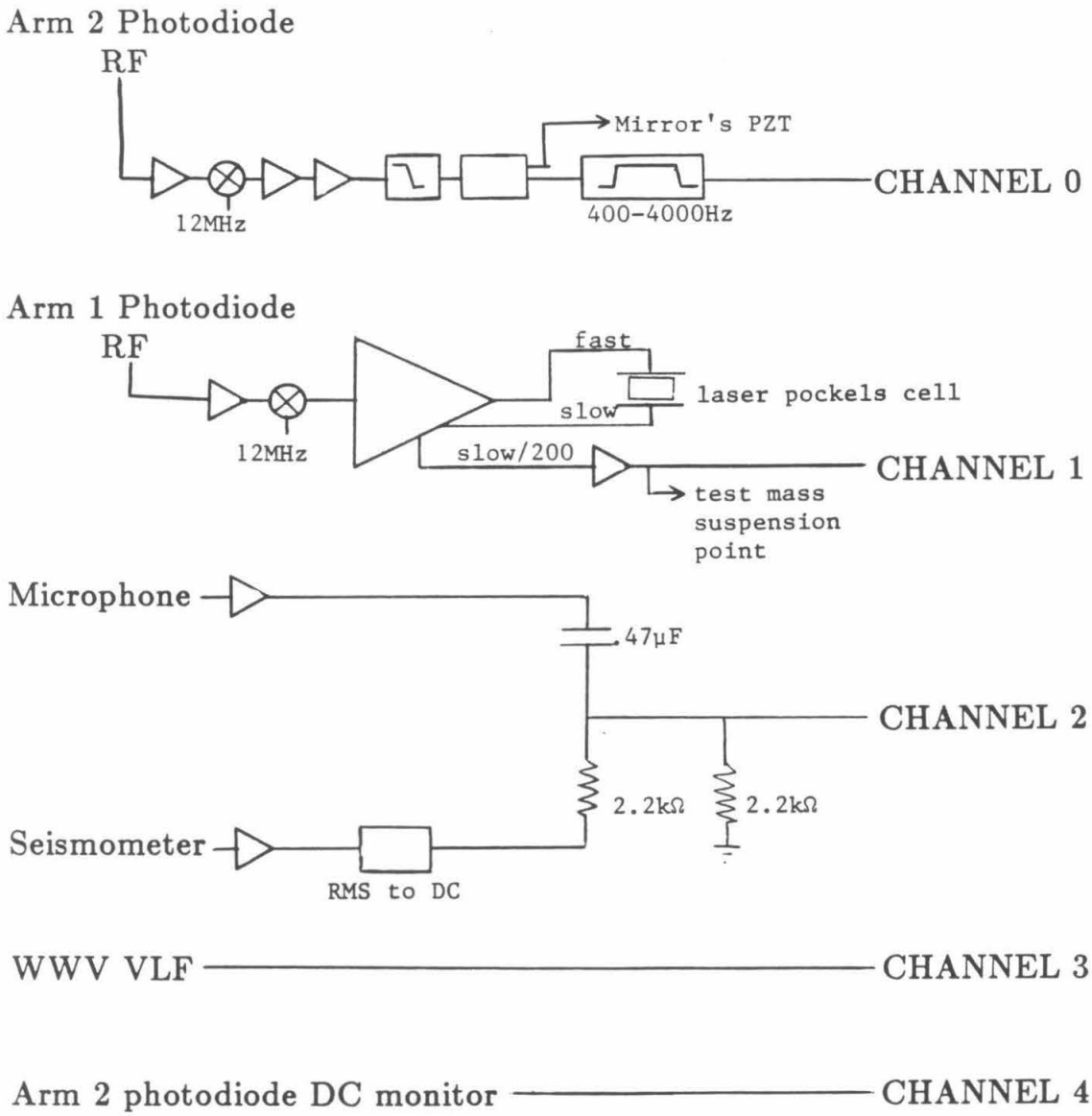

Figure 5.3: The signals recorded on tape.

drive, this cut down the "live" time significantly. The precise arrangement of the signals recorded on tape is shown in Figure 5.3.

In addition to the signals recorded on tape, signals were also recorded on a chart recorder. The chart recorder set up is shown in Figure 5.4. This record was used to track down what was limiting the detector's stability, but it was not used in the final analysis, because the timing resolution on the chart was so poor.

As mentioned earlier (in Section 3.1.1) the gravity wave signal is the feedback signal to the second arm followed by a few filters to keep it within range of our ADC, without introducing digitization error. There is also a 4kHz low pass filter to prevent aliasing.

The WWV signal was recorded so that we could recover timing information if necessary, and to be sure no blocks of data were "lost." The other three signals were recorded to help distinguish between "good" and "bad" data. "Good" data are data which are recorded when the detector's output is related to the strain of space-time, and not to a servo trying to acquire lock, or to the acoustic noise in the lab. It is important to "veto" data collected when the detector is not resonating, or is unusually noisy. It is even more important not to veto data because the gravity wave signal is high; if one were to do that then any real gravity waves would be vetoed, and the data would be called "bad" because gravity waves were present. The method used in this search, to determine which data should be vetoed and which should be called "good," is described in Section 5.2.3. A program was written to examine the tapes and, using the information stored on the auxiliary channels, create a table of what data are "good" and should be searched for gravity waves. This table contains the block and sample number of where the data analysis should begin and end for each stretch of "good" data.

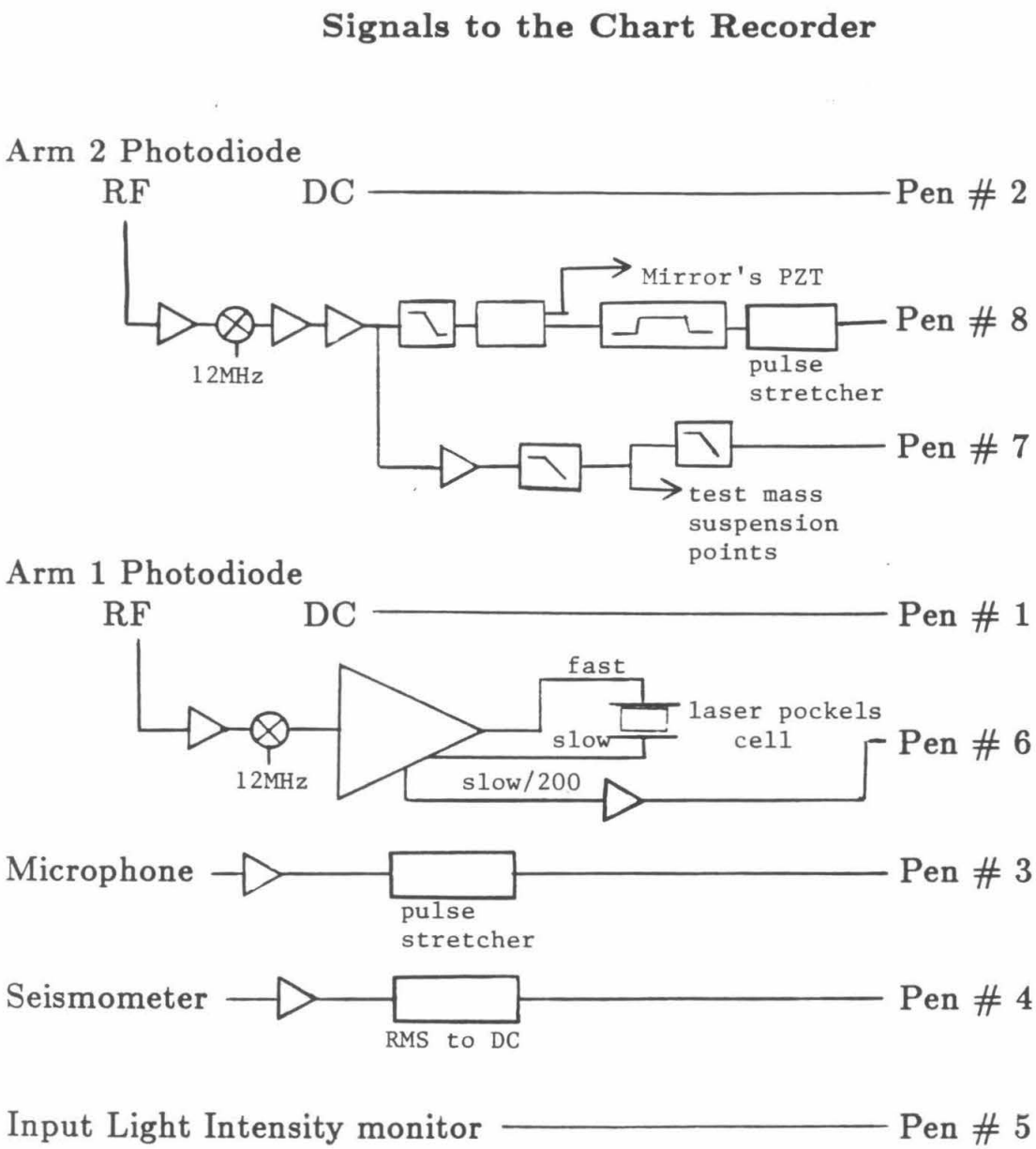

Figure 5.4: The signals recorded on the chart recorder.

5.2.3 Vetos

Four signals were looked at to determine whether or not the data were contaminated by spurious effects. The most important of these was the light level of the second arm. If the second cavity stops resonating, then the light is no longer held on a dark fringe and the light level jumps to a higher value, therefore this light level is a good way to know when "the gravity wave signal" is related to the strain. Of course if the first arm stops resonating then the signal would be equally bad, however if this arm loses resonance then the second arm will also immediately stop resonating. This is because the light from the laser becomes much noisier, (since it is no longer servoed to the the first arm) and this invariably causes the second arm to lose lock, because its servo cannot cope with the higher noise level. The cutoff was chosen by sampling at 40Hz the light level recorded on tape, and examining a histogram of the output. This histogram should have two clear peaks in it; the broadening of the peaks is caused by fluctuations in the laser power and the cavity alignment, (see Figure 5.5). The threshold was chosen to be in the valley between the two peaks. The data were rejected not only on the basis of the DC level of the light, but also if the light level changed too rapidly. This could be caused by the laser's power changing suddenly, or by bad modes in the detector, (as mentioned in Chapter 3, the mirrors were slightly deformed at the time of this run, and this sometimes led to strange modes resonating in the detector). Either effect could cause the output level of the detector to be anomalously noisy. Figure 5.6 shows the DC light level as a function of time. The data collected at this time would be rejected on two counts: first, the light level is too high after .5 seconds, indicating that the second cavity is not resonating; second, the light level changes too quickly at $t = .23$ seconds.

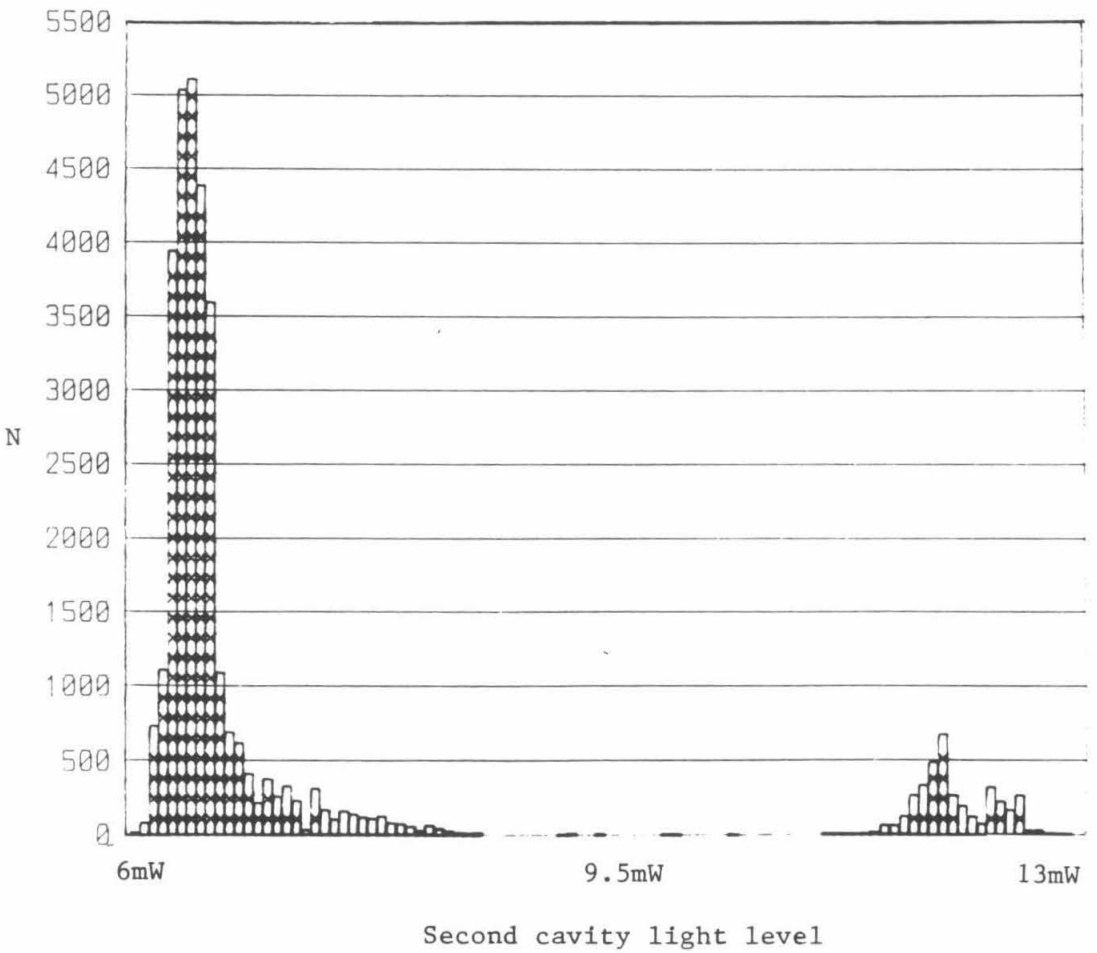

Figure 5.5: A histogram of the power of the light back-reflected from the second cavity. The points near P=12mW correspond to the cavity not resonating, those on the right, near P=6.3mW, correspond to the cavity resonating with $\approx$ 47% contrast. The DC threshold for this tape was P=9.5mW. The broadening of the two peaks is caused by fluctuations in the cavity's contrast and the power of the input light.

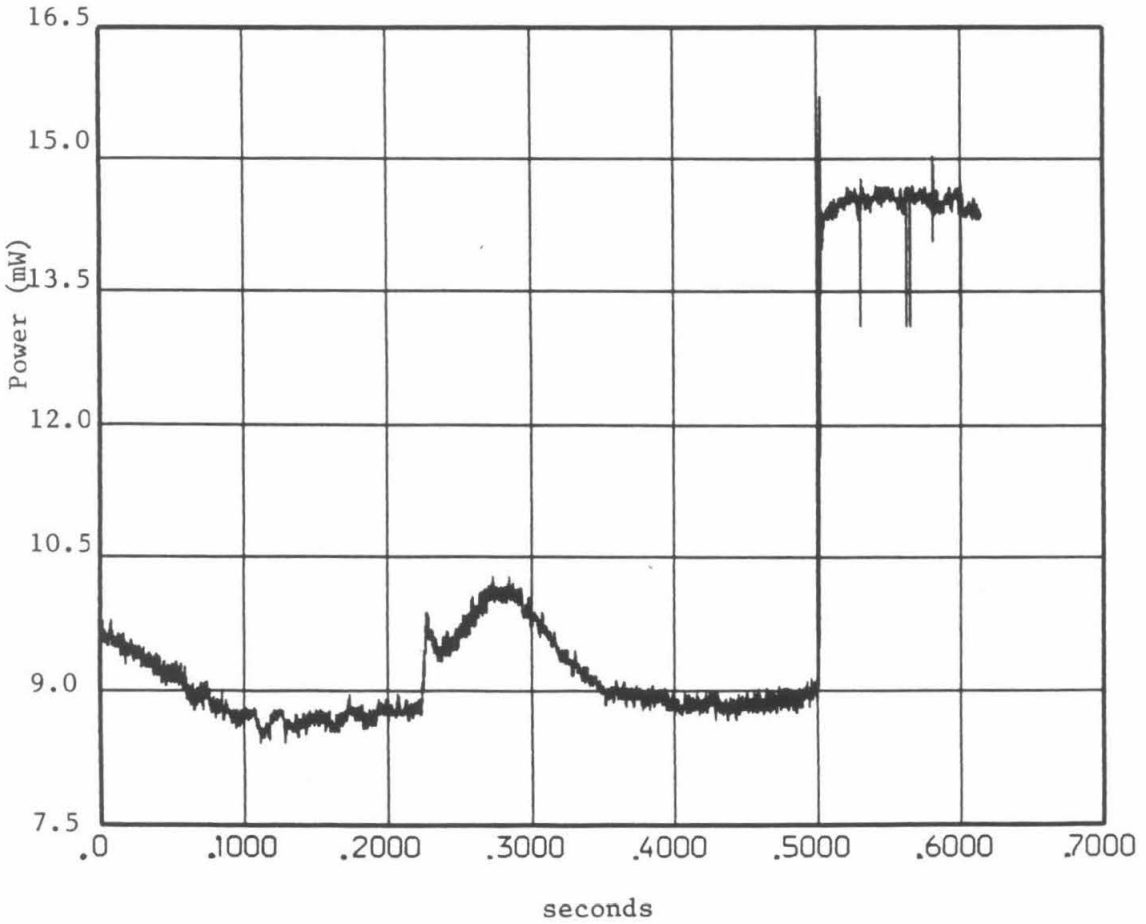

Figure 5.6: The light level as a function of time. The data stored at this time would be rejected for two reasons—after $t = .5$seconds the level is too high, and at $t = .23$seconds the derivative is too large.

Both are correlated with the detector being anomalously noisy. In addition to rejecting the data right when the light level is high, or changing rapidly, the data both 1 second before and .1 second after these events is rejected. The data 1 second before are rejected because usually just prior to the light level going high the second arm servo is near the end of its range, and the gravity wave data will be noisy. The data .1 second after are rejected because it usually takes a short amount of time for the detector to settle down after acquiring lock, or any other disruptive event.

The low frequency feedback signal to the first arm was recorded because we know from experience that as this servo reaches the edge of its dynamic range, the noise in the detector becomes worse. If the signal was within the final 5% of its range then the data taken at that time were rejected.

A seismometer and microphone signal were added together and recorded. The seismometer used was a ranger seismometer, located near the central tank of our vacuum system. This was recorded so that we could distinguish between large ground motion and a gravity wave signal. Excess ground motion did not turn out to be a problem in this data run, so that the seismometer signal was not used to veto any data. The microphone signal was sampled at 10kHz so that we would have information about the acoustic noise at all frequencies of interest. The detector is known to be sensitive to acoustic noise and it is important to be able to distinguish between a gravity wave signal and acoustic noise, which could be due to something as mundane as someone slamming a door. Data collected when there was excess acoustic noise in the lab were vetoed. It was important to sample the microphone at 10kHz so that it could also be used to reject spurious periodic signals. [13]

The fourth signal examined was the gravity wave signal itself, however this

was only looked at for veto purposes to be certain that the analog to digital converter (ADC) was within range. The detector has a resonance at 212Hz. When this was excited, there were times that it caused the gravity wave signal to exceed the range of the ADC. The signals at other frequencies were well within range of the ADC, so that eliminating data because of an overload of the ADC was not going to eliminate potential gravity wave events.

The analysis of these signals is discussed in greater detail in Appendix B.

5.2.4 Whitening the Data

Before conducting a search for any burst source it is useful to "whiten" the data. This is because an optimum filter depends not only on the signal waveform, but also on the noise of the instrument, (see Equation 5.1). If one whitens the data first, then one can use a matched filter, rather than the more complicated optimum filter, (the matched filter must look for the waveform expected from the signal after having gone through the whitening filter rather then the original signal). The optimum filter is more complicated than the matched filter because if one is searching for a signal which lasts only 1msec, and one's instrument has excess noise at 100Hz, then an optimum filter must be .01sec long, rather then .001sec. All the data examined were whitened separately so if these data are later analyzed for sources other then coalescing binaries the whitening step would already have been performed.

The whitening filter used an FFT to perform the filtering. First the data were windowed using a Hamming window,

$$W(n) = .54 - .46\cos\left(\frac{2\pi n}{N}\right) \tag{5.11}$$

then an FFT was performed, the output of this FFT was multiplied by the

filter, and then an inverse FFT was performed. The effects of windowing were compensated for by using an overlap and add method.[37] N points were read from the tape into a buffer, (where N = a power of 2), these were multiplied by the window and then filtered. The first $N/2$ points were then written to disc, the latter $N/2$ points were saved. The latter $N/2$ points of *raw* data were then shifted to the beginning of the buffer and an additional $N/2$ points were read from the tape. The buffer was again windowed and filtered, then the first $N/2$ points were added to the last $N/2$ points from the previous segment of filtered data, this compensated for the shape of the window. If one examines Equation 5.11 carefully one will notice that $W(n) + W(n + N/2) = 1.08$, a constant. So the data at the edges of the window were not attenuated at the output of the filter.

The filter used was a combination high-pass and whitening filter. A high-pass was used because the signal-to-noise ratio at frequencies below 300Hz was much worse then at higher frequencies, (see Figure 5.2). The cutoff chosen was 305Hz to avoid a line spike at 300Hz. The shape of the whitening filter was obtained by averaging many FFTs from the beginning of the data set (340 1024point FFTs were averaged). The filter is shown in Figure 5.7.

The Fourier transform of the output of this filter is shown in Figure 5.8, the data used to make this figure were not the same data which were averaged to make the filter. Notice that frequencies below 305Hz are attenuated by 30dB, and that above this all the data are within 10dB.

Another advantage of whitening the data is that fewer bits of data per sample can be stored without loss of signal-to-noise. If the data are all within 50 dB, then only 8 bits need be stored. We do not currently take advantage of this, but it would be important for a fully operational observatory, where data are being collected at least twelve hours per day. In that case the problem of data storage

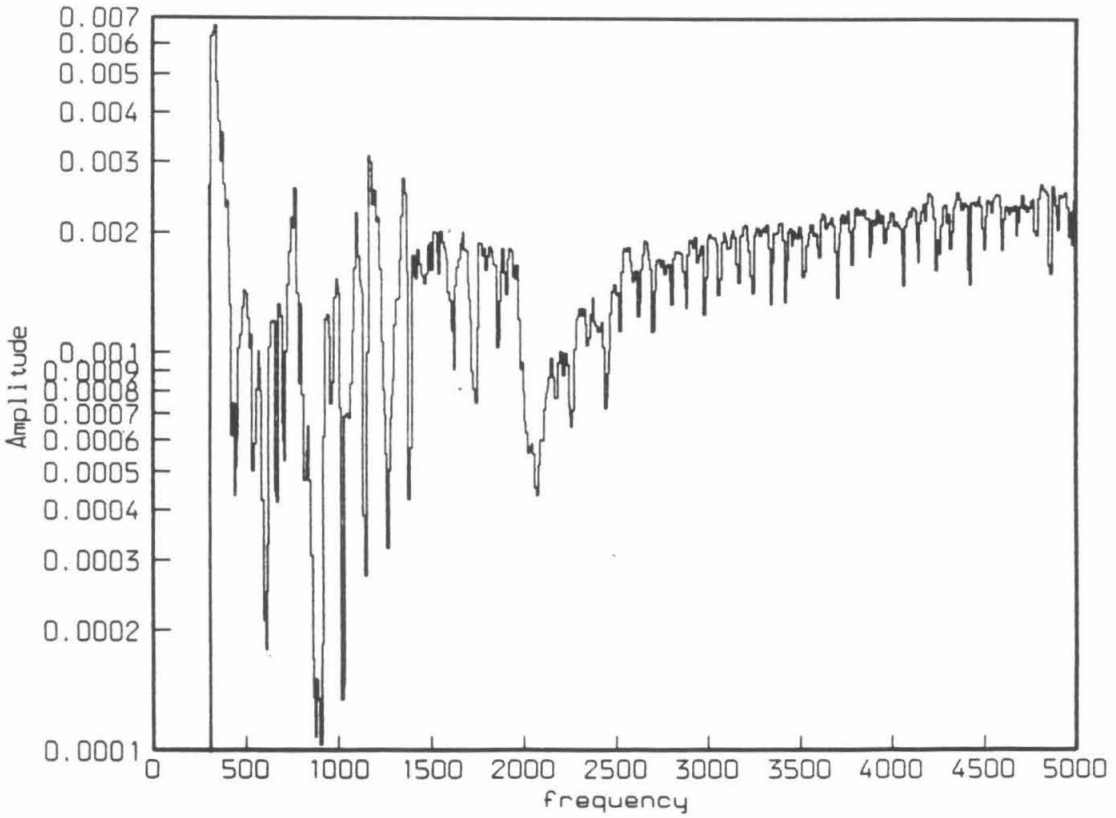

Figure 5.7: The whitening filter.

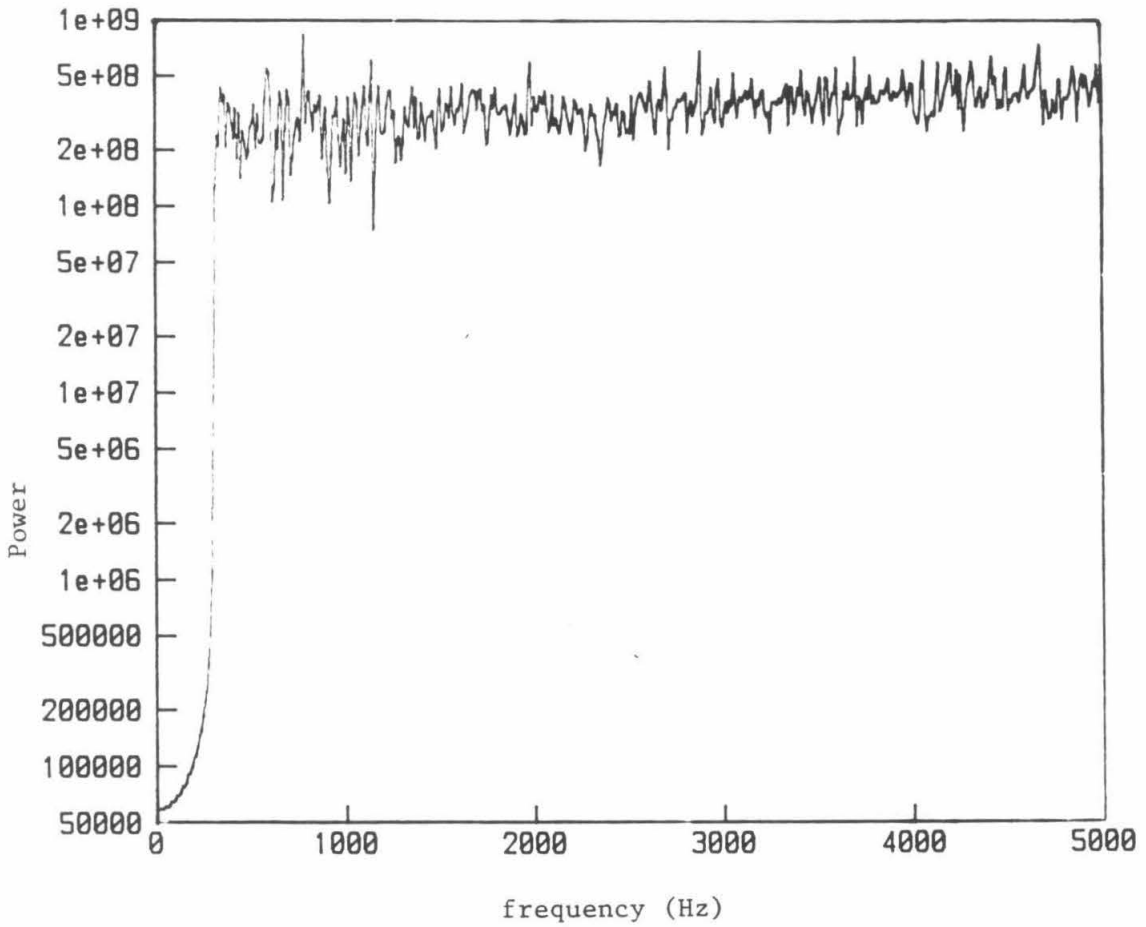

Figure 5.8: Output of the whitening filter.

becomes daunting, and one should use every technique available to improve the efficiency of the data storage.

The whitening filter is included in Appendix B.

5.2.5 Implementing the Binary Star Filter

The computer codes used to analyze these data are all included in Appendix B. This section outlines what each of these programs did.

There are certain parameters in this filter which must be set before applying this filter to data. These include the integration time and the step size in τ. For simplicity I defined τ = 1sec. The integration time chosen was from $\tau - t$ = .11sec (t_0 = .89sec) to $\tau - t$ = .003sec (t_{final} = .997sec). At $\tau - t$ = .11sec the frequency of a binary made of two $1.4M_\odot$ stars would be equal to the minimum frequency that the detector is sensitive to: $f(.89) = f_{min}$ = 305Hz. Tidal disruption of two $1.4M_\odot$ neutron stars is expected .003 sec before coalescence. Heavier stars would have lower frequencies at the beginning of the integration time, but because of the prefilter this should not harm the signal-to-noise ratio too much.

The step size in τ, how often one repeats the filter, was chosen so that the signal-to-noise would not be compromised by more then 15% (30% in power) because of an error in τ. This is discussed more in Section 5.3. If one were willing to accept a loss in the signal-to-noise ratio, then the speed of this algorithm could be improved.

Only the data which were considered "good" were analyzed. This was done by reading in a table which labeled which chunks of data were considered "good," and skipping over those data not included in the table. The program which created this table is in Appendix B, and what criteria it used is discussed in

Section 5.2.3.

During this data run I wished to collect more information than just whether or not the data was over a certain threshold. Whenever the data was over a low threshold, the computer code output both the time of the event and all channels of the FFT which were over the threshold, rather than just the channel which "fit" the data the best (had the highest peak). In addition a histogram of each channel was created and at the end of each tape this too was output. The time it took for this filter to analyze the data was increased because of the time it took to create and output this additional information. If the filter and detector were both fully developed and tested, then the code would not need to output all these extraneous data, and the filter's efficiency would be improved. This code has been altered so that only those points greater than the final threshold used in this search were output, and the time it took to analyze one tape, (tape # 47) improved from 202 minutes to 90 minutes, using the Masscomp computer in both instances. This tape contained seven minutes of data; four minutes were analyzed, the other three minutes had been vetoed.

Because the binary star filter output so much information, the final results were obtained by reducing the output of this program. This was done in two steps, the first (using a program called *readlog.f*, see Appendix B) searched for the largest peak within the calibrated channels in a time equal to twice the filter length (some of the channels of the FFT were not well calibrated, because the signal corresponding to that channel would not cleanly fit within the bandwidth of the detector during the integration time; the calibration is discussed more in Section 5.3). The reason for a "dead-time" around each event is that if a signal at $t = 0$ sets off the filter, then it will also trigger the filter at $t = -\delta t$ and at $t = +\delta t$ (where δt is the length of the filter). Though the output peak will not be

as high at $t = \pm\delta t$, it should not be counted as a separate event.* The program *readlog.f* output the time of each event, the channel of the FFT that the peak occurred in, and the size of the peak in "filter" units. Filter units are simply the numbers output by the binary star filter. The conversion of these to strain units depends on the channel of the FFT (which is equivalent to the value of η), this is discussed in Section 5.3.

A second program then read through these events and output those which had an event size above a certain threshold, given in filter units. The reason that the threshold was set in filter units, rather than in strain, was that for most of the channels the variance of the noise was approximately the same in terms of filter units, but wildly different in terms of strain. Those channels which corresponded to waveforms which have a frequency less then $f_{min} = 305$Hz during part of the filtering time tended to have a lower variance because the noise below f_{min} was suppressed by the prefilter. This program is also included in Appendix B, and is called *thrshevent.f*.

5.3 Calibration

Calibration of this search was done in two steps. First the conversion from strain into "tape" units had to be measured, then, using this, the output of the binary star filter had to be converted to an equivalent strain.

We frequently collected calibration signals on tape, before or after most coincidence runs, we would collect some data with a calibration signal on. This was done by putting a known displacement on one mirror in the detector, and

*For simplicity, the histograms do not have a "dead-time," so events in the histogram are multiply counted; one spike in the data could be counted as many as 22 times.

collecting data in the usual fashion. We recorded both white displacement noise and sine waves. The white noise gives the shape of the detector's response, the sine wave is a cleaner way to measure the absolute amplitude. The transfer function of the detector was also measured using a Hewlett Packard signal analyzer. Fourier transforms of both the data containing white noise and the data containing a 10fm_{rms} 1.53kHz sine wave were taken using the computer. Using the same routine, the FFT of a computer-generated 1.53kHz sine wave was also taken. When the computer-generated sine wave had an rms amplitude of 115 "tape" units, the output peaks of the two FFTs agreed, implying that at 1.53kHz $1\text{fm}=2.5\times10^{-17}\text{strain} = 11.5$"tape" units. The shape of the response was gotten from the transfer function stored on the Hewlett Packard signal analyzer, (file name XFER-142). The amplitude was measured every 100Hz and a spline fit [38] was used to determine the detector response. This agreed within error with the white noise recorded on tape. The spline fit is shown in Figure 5.9.

To calibrate the binary star filter a long file was created with a chirp waveform in the middle,

$$S(t) = 10^{-16}(\text{strain}) \times (1 - t/\tau)^{-1/4} \times d(f(t)) \times \cos\left(2\pi f_0(1 - t/\tau)^{5/8}\right) \quad (5.12)$$

where $d(f)$ was the detector's response at the frequency f, ($d(f)$ converted strain to tape units), and $\tau = 1\text{sec}$. This signal was then put through both the whitening prefilter and the binary star filter. The maximum peak output and the channel of the FFT that it occurred in were recorded. This was done for many values of η, varying from $2.45\times10^{-9}\text{sec}^{5/3}$ (corresponding to two $.15M_\odot$ stars) to $1.1\times10^{-6}\text{sec}^{5/3}$ (corresponding to two $6.M_\odot$ stars). See Table 5.2. Higher and lower values of η led to signals which did not cleanly fall in the detector's frequency range over the integration time chosen. Finally a curve was fit to the

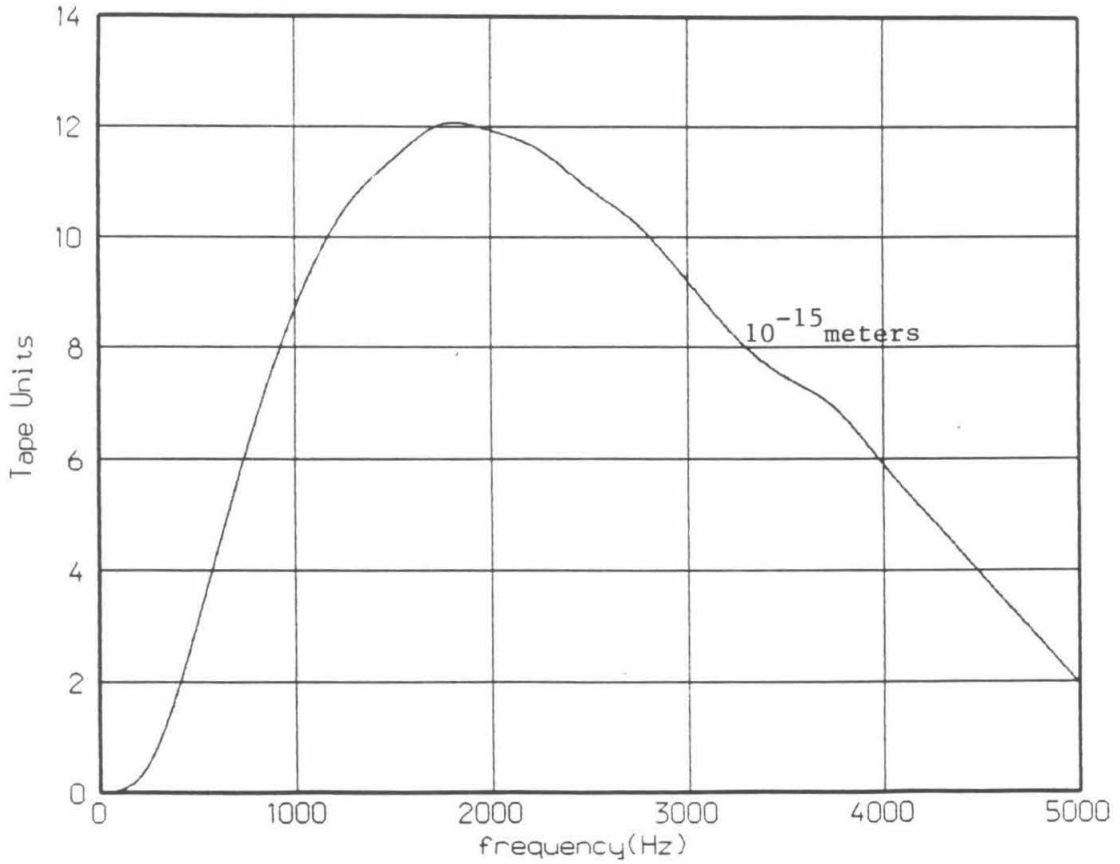

Figure 5.9: The detector's response in "tape" units as a function of frequency. A 1.53kHz sine wave with an amplitude of $h = 2.5 \times 10^{-17}$ would have an amplitude of 11.5 tape units.

η (in $\sec^{\frac{5}{3}}$)	$M_1 = M_2$ (in $M_\odot$)	$f(\tau - t) = .11\text{sec}$ (in Hertz)	Output peak height (in "filter" units)	Channel of FFT
2.45×10^{-9}	.15	1230	6750	195
3.32×10^{-9}	.18	1100	7600	174
3.96×10^{-9}	.2	1030	7150	163
7.79×10^{-9}	.3	800	4250	127
1.26×10^{-8}	.4	668	3900	106
1.82×10^{-8}	.5	582	2100	92
2.47×10^{-8}	.6	519	1600	83
3.20×10^{-8}	.7	471	2000	75
3.99×10^{-8}	.8	433	1500	69
4.86×10^{-8}	.9	403	1000	64
5.79×10^{-8}	1.0	377	870	60
9.55×10^{-8}	1.35	312	820	50
1.01×10^{-7}	1.40	306	845	49
1.08×10^{-7}	1.45	298	750	48
1.84×10^{-7}	2.0	244	280	39
3.62×10^{-7}	3.0	190	130	31
5.84×10^{-7}	4.0	158	75	26
8.47×10^{-7}	5.0	138	38	23
1.15×10^{-6}	6.0	123	50	21
1.48×10^{-6}	7.0	112	23	21
1.85×10^{-6}	8.0	103	16	20
2.69×10^{-6}	10.	89	3.8	21
3.93×10^{-5}	50.	33	.003	20

Table 5.2: Calibration of the filter.

points listed in Table 5.2. This curve is shown in Figure 5.10. The fit is purely empirical. The change in slope at channel 49 is due to the fact that at $t = t_0$, when the filter begins, the channels below 49 correspond to signals whose frequencies are not yet above $f_{min} = 305$Hz, so that any signal corresponding to these channels will be attenuated by the prefilter until the frequency of the signal sweeps above f_{min}.

These files were also used to discover what was an acceptable error in τ. If the error in τ is too large then one risks missing a signal. The dependence of the output peak height versus the error in τ, $\Delta\tau$, is shown in Table 5.3. I decided that an attenuation in the filter output of greater then 30% in power was unacceptable. For this reason the step size $\Delta\tau = .0005$sec $= 5$ samples was chosen. With $\Delta\tau = .5$msec the error in τ can never be greater then .25msec, which implies that no more than 30% of the signal power will ever be "lost."

In converting the signal output from this filter into units of strain, it was assumed that the the error in τ was maximum. The conversion of "filter" units to strain is shown in Figure 5.10.

In the next chapter the results of this data analysis, and the conclusions that one can draw from these results are discussed.

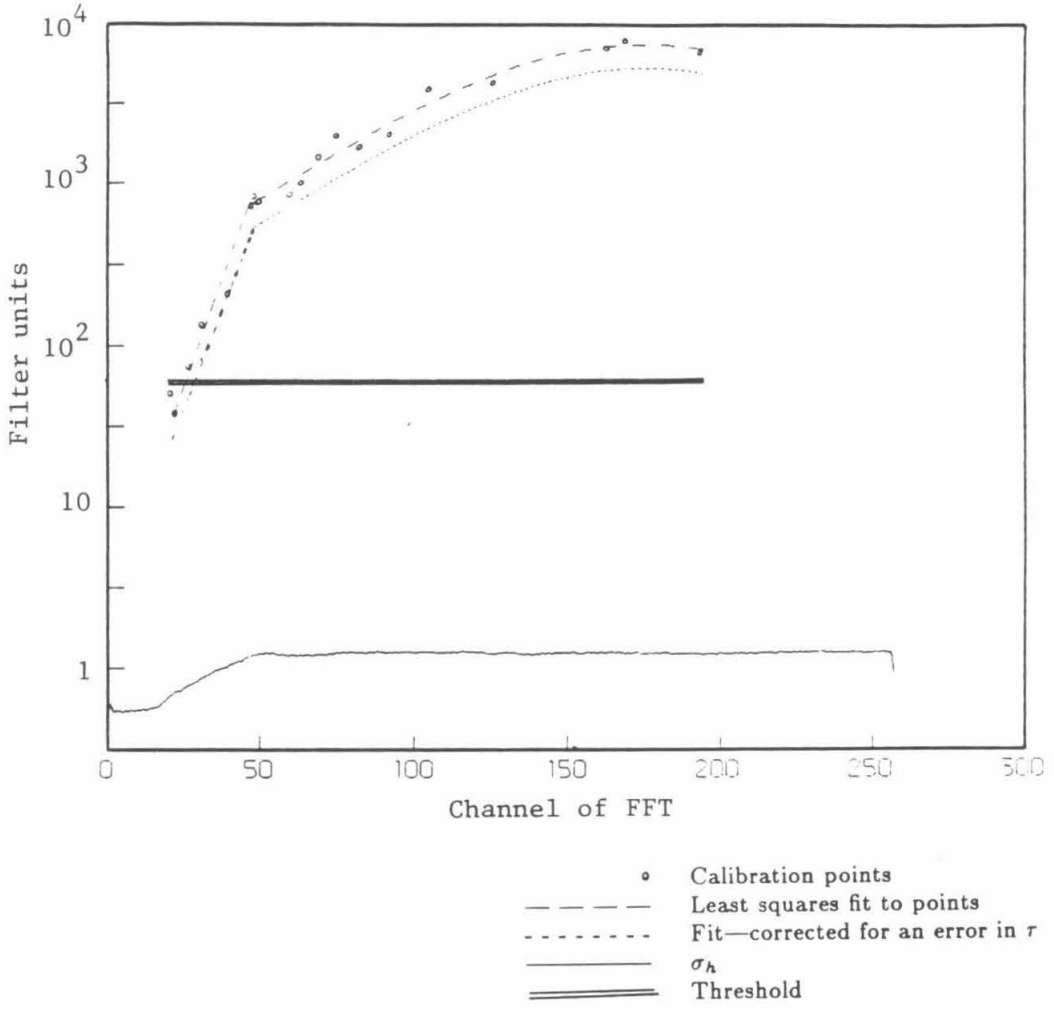

Figure 5.10: The calibration of the binary star filter.

η (in $\sec^{\frac{5}{3}}$)	$\Delta\tau$ (in seconds)	Loss in filter output	
		Power ($\propto h^2$)	Amplitude ($\propto h$)
10^{-7}	+.005	83%	60%
($e.g.\ M_1 = M_2 = 1.4M_\odot$)	+.001	45%	26%
	+.0005	43%	25%
	+.0004	46%	27%
	+.0003	40%	22%
	+.0002	28%	15%
	+.0001	4%	2%
	0	0%	0%
	-.0001	0%	0%
	-.0002	6%	3%
	-.0003	23%	12%
	-.0004	37%	21%
	-.0005	48%	28%
	-.001	55%	33%
4×10^{-9}	+.0005	55%	33%
($e.g.\ M_1 = M_2 = .2M_\odot$)	+.0004	45%	26%
	+.0003	30%	16%
	+.0002	25%	13%
	+.0001	19%	10%
	0	0%	0%
	-.0001	.2%	.1%
	-.0002	13%	7%
	-.0003	49%	29%
	-.0004	59%	36%
	-.0005	54%	32%

Table 5.3: Effect of an error in τ.

Chapter 6

Results and Conclusions

6.1 Results

6.1.1 Events Found by the Filter

All the events over a set threshold were closely examined. The threshold was chosen such that the total number of events was not prohibitively large. The threshold chosen is shown in Figures 5.10 and 6.3. A list of events, the times they occurred, the channel of the filter they appeared in, and the size of the peak in both filter units and σ (the standard deviation of the channel in which the event appeared) is given in Table 6.1.* After locating these events the raw data were examined more closely.

*The conversion of filter units to strain is given in Table 5.2, and Figure 5.10. The output channel is proportional to f_0, the frequency of the signal's waveform one second from coalescence, it is a function of the mass parameter of the binary stars, η.

Tape	Universal Time (dd:hh:mm:ss)	Peak Height filter units ($\propto h^2$)	Peak Height σ ($\propto h$)	Channel of FFT	Comments
44	68:01:00:25.2	67.7	7.3σ	162	bump
	68:01:00:27.2	63.1	7.1σ	151	bump
	68:01:00:36.2	64.6	7.3σ	195	bump
	68:01:00:49.1	61.8	7.0σ	164	
	68:01:00:54.5	62.3	7.1σ	176	bump
	68:01:01:45.4	63.1	7.1σ	181	bump
	68:01:01:51.0	95.2	8.9σ	47	
	68:01:01:51.4	65.1	7.2σ	54	spikes
	68:01:02:11.9	72.0	7.7σ	55	spikes
	68:01:02:43.4	68.5	7.3σ	116	
45	68:01:10:14.9	116.1	10.0σ	46	
	68:01:11:02.6	66.0	7.2σ	108	bump
46	68:01:21:43.9	76.3	7.8σ	74	
	68:01:22:59.1	609.0	22.3σ	195	spikes
47	68:01:30:15.6	65.1	7.2σ	154	
	68:01:32:59.7	84.4	8.3σ	178	spikes & bump
	68:01:35:24.7	73.6	8.0σ	45	
48	68:01:40:50.4	75.9	8.1σ	45	
	68:01:40:52.1	63.1	7.2σ	191	bump
49	68:01:51:17.9	89.8	8.8σ	45	
	68:01:53:29.5	62.8	7.2σ	56	spikes
	68:01:53:32.8	131.7	10.4σ	57	spikes
	68:01:53:33.9	210.4	13.7σ	44	spikes & bump
	68:01:53:46.8	63.8	7.4σ	46	
	68:01:54:08.2	81.8	8.4σ	45	
	68:01:56:32.8	61.5	8.3σ	33	spikes
50	68:02:03:54.0	85.4	8.6σ	45	
	68:02:04:40.6	72.9	7.9σ	46	bump
	68:02:06:22.6	71.6	8.1σ	42	212Hz oscillation
	68:02:08:32.4	65.2	7.4σ	46	
	68:02:08:46.2	62.8	7.1σ	128	spikes

Table 6.1: Events found by the filter.

6.1.2 A Closer Look at the Events

Once the largest events had been located by the binary star filter, the raw gravity wave signal as well as the auxiliary signals were extracted from the tapes. These were examined to see if a correlation between one of the other signals and the gravity wave signal could be found. The first thing that became apparent was that although one might not be able to rule out the possibility that some of the events were caused by gravitational radiation, they certainly were not coalescing binary stars. Nine of the 31 events were not due to a "chirp," as expected from a coalescing binary, but to a few cycles of a very large sine wave. Many of these could have been caused by part of the second cavity servoloop saturating. These events are discussed more in Section 6.1.3.

Many of the events occurred when there were also "bumps" in the DC light level,[†] (see Figure 6.1). These bumps could be due to a fluctuation in the input light level, a fluctuation in the alignment, or because the cavity was falling off the fringe, ($L \neq n\lambda/2$). During these bumps the slope of the DC light level was not great enough for the veto program to catch them. To see if these bumps were truly correlated with the noise another program was written, (*bumps.f*, also in Appendix B). This program did a linear fit of the DC light level, and output the slope when it was greater than a fairly low threshold. The times at which the light level was changing rapidly were then compared with the output of the binary star filter. When the slope of the DC light was greater than 24mW/sec, (.08 tape units/sample) there was a definite correlation; there were 112 bumps in the data analyzed with a slope greater than 24mW/sec, 33 of these bumps

[†]This DC light level is the power of the light back reflected from the second cavity. This is discussed in Chapter 3.

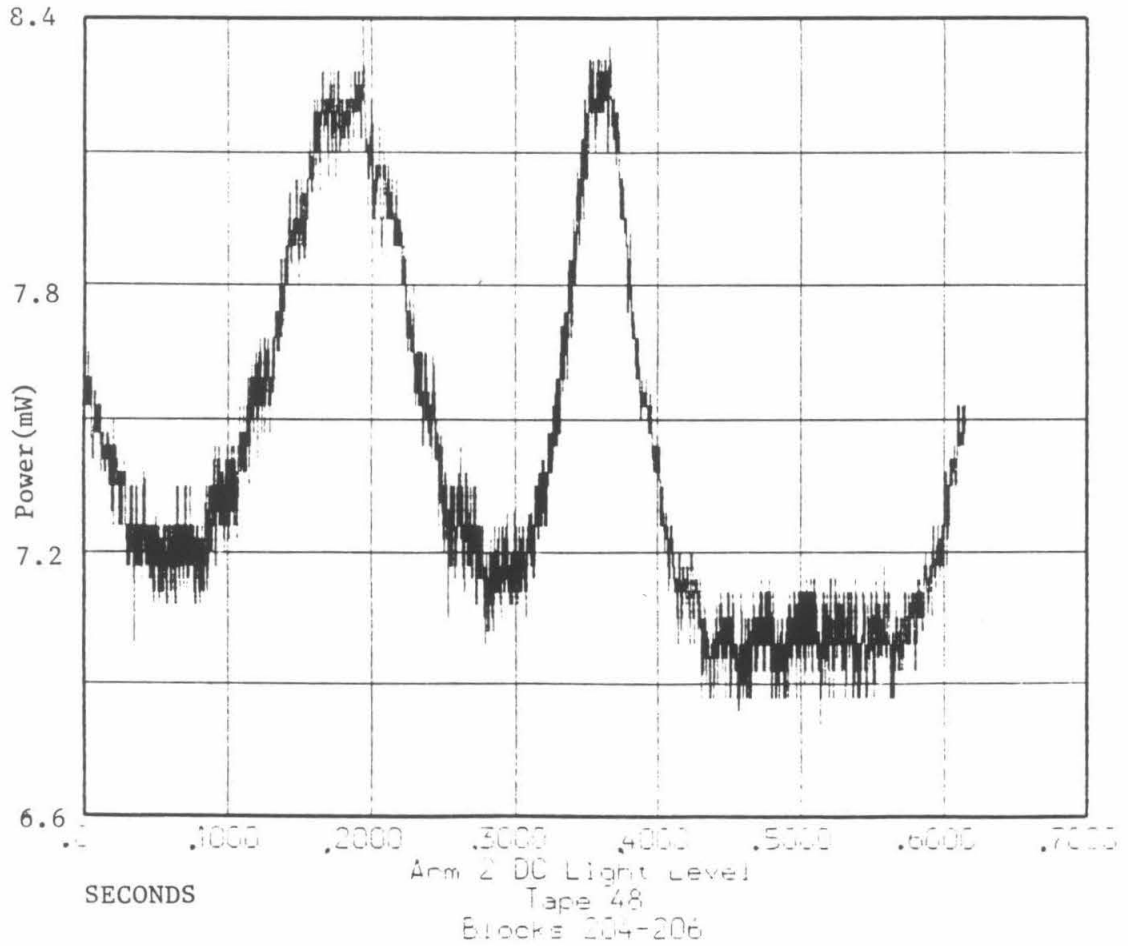

Figure 6.1: "Bumps" in the DC light level.

were coincident with signals in the gravity wave data greater than 50 "filter" units (approximately 6.5σ). Cutting out *all* the data associated with these DC light fluctuations removed approximately 20 seconds of the 36 minutes of data analyzed. This eliminated ten of the largest "events."

6.1.3 The "Spikes" in the Gravity Wave Signal

Those events which resembled short spikes, rather than a coalescing binary, were examined more closely. The raw data for these events are given in Appendix C. Both the chart recorder and tape signal were inspected for correlations with other signals. The results of this examination are presented in Table 6.2. By examining the chart recorder signals, one discovers that many of these events occurred when the second cavity servo was near the end of its dynamic range. Because of the poor timing resolution of the chart recorder, it is impossible to state whether the servo actually reached its limit at the time of these events or not. All the events which occurred when the servo was near the end of its range have the same form, a few cycles of a damped sine wave; this is further evidence that they were caused by the same effect. Four of these occurred when there were also bumps in the DC light level, (though two of these were under the threshold used to eliminate "bad" data). These fluctuations in the light level could have been caused by the light falling off the fringe, which one would expect if the servo were saturated.

Only two of the spikes did not have this characteristic shape. One of these had the same characteristic frequency, but only lasted for one cycle. This resembles the detector's response to a step impulse. The second is more mysterious. This was the largest event found in the data; it was a few cycles of a 5kHz sine wave with fluctuating amplitude. What makes this event so unusual is that

Universal Time (dd:hh:mm:ss)	Auxiliary Signals		Type of Spike
	Chart recorder	Tape	
68:01:01:51.4	2^{nd} cavity servo near limit	—	1
68:01:02:11.9	2^{nd} cavity servo near limit	bump(16mW/sec)	1′
68:01:22:59.1	—	—	3
68:01:32:59.7	—	bump(30mW/sec)	1′
68:01:53:29.5	2^{nd} cavity servo near limit	—	1
68:01:53:32.8	2^{nd} cavity servo near limit	bump(10mW/sec)	1′
68:01:53:33.9	2^{nd} cavity servo near limit	bump(30mW/sec)	1′
68:01:56:32.8	—	—	2
68:02:08:46.2	—	—	1′

Type 1: Three or more cycles of a $\approx$1kHz damped sine wave.

Type 1′: A type 1 spike, with another located within .2sec, if a bump occurred in the DC light level it was between the two spikes.

Type 2: One cycle of a $\approx$1kHz sine wave.

Type 3: Over 10 cycles of a 5kHz sine wave.

Table 6.2: Spikes in the output.

the output of the detector was filtered with a 4kHz 4-pole low pass filter before being recorded on tape. Either this event was seven times larger before the filter, (implying the spikes were 100 times as large as the background noise level), or it was due to some electronic pick-up between the filter and the analog to digital converter.

6.1.4 Distribution of the Output

As stated in Section 5.2.5, not only were the large events output by the filter, but a histogram of the events was output for each channel of the FFT. The histograms from each tape have been added together. A few samples of these histograms are shown in Figure 6.2. From these histograms the variance of each channel can be calculated. The variance of each channel is shown in Figure 5.10, this is in filter units. Figure 6.3 gives σ(Channel) in units of strain.

If the noise were purely gaussian, then the number of events in each bin would fall off exponentially, following the lines shown in Figure 6.2. As in any real detector, the noise in the Caltech prototype has a non-gaussian tail. This is due to sporadic noise sources, such as the bumps in the light level mentioned earlier. As mentioned in Section 5.2.5, one event in the data will appear numerous times in the histograms; all the events above 60 filter units are due to the 31 events listed in Table 6.1. Some events have not been included in the histograms because they exceeded the upper limit of the binning routine; all those omitted were due to one "spike" in the data at universal time=68:01:22:59.1. These histograms include data taken when there were fluctuations in the DC light level, this accounts for some, but not all, of the non-gaussian noise. Unfortunately not all the non-gaussian noise in the detector can be correlated with the auxiliary

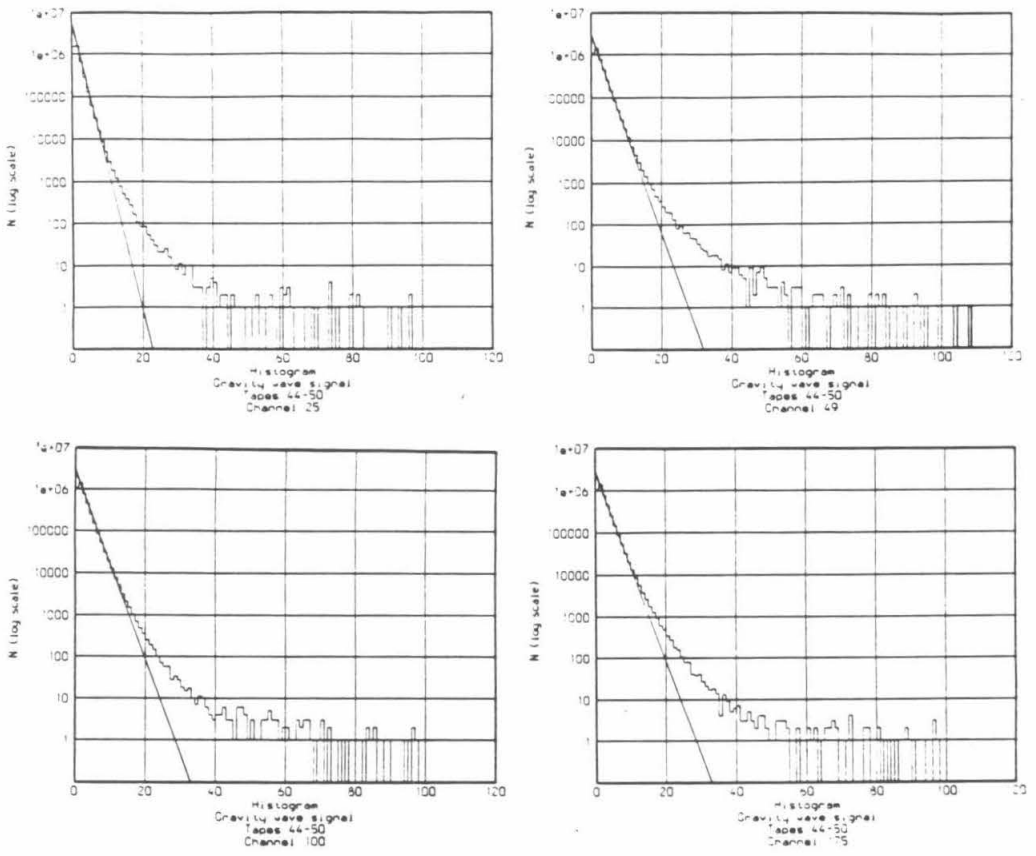

Figure 6.2: Histograms of the output for four of the channels.

signals recorded.

6.2 Conclusions

This section will explore what the results of this data analysis imply, both astrophysically and experimentally.

Table 6.3 shows a list of times at which the detector registered a signal, either due to gravitational waves or due to some spurious non-gaussian noise in the detector. These events cannot be objectively ruled out as possible gravity waves, since they cannot be correlated with a source of noise in the interferometer, such as the noise in the light level. Nor can one state that they definitely were due to gravitational radiation. Two detectors are required to differentiate between noise in one detector and gravity waves, this is because no matter how well designed a detector is, there will always be a non-gaussian tail to its noise distribution. This can be due to things which can be independently detected, such as acoustic noise in the lab, or effects which are difficult to see anywhere but in the detector output, such as a sudden release of internal stress in the test masses themselves.

Although any of the events in Table 6.3 might be due to gravitational radiation, a closer look at some of them shows that they are definitely not due to coalescing compact binaries. As mentioned in Section 6.1.2, some of the events were caused by spikes in the detector output. If the output of the detector contains large enough spikes, they will overlap with almost any filter, and appear significantly large at the output of the filter. Seven of the twenty-one events in Table 6.3 turned out to be due to such spikes, and not to anything in the de-

Tape	Universal Time	Peak Height		Channel	Comments
	(dd:hh:mm:ss)	filter units	h	of FFT	
44	68:01:00:49.1	61.8	1×10^{-17}	164	
	68:01:01:51.0	95.2	4×10^{-17}	47	
	68:01:01:51.4	65.1	3×10^{-17}	54	spikes
	68:01:02:11.9	72.0	3×10^{-17}	55	spikes
	68:01:02:43.4	68.5	2×10^{-17}	116	
45	68:01:10:14.9	116.1	5×10^{-17}	46	
46	68:01:21:43.9	76.3	3×10^{-17}	74	
	68:01:22:59.1	609.0	4×10^{-17}	195	spikes
47	68:01:30:15.6	65.1	1×10^{-17}	154	
	68:01:35:24.7	73.6	5×10^{-17}	45	
48	68:01:40:50.4	75.9	5×10^{-17}	45	
49	68:01:51:17.9	89.8	5×10^{-17}	45	
	68:01:53:29.5	62.8	3×10^{-17}	56	spikes
	68:01:53:32.8	131.7	4×10^{-17}	57	spikes
	68:01:53:46.8	63.8	4×10^{-17}	46	
	68:01:54:08.2	81.8	5×10^{-17}	45	
	68:01:56:32.8	61.5	8×10^{-17}	33	spikes
50	68:02:03:54.0	85.4	5×10^{-17}	45	
	68:02:06:22.6	71.6	5×10^{-17}	42	212Hz oscillation
	68:02:08:32.4	65.2	4×10^{-17}	46	
	68:02:08:46.2	62.8	1×10^{-17}	128	spikes

Table 6.3: Events which could not be vetoed.

tector output resembling a coalescing binary.[‡] For this reason, these events will be neglected in any discussion of the implications one can draw from this search about compact binaries.

6.2.1 Astrophysical Implications

Sensitivity Limits

I feel that the best way to present the limits this search sets is graphically. Figure 6.3 shows the threshold of this search, the events found, and the upper limit one can set, all in terms of strain. It also shows σ, which sets a basic limit on the limits one can set, even if there are two detectors, or one detector whose noise is purely gaussian. If the Caltech detector's noise were strictly gaussian, then you would expect only about one event greater than 25 filter units. This implies that the limit one could set would be roughly half that shown in Figure 6.3.

Figure 6.4 shows the same results presented in Figure 6.3 but the strain has been converted to an equivalent range, assuming that a quarter of the signal has been lost due to the random alignment of the source and detector.

The most optimistic theoretical prediction of event rates, in which one assumes all the missing mass in the galaxy is in the form of black holes, gives an expected event rate of about three events per year at the level of this study.[9,20] A more conservative estimate of the rate of neutron star coalescences has been made by Clark, van den Heuvel, and Sutantyo [19]; they estimate that in order to see three coalescences per year one must have a range of 100Mpc. To achieve this range would require the LIGO, the Caltech prototype will not reach this sensitivity (see Figure 2.2).

[‡]The raw data for these events and all the others listed in Table 6.3 are plotted in Appendix C.

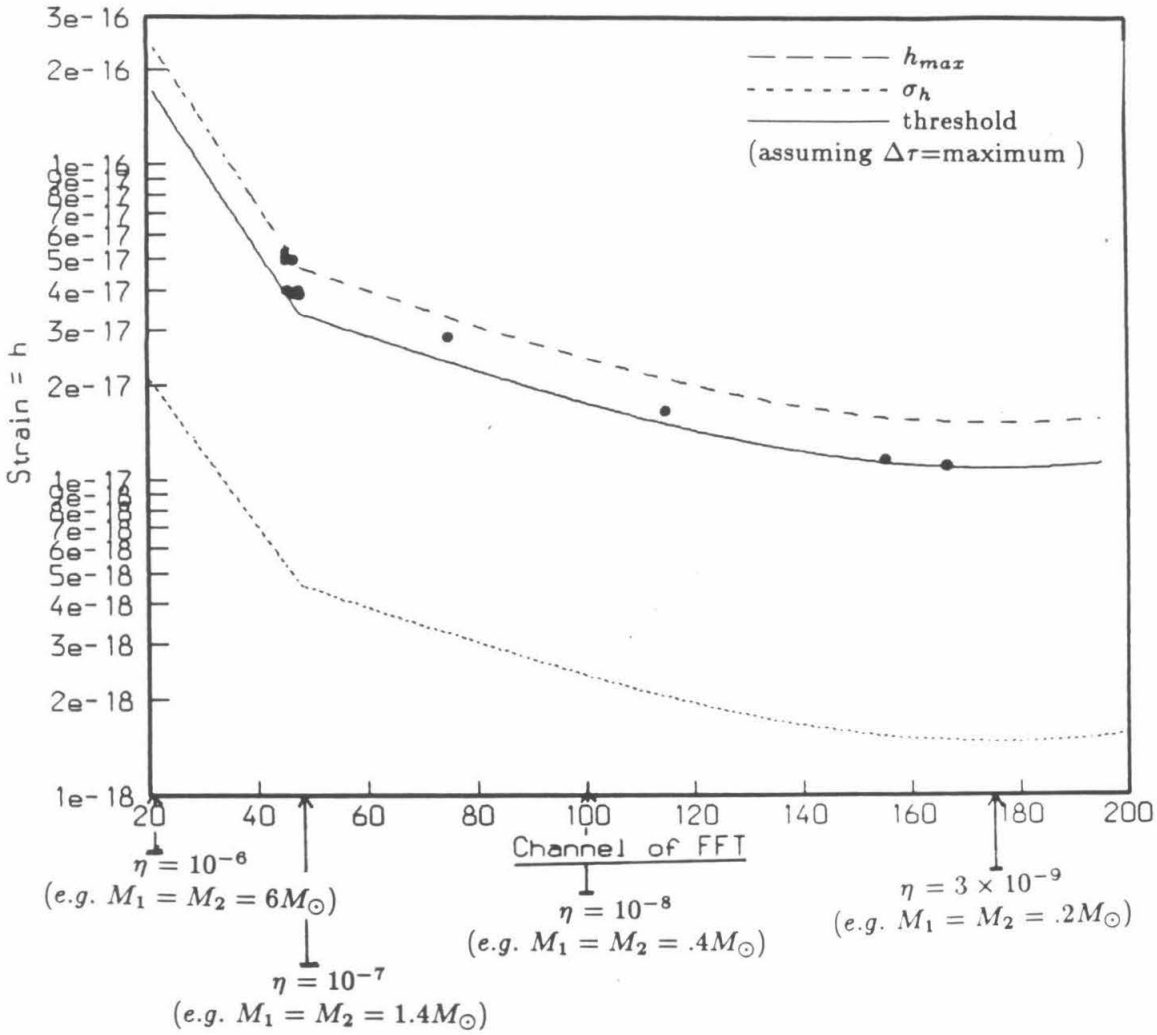

Figure 6.3: "Possible" coalescing binaries, in units of strain.

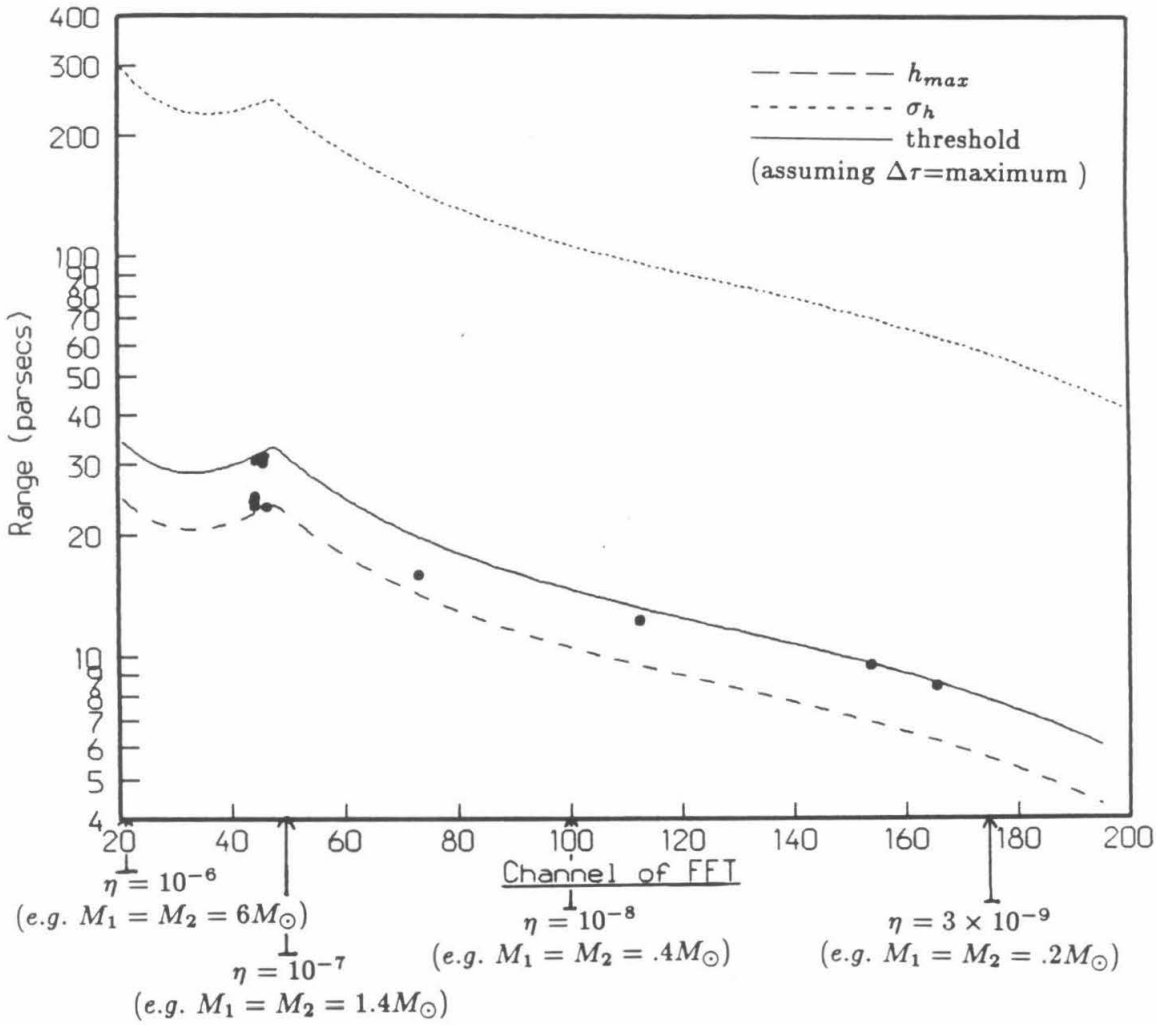

Figure 6.4: "Possible" coalescing binaries, in terms of distance.

Comparison with other Searches

This search represents the first attempt to use a broad band detector to look for coalescing binary stars. Bar detectors are still more sensitive to burst sources than interferometric detectors. They are narrow band and therefore do not carry as much information as a comparably sensitive interferometric detector would. The best limit set to date on coalescing binaries has been set by a coincidence run between cryogenic bar detectors at Stanford, LSU, and Rome.[39] Stanford and Rome ran in coincidence for approximately 35 days. Their search was approximately 100 times more sensitive than the results I've presented. (If they were to set a threshold which yielded one event every 36 minutes, then that threshold would correspond to a binary approximately 100 times further away than the largest event found in the 36 minutes of data from this run.[40]) It is possible that they would be completely insensitive to very light and very heavy binaries because the signal might never enter their frequency band. Light neutron stars would tidally disrupt before reaching the bar's resonant frequency.[18] Heavier black holes may never reach that frequency because the approximations that went into calculating the waveform may no longer be valid in the last millisecond of a black hole coalescence.[15]

6.2.2 Relevance to the Detector Development

Although the likelihood of detecting anything was small, it is important to begin developing techniques for use in the LIGO. This filter improved the detector's sensitivity by a factor of 20 for searches for $1.4M_{\odot}$ neutron stars. Increasing the sensitivity by a factor of 20 increases the expected event rate by a factor of 8000. Since gravity waves are rare, and the output of any detector will probably

be dominated by the detector's noise, rather than gravity waves, it is important that filters be developed to enhance the detector's performance.

This search represents the first time that the Caltech detector was used to search for burst sources.[§] It is important to develop an understanding of what can cause spurious noise in the detector. One result of this search is that we now know that we must strive to cut down on the sensitivity of the detector to acoustic noise. Many of the events in the detector output were correlated with the light level of the second cavity. Some of the excessive noise was probably due to non-gaussian modes in that cavity. Since these data were obtained the mirrors in the cavities have been replaced, so that these modes are no longer present.

The light level of the second cavity could be correlated with spurious events via two other effects. If the cavity was falling off the fringe, then not only would the error signal be noisier then usual, but the fact that it is falling off the fringe indicates that part of the second cavity locking servo is probably saturated. Most of the spikes in the data were probably due to this effect. If the input light was fluctuating, then this can come through directly, or it could indicate that the laser was hopping a mode, which would put excessive frequency noise on the light. (Usually when the laser hops a mode the servoloop loses lock, and both cavities stop resonating.) It is difficult to be certain which of these effects caused any particular fluctuation in the DC light level without more information. If there were more information so that these effects could be distinguished, then it would be possible to set separate thresholds for each, and thereby remove more of the contaminated data without needlessly throwing away data collected when

[§] In 1983, Mark Hereld used this detector to search for periodic radiation from the millisecond pulsar.[6] The data discussed in this thesis have also been analyzed for periodic radiation. This sets the best limit to date on periodic sources of gravitational radiation.[13]

the detector's noise was low.

The "live" time[¶] of this experiment was limited by the dynamic range of the second cavity servo. Since then this has been improved by replacing the PZT transducer on the far test mass with a coil/magnet arrangement. This should also cut down on the noise caused by this servo reaching the end of its dynamic range.

The sensitivity of this detector to coalescing binaries could be improved by improving its low frequency noise. The sensitivity of the detector to coalescing binary stars is proportional to $f_{min}^{2/3}$.

6.3 Suggestions for the Future

In this section I make some suggestions for the future. Some are short term tasks, and others deal with general policy on the development of this detector.

First of all, more time should be spent tracking down the cause of the non-gaussian noise in the detector. This could be done in much the same manner we search for what is limiting the spectral noise density. To discover what is limiting the gaussian noise of the detector we look for correlations between the detector's noise spectrum and possible sources of noise. This is done in many ways. The simplest is to impose excessive noise at a fixed frequency f on whatever is suspected of causing noise in the interferometer, such as the angular motion of a test mass, and see if it affects the detector output by looking at the noise spectrum at f and harmonics of f. By studying histograms of the detector

[¶] The "live" time is the time that the output of the detector was not being contaminated by spurious events, in this experiment this was 36 minutes out of 50 minutes, neglecting the time it took to change tapes.

output in addition to the noise spectrum, correlations between the non-gaussian noise and other events in the lab could be searched for.[‖] (Our Hewlett Packard signal analyzer is capable of creating histograms as well as noise spectrums, so that this suggestion should be trivial to implement.)

I would like to suggest that we strive to reduce one known cause of non-gaussian noise, the detector's acoustic sensitivity. Although acoustic noise can be sensed directly, and events due to this can then be removed, this results in the loss of a great deal of data. Removal of the optical fiber, which is already planned, should help alleviate this problem.

One thing that became clear in trying to understand what was causing the non-gaussian events was that we need more information about what else is happening in the lab. Additional data should be collected, including:

1. The low frequency feedback to the second cavity, to be certain that the servoloop is not near saturation.

2. The intensity of the input light.

3. The DC light level of the first cavity.

4. Additional seismometers located at other positions in the lab.

5. Information about the orientation control servos.

The only signals which need to be sampled at the full detector bandwidth are the detector output itself, and the microphone.

The low frequency feedback signal to the second cavity gives a direct measure of when that servo is near saturation and hence is a much more reliable

[‖]The histogram should be taken of the detector output followed by a narrow band filter, so that the histogram will not be dominated by resonances in the detector.

sensor then the light level of the second cavity. When either cavity's servo is near saturation, the detector's output becomes noisy; it is therefore advisable to minimize the time that this occurs. This could be done by opening the servoloop whenever it gets close to its saturation level. The cavity will stop resonating and the servo will have to reacquire lock; it usually acquires lock in the middle of the servoloop's dynamic range. Although this will cut down on the amount of time the two cavities are resonating, it should maximize the amount of "good" data collected.

By more frequently studying histograms of the detector output, we should develop intuition about what other signals are important, and how to increase the fraction of the collected data which is not contaminated by spurious effects.

Appendix A

Calculation of Noise due to Off-Axis Modes

This appendix presents the contribution to the detector's noise level caused by coupling of light into off-axis modes in more detail than that presented in Section 4.1.2. Excitation of other modes causes "phase noise," which is indistinguishable from a change in length of the cavity. Other modes are excited when the input beam does not spatially match the TEM_{00} mode of the cavity. The TEM_{00} mode can be described by its field distribution at the waist of the cavity:

$$\psi_{00} = A_{inc} U_0(x) U_0(y) \tag{A.1}$$

where:

$$U_0(y) = \sqrt{\frac{2}{\pi y_0^2}}\, e^{-\left(\frac{y}{y_0}\right)^2}. \tag{A.2}$$

The TEM_{01} mode has the form:

$$\psi_{01} = A_{inc} U_0(x) U_1(y) \tag{A.3}$$

where:

$$U_1(y) = \left(\frac{2y}{y_0}\right) U_0(y). \tag{A.4}$$

$U_i(y)$ are Hermite-Gaussian polynomials; these polynomials form an orthonormal set.

First consider a cavity in which only the TEM_{00} mode has been excited. Suppose the incident light has amplitude A_{inc}, and is perfectly aligned with the cavity. Define the leakage field to be the light which has been stored in the cavity, and leaks out the input mirror, [25,41]

$$A_{leak} = A_{reflected} - r_1 A_{inc} \tag{A.5}$$

$$A_{leak} = \left(\frac{\mid t_1 \mid^2 r_2 e^{i\delta}}{1 - r_1 r_2 e^{i\delta}} \right) A_{inc} \tag{A.6}$$

where t_i and r_i are the amplitude transmissivity and reflectivity of the cavity mirrors.

The phase of the leakage field is measured relative to the incident light using a phase modulation technique.[22] The signal:

$$S \propto \mathrm{real}(A_{inc}) \times \mathrm{imag}(A_{leak}) \tag{A.7}$$

$$= |A_{inc}|^2 \left(\frac{r_2 \mid t_1 \mid^2}{1 - 2r_1 r_2 \cos(\delta) + (r_1 r_2)^2} \right) \sin(\delta). \tag{A.8}$$

On resonance $\delta = 4\pi L/\lambda = 2\pi n$, which implies that $S = 0$. If the cavity changes length by a small amount ΔL then

$$\delta = 2\pi n + \frac{4\pi \Delta L}{\lambda}. \tag{A.9}$$

To first order in ΔL :

$$S \propto |A_{inc}|^2 \left(\frac{r_2 \mid t_1 \mid^2}{1 - 2r_1 r_2 + (r_1 r_2)^2} \right) \left(\frac{4\pi \Delta L}{\lambda} \right). \tag{A.10}$$

Now consider the case where A_{inc} does not totally agree with the TEM_{00} mode of the cavity but is "contaminated" with some light which spatially matches the TEM_{01} mode.

$$\psi_{inc} = A_{inc_{00}} U_0(x) U_0(y) + A_{inc_{01}} U_0(x) U_1(y) \tag{A.11}$$

where $A_{inc_{01}} = \epsilon A_{inc_{00}}$, $\epsilon \ll 1$. Let f_0 be the resonant frequency of the TEM_{00} mode, and f_1 be the resonant frequency of the TEM_{01} mode.

$$f_1 = f_0 + \frac{c}{2\pi L}\cos^{-1}\sqrt{1 - L/R} \tag{A.12}$$

$$f_1 = f_0 + \Delta f. \tag{A.13}$$

For the light in the TEM_{00} mode $\delta_0 = 4\pi L/\lambda_0 = 2\pi n$, because this is the mode which is held on resonance. For the light in the TEM_{01} mode $\delta_1 = 4\pi L/\lambda_1$, ($\lambda_n = c/f_n$).

$$\psi_{leak} = A_{leak_{00}} U_0(x)U_0(y) + A_{leak_{01}} U_0(x)U_1(y) \tag{A.14}$$

$$A_{leak_{00}} = \left(\frac{|\, t_1 \,|^2 \, r_2}{1 - r_1 r_2}\right) A_{inc_{00}} \tag{A.15}$$

$$A_{leak_{01}} = \left(\frac{|\, t_1 \,|^2 \, r_2 e^{i\delta_1}}{1 - r_1 r_2 e^{i\delta_1}}\right) \epsilon A_{inc_{00}}. \tag{A.16}$$

The photodiode measures the intensity integrated over the entire spot.

$$I(x,y) = |\psi_{reflected}|^2 = |A_{reflected_{00}} U_0(x)U_0(y) + A_{reflected_{01}} U_0(x)U_1(y)|^2. \tag{A.17}$$

Since $U_0(y)$ and $U_1(y)$ are orthonormal, when one integrates over the entire spot the cross terms drop out and one is left with a signal,

$$P \propto |A_{reflected_{00}}|^2 + |A_{reflected_{01}}|^2. \tag{A.18}$$

So the light in each mode can be treated separately. Demodulating this signal gives one the weighted sum of the phase error for each mode. The phase error for the TEM_{00} mode is essentially zero, since this is the mode held on resonance. The error signal due to the TEM_{01} mode is:

$$S \propto \text{real}(A_{inc_{01}}) \times \text{imag}(A_{leak_{01}}) \tag{A.19}$$

$$= |\epsilon A_{inc_{00}}|^2 \left(\frac{r_2 |\ t_1\ |^2}{1 - 2r_1 r_2 \cos(\delta_1) + (r_1 r_2)^2} \right) \sin(\delta_1). \qquad (A.20)$$

By combining Equations A.10 and A.20 one sees that the misalignment mimics apparent displacement:

$$\Delta L = \epsilon^2 \frac{\lambda}{4\pi} \sin(\delta_1) \left(\frac{1 - 2r_1 r_2 + (r_1 r_2)^2}{1 - 2r_1 r_2 \cos(\delta_1) + (r_1 r_2)^2} \right) \qquad (A.21)$$

where $\delta_1 = 2\cos^{-1}(\sqrt{1 - L/R})$.

To calculate how large ΔL is, one must first calculate ϵ. This calculation has been done before, [32,35]; it is presented here for completeness. Suppose that the input beam is misaligned along one dimension. If it is at a small angle, α, to the axis of the TEM_{00} mode and is displaced by a small amount, a, at the waist, then at the cavity's waist it can be described by:

$$\psi = A_{inc} U_0(x) U_0(y - a) e^{\frac{2\pi i \alpha (y-a)}{\lambda}}. \qquad (A.22)$$

To first order in a and α:

$$\psi = A_{inc} U_0(x) \left[U_0(y) + \left(\frac{a}{y_0} + \frac{\pi i \alpha y_0}{\lambda} \right) U_1(y) \right]. \qquad (A.23)$$

This polynomial describes the spatial field distribution of the TEM_{01} mode. Clearly:

$$\epsilon = \left(\frac{a}{y_0} + \frac{\pi i \alpha y_0}{\lambda} \right). \qquad (A.24)$$

Appendix B

The Computer Codes

B.1 The Data Acquisition Software

This program sampled five channels of the 12 bit analog to digital converter of a Masscomp 500 computer. Each channel was sampled at 10kHz. The data was written to tape in blocks of 10240 points, each point a 2 byte integer. The data was written sequentially; every fifth point would be from a particular channel of the ADC. This program was written by A. Bostick, and is entitled *gravwave.c*.

```
#include <mr.h>
#include <stdio.h>
#include <fcntl.h>
#define NULL 0
#define SAMPLES 10240
#define NUMBUFS 20
#define SHORTS 3

main()
{
        int exwrit, adpn, clkpn, fd, fchan, nchans, incr, gain, i;
        int bufindex;
        short buffer[SAMPLES*NUMBUFS];

        adpn = clkpn = -1;
        exwrit = 0;
        printf("Opening the A/D converter\n");
        mropen(&adpn, "/dev/dacp0/adf0", exwrit);
        printf("Opening the tape drive\n");
        fd = open("/dev/r1600mt0", O_WRONLY);
        printf("Establishing the multiple buffer for the transfer\n");
        mrbufall(adpn, buffer, NUMBUFS, (SAMPLES*2));
        fchan = 0;
        nchans = 5;
        gain = 0;
        incr = 1;
        printf("Establishing A/D channel sampling mode\n");
        mradinc(adpn, fchan, nchans, incr, gain);
        printf("Starting the transfer\n");
        mrxinq(adpn, SAMPLES, NULL, NULL);

        for (i=0; i<2099; i++)
        {
                mrbufwt(adpn, 20000);
                mrbufget(adpn, SHORTS, &bufindex);
                write(fd, &buffer[bufindex], (SAMPLES*2));
                mrbufrel(adpn, &buffer[bufindex]);
        }

        mrbufwt(adpn, 20000);
        mrbufget(adpn, SHORTS, &bufindex);
        write(fd, &buffer[bufindex], SAMPLES);
        printf("Closing the devices\n");
        mrclosall();
        close(fd);
}
```

B.2 The Tape Scanning Program

The first step in analyzing a tape is to choose the proper limits for the veto program. This is done with the aid of the program *limits.f*, which reads in the tape and outputs DC light signal from the second cavity, and the low frequency feedback signal from the first cavity. The tape is read using *C* subroutines in the file *tapesubs.c*.

By plotting a histogram of the DC light level, one can find the appropriate cut off between when the cavity was resonating and when it was not. On a few tapes, which were not analyzed, the cut off is not clear. This could be because the cavity would occasionally resonate in the wrong mode, or because the input light level was fluctuating too much. When the cavity is resonating in the TEM_{00} mode, the contrast is usually fairly good, (the DC light level is low); when resonating in the wrong mode, the contrast is poor and the noise in the detector is high. Since the input light level tends to fluctuate, it is difficult to set a limit which clearly differentiates between the TEM_{00} and TEM_{01} modes.

The low frequency feedback signal from the first cavity was recorded so that one could detect when that servo was near saturation. By finding the highest and lowest points in this signal, one can determine where saturation will take place. It is not necessary to find the highest and lowest points on each tape—one merely needs to find the overall high and low points. One can then set a threshold so that all data collected within the final 5% of this servo's dynamic range is rejected.

This program takes approximately eleven minutes to analyze one seven minute tape.

```
c          limits.f
c this program creates files of samples from
c channels 1 and 4 (hv and arm 2 dc light)
c to compile type "f77 limits.f tapesubs.c"
         parameter (IBLKSZ=10240)
c IBLKSZ=total number of data points in 1 block,
c there are IBLKSZ/5 gw points in a block
c (assuming there are 5 channels of data recorded)
c INC-1=points per channel to be skipped,
c INC=1 implies you sample every point in a channel
c NBLKS=number of blocks on tape minus one
c
         integer*2 buffer(0:IBLKSZ-1)
         integer j,fd,CHA,CHB
         common/buf/buffer
         common/lblk/LBLK
         common/fd/filedescript
c open tape
         call copen$
         open(11,file="CH1smple.dat")
         open(12,file="CH4smple.dat")
         INC=128
         NBLKS=2099
         CHA=1
         CHB=4
         INC2=5*INC
c CHA &CHB=the two channels you want sampled
c INC2=number of channels times INC
         LBLK=-1
c begin reading blocks of data from tape
c LBLK=number of block last read(starting with zero)
    5              call cblock$
                   do 10 j=CHA,IBLKSZ,INC2
   10              write(11,*) buffer(j)
                   do 20 j=CHB,IBLKSZ,INC2
   20              write(12,*) buffer(j)
         if(LBLK.lt.NBLKS) goto 5
         call cclose$
         close(11)
         close(12)
         end
```

```
/*                  tapesubs.c                          */
/* These routines open the tape drive,                  */
/* read the data, and increase LBLK by one,             */
/* and close the tape drive.                            */
#include <stdio.h>
#include <fcntl.h>
#define IBLKSZ 10240
#define IFILT 2048
copen()
{
        extern int fd_;
        fd_ = open("/dev/r1600mt0", O_RDONLY);
        return;
}
cblock()
{
        extern int fd_;
        extern int lblk_;
        extern short buf_[IBLKSZ];
        read(fd_, buf_, 2*IBLKSZ);
        lblk_=lblk_++;
        return(lblk_);
}
cclose()
{
        extern int fd_;
        close(fd_);
        return;
}
```

B.3 The Prefilter and Veto Routines

In order to minimize the number of times each tape must be read, one program, *pre-table.f*, both creates the table of where the data are "good" and whitens the data. A sample table for one of the tapes follows this program. This program takes fifty minutes to analyze one seven minute tape.

The whitening filter is discussed in Section 5.2.4. The program *pre-table.f* uses the Masscomp array processor to perform a 16384 point FFT. This is then multiplied by a real filter, so that no phase distortion is introduced. The array processor then does an inverse FFT. A Hamming window is used; this is discussed in Section 5.2.4. In order to avoid any unnecessary digitization error, and to improve the speed of this program, the data are not multiplied by the usual scaling factor (1/16384). The data are converted to 2 byte integers and written to disc. Because the filter removes the excess noise at low frequencies, the numbers are still small enough to be written as 2 byte integers, even though they have essentially been multiplied by 16384.

The veto table is created by the subroutine table. It is fully explained in the program itself and in Section 5.2.3. This routine uses 9 different parameters:

LIMIT4: The threshold on the DC light level, (channel 4 on the tape).

mklimit: The threshold on the microphone.

sllimit,msllimit: The positive and negative thresholds on the change of the DC light level.

LIMIT1low,LIMIT1up: The thresholds on the feedback signal to the first cavity, (channel 1 on the tape).

DLY,NDLY: The delay (both positive and negative) between when all the signals are within the appropriate thresholds and when the data is considered "good." The microphone veto does not use this delay.

minlock: The minimum time the signal must be considered "good" in order to be included in the table.

Most of these parameters are read from the standard input. This routine also checks that the gravity wave signal was not saturating the ADC; it requires that this signal be between ± 2000, (the full range of the ADC is ± 2048).

```
c
c                pre_table.f
c
c  Feb 29, 1988
c
c This program prefilters the data (a high pass and whitening
c filter) and creates a table to locate the "good" data,
c this program calls subroutines found in the file tapesubs.c
c to compile: f77 pre_table.f tapesubs.c -llap -o pre_table
c
c Output is written to
c /usr/sheri/analysis/T.tab, after running this program move T.tab
c to T#.tab where #= the number of the tape."
c
c  LIMIT4 sets limits on arm 2 light level (Ch 4 on tape);
c  LIMIT1 sets limits on arm 1 HV
c  LIMIT4 should be chosen on the basis of a histogram of channel 4 of the
c  tape, the data can be sampled using the program limits.f
c  MINLOCK=minimum number of samples the interferometer has to be resonating
c  for data to be included in table, (MINLOCK=1000 corresponds to .1 sec)
c  DLY=number of points to be skipped after vetos say that the data
c  is "good" before it is really considered to be "good,"
c  (DLY=100 corresponds to .01 sec).
c  NDLY=number of points to be omitted from the end of a string of "good" data.
c  TAPENO=number of the tape being analyzed.
c  mklimit=microphone threshold,
c  islomax=threshold on change in the DC light level.
c coeffs doesn't seem to use elements above 192 for IFFTSZ=16384, or above 48
c for IFFTSZ=512 or 1024, dimension needed seems to be dim=3*(2**(loglen/2-1)).
c This program makes some assumptions about the format of the data and the size
c of the FFTs, where these assumptions are made are labelled with C:ASSUMP
c followed by the assumption being made, and how to change it.
C
C:ASSUMP this program assumes that the input is in the form of 2 byte integers,
C        and that (NBLKS+1)/4 is an integer.
C        Do not change IFFTSZ without also changing the size of coeffs
C
        parameter(IAPFINC=1,IAPCINC=2,IHFINC=4,IHCINC=8)
        parameter(IFFTSZ=16384,IFFThalf=8192,IFFTSZZ=8193,loglen=14)
        parameter(IBLKSZ=10240,IBLKSZg=2048,NBLKS=2099)
        complex sig(IFFTSZ),coeffs(192),fourier(IFFTSZ)
c       complex sig(IFFTSZ),coeffs(IFFTSZ),fourier(IFFTSZ)
        complex filter(IFFTSZ2)
        real raw(IFFTSZ),window(IFFTSZ)
        integer*2 buffer(0:IBLKSZ-1),b4(30),micro(NBLKS)
        integer*2 insig(IFFThalf),ovlpadd(IFFThalf)
        integer i, j, ilock, jlock, LOCKFLAG, filedescript,DLY,NDLY
        integer dev,mklimit
        common/buf/buffer
        common/lblk/LBLK
        common/fd/filedescript
        common/tab1/LOCKFLAG,ilock,jlock,LIMIT1low,LIMIT1up
        common/tab2/LIMIT4,MINLOCK,DLY,NDLY,b4
        common/tab3/dev,mklimit,micro
        common/ARAYS/ sig,filter,coeffs,fourier,raw,window
c       prepare input and output
```

```
      call copen$
      open(9,file="/usr/sheri/analysis/Tnumpre.dat",
     &  form='unformatted',access='direct',recl=IFFTSZ)
      open(10,file="/usr/sheri/analysis/Tnum.tab")
      open(11,file="/usr/sheri/analysis/fftavg.dat")
      rewind(10)
      rewind(11)
c Input limits to determine where the data is "good"
      print*,"enter LIMIT1low,LIMIT1up,LIMIT4,MINLOCK,DLY,NDLY,TAPENO:"
      read*, LIMIT1low,LIMIT1up,LIMIT4,MINLOCK,DLY,NDLY,TAPENO
c Initialize constants for table.
c LOCKFLAG=0 when in lock, 1 when out of lock
      LOCKFLAG=1
      write(10,*)LIMIT1low,LIMIT1up,LIMIT4,MINLOCK,DLY,NDLY,TAPENO
c initialize constants for prefilter
      dt=1./10000.
      df=1./(IFFTSZ*dt)
      irec=1
c irec=record number to be output next.
c LOAD FILTER
c first and last elements of filter must be real!
c read "whitening" into filter(i),this was generated by averaging many FFTs,
c and taking the inverse.
c set minimum frequency for high pass,(in Hz)
      fmin=305
      call white(fmin,df)
      print*,"returned from white"
c Initialize AP and calculate table for FFT(coeffs)
      call bigprep
      print*,"returned from bigprep"
c Calculate window
      call Hamming
      print*,"returned from Hamming"
c begin main loop through data
c read in signal
c           loc=key to location on the tape.
c               loc=0 at the beginning
c               loc=1 in the middle
c               loc=2 at the end
c           irec=record number of next data to be written to disc
c LBLK= # of last block read in, blocks are numbered from zero to NBLKS.
      loc=0
      irec=1
      LBLK=-1
 11   call loadraw(loc)
      if(LBLK.eq.NBLKS) loc=2
c window data
      do 12 i=1,IFFTSZ
      sig(i)=raw(i)*window(i)
 12   continue
c filter data
      call prefiltb
c output filtered data
      if(loc.eq.0) then
c               you're at the beginning of the tape,
c               there is nothing to overlap and add to.
```

```
                do 30 i=1,IFFThalf
                rsig=real(sig(i))
                insig(i)=nint(rsig)
  30            continue
                loc=1
        else
c               you need to output the sum of the first half of
c               sig plus ovlpadd(i)
                do 31 i=1,IFFThalf
                rsig=real(sig(i))
                insig(i)=nint(rsig)+ovlpadd(i)
  31            continue
        endif
c output insig
        write(9,rec=irec) insig
        irec=irec+1
c now store second half of sig in ovlpadd so that it can be
c output the next time around, unless you're
c at the end of the tape then output the second half of sig.
        if(loc.eq.2) then
        do 32 i=IFFThalf+1,IFFTSZ
                rsig=real(sig(i))
                insig(i-IFFThalf)=nint(rsig)
  32            continue
                write(9,rec=irec) insig
        else
                do 33 i=1,IFFThalf
                rsig=real(sig(i+IFFThalf))
                ovlpadd(i)=nint(rsig)
  33            continue
                goto 11
        endif
        call mapfree()
c if data at end of tape was good, print out limits of last
c good chunk of data.
        if (LOCKFLAG.EQ.0) write(10,*)ilock,ilock+5,IBLK,IBLKSZg-1
c mark end of table with ilock=5000
        write(10,*) 5000,0,0,0
c
        close(9)
        close(10)
        close(11)
        call cclose$
        end


        subroutine bigprep
c This routine prepares the array processor.
        parameter(IHPFINC=1,IAPCINC=2,IHFINC=4,IHCINC=8)
        parameter(IFFTSZ=16384,IFFTSZ2=8193,loglen=14)
        parameter(IBLKSZ=10240,IBLKSZg=2048,NBLKS=2099)
        complex sig(IFFTSZ),coeffs(192),fourier(IFFTSZ)
c       complex sig(IFFTSZ),coeffs(IFFTSZ),fourier(IFFTSZ)
        complex filter(IFFTSZ2)
        real raw(IFFTSZ),window(IFFTSZ)
c       integer*4 rbereturn
```

```
      common/ARAYS/ sig,filter,coeffs,fourier,raw,window
      call mapinit(1)
      call mapbigfft(sig,coeffs,fourier,loglen,1,-1)
      call mapwaitrbe()
      return
      end

      subroutine loadraw(index)
c     This routine orchestrates the handling of the raw data.
c     parameter(IAPFINC=1,IAPCINC=2,IHFINC=4,IHCINC=8)
      parameter(IFFTSZ=16384,IFFThalf=8192,IFFTSZ2=8193,loglen=14)
      parameter(IBLKSZ=10240,IBLKSZg=2048,NBLKS=2099)
      complex sig(IFFTSZ),coeffs(192),fourier(IFFTSZ)
c     complex sig(IFFTSZ),coeffs(IFFTSZ),fourier(IFFTSZ)
      complex filter(IFFTSZ2)
      real raw(IFFTSZ),window(IFFTSZ)
      integer*2 buffer(0:IBLKSZ-1),b4(30),micro(NBLKS)
      integer j3,slp
      integer LIMIT4,MINLOCK,DLY,NDLY,dev,mklimit
      integer i, j, ilock, jlock, LOCKFLAG, filedescript
      common/buf/buffer
      common/lblk/LBLK
      common/fd/filedescript
      common/tab1/LOCKFLAG,ilock,jlock,LIMIT1low,LIMIT1up
      common/tab2/LIMIT4,MINLOCK,DLY,NDLY,b4
      common/tab3/dev,mklimit,micro
      common/ARAYS/ sig,filter,coeffs,fourier,raw,window
      mstep=IBLKSZ-151
c
c index=1 implies reading in data from the middle of the tape,
c         data in raw must be shifted from end to beginning and
c         then new data must be read into end.
      ishift=IFFTSZ/2
      if(index.eq.1) then
              numreads=IFFTSZ/(2*IBLKSZg)
              do 10 i=1,ishift
 10           raw(i)=raw(i+ishift)
              do 20 j=1,numreads
c Load b4(this array is used by table, which needs some points
c         from the end of the last block)
              do 15 m=1,30
 15           b4(m)=buffer(mstep+(5*m))
              call cblock$
              call mike
              call table
              i=ishift+((j-1)*IBLKSZg)+1
              do 30 k=0,IBLKSZg-1
              raw(i)=buffer(5*k)
              i=i+1
 30           continue
 20           continue
      endif
c index=0 implies reading in data for the first time, so you don't need to
c         shift any data
      if(index.eq.0) then
              numreads=IFFTSZ/IBLKSZg
```

```
                do 40 j=1,numreads
c Load b4( this array is used by table, which needs some points
c          from the end of the last block)
                if(LBLK.ne.0) then
                    do 35 m=1,30
 35                 b4(m)=buffer(mstep+(5*m))
                endif
                call cblock$
                call mike
                call table
C:ASSUMP cblock$ reads in 102480 points=1 block of data, of these IBLKSZg=2048
C        are the strain signal. Also, raw(i)=buffer(5*k) assumes that the strain
C        data is stored on the tape in channel 0 of 5 channels, 1 point from
C        each channel written to tape at a time.
C
                i=((j-1)*IBLKSZg)+1
                do 50 k=0,IBLKSZg-1
                raw(i)=buffer(5*k)
                i=i+1
 50             continue
 40             continue
        endif
        return
        end

        subroutine white(fmin,df)
c This subroutine creates the filter used in prefiltb.
        parameter(IAPFINC=1,IAPCINC=2,IHFINC=4,IHCINC=8)
        parameter(IFFTSZ=16384,IFFTSZ2=8193,loglen=14)
        parameter(IBLKSZ=10240,IBLKSZg=2048,NBLKS=2099)
        complex sig(IFFTSZ),coeffs(192),fourier(IFFTSZ)
c       complex sig(IFFTSZ),coeffs(IFFTSZ),fourier(IFFTSZ)
        complex filter(IFFTSZ2)
        real raw(IFFTSZ),window(IFFTSZ)
        common/ARAYS/ sig,filter,coeffs,fourier,raw,window
C:ASSUMP
c this subroutine assumes that you are using fftavg.dat for
c information on how to whiten the spectrum. fftavg.dat
c contains the average of 34 power spectrums, taken from
c tape number 7. There are
c 513 points, for a 8193=IFFTSZ2 filter you need to use
c each of these points about 16 times each.
        m=IFFTSZ/1024
        do 10 i=1,512
        read(11,*) fftavg
        filt=sqrt(1/fftavg)
        do 20 j=1,m
        n=m*(i-1)+j
        f=(n-1)*df
        if(f.lt.fmin) then
           filter(n)=cmplx(0.)
        else
           filter(n)=cmplx(filt)
        endif
 20     continue
 10     continue
```

```
      read(11,*) fftavg
      filt=sqrt(1/fftavg)
      filter(IFFTSZ2)=cmplx(filt)
      return
      end


      subroutine prefiltb
c This subroutine performs an FFT, multiplies by a filter
c and then performs an inverse FFT.  It uses the array
c processor.
      parameter(IAPFINC=1,IAPCINC=2,IHFINC=4,IHCINC=8)
      parameter(IFFTSZ=16384,IFFTSZ2=8193,loglen=14)
      parameter(IBLKSZ=10240,IBLKSZg=2048,NBLKS=2099)
      complex sig(IFFTSZ),coeffs(192),fourier(IFFTSZ)
c     complex sig(IFFTSZ),coeffs(IFFTSZ),fourier(IFFTSZ)
      complex filter(IFFTSZ2)
      real raw(IFFTSZ),window(IFFTSZ)
      common/ARAYS/ sig,filter,coeffs,fourier,raw,window
c fft
      call mapbigfft(sig,coeffs,fourier,loglen,1,0)
      call mapwaitrbe()
c multiply by filter
      fourier(1)=filter(1)*fourier(1)
      do 20 i=2,IFFTSZ2
      fourier(i)=filter(i)*fourier(i)
      index=IFFTSZ+2-i
      fltrindx=conjg(filter(i))
      fourier(index)=fltrindx*fourier(index)
   20 continue
c inverse fft
      call mapbigfft(fourier,coeffs,sig,loglen,-1,0)
      call mapwaitrbe()
      return
      end

      subroutine Hamming
c This subroutine will compute a Hamming window.
c
      parameter(IAPFINC=1,IAPCINC=2,IHFINC=4,IHCINC=8)
      parameter(IFFTSZ=16384,IFFTSZ2=8193,loglen=14)
      parameter(IBLKSZ=10240,IBLKSZg=2048,NBLKS=2099)
      complex sig(IFFTSZ),coeffs(192),fourier(IFFTSZ)
c     complex sig(IFFTSZ),coeffs(IFFTSZ),fourier(IFFTSZ)
      complex filter(IFFTSZ2)
      real raw(IFFTSZ),window(IFFTSZ)
      common/ARAYS/ sig,filter,coeffs,fourier,raw,window
      a=2.*3.141592654/IFFTSZ
      Do 10 n=1,IFFTSZ
   10 window(n)=0.54-(0.46*cos((n-1)*a))
      return
      end
c
      subroutine outgood(j)
c This subroutine outputs the table.
      parameter(IBLKSZ=10240,IBLKSZg=2048,NBLKS=2099)
```

```
      integer*2 buffer(0:IBLKSZ-1),b4(30),micro(NBLKS)
      integer j,ilock,jlock,lock,LOCKFLAG,filedescript
      integer DLY, NDLY, minlock,dev,mklimit
      common/buf/buffer
      common/lblk/LBLK
      common/fd/filedescript
      common/tab1/LOCKFLAG,ilock,jlock,LIMIT1low,LIMIT1up
      common/tab2/LIMIT4,MINLOCK,DLY,NDLY,b4
      common/tab3/dev,mklimit,micro
c
      LOCKFLAG=1
      iout=LBLK
      jout=j-5-(5*NDLY)
 31   if(jout.lt.0) then
          iout=iout-1
          jout=jout+IBLKSZ
          goto 31
          endif
      if(iout.lt.0) return
c check microphone veto
      i1=ilock
      do 10 iblk=i1,iout
      if(micro(iblk).eq.-1) then
c lab was too loud
              imkout=iblk-1
              jmkout=10235
      lock=(imkout-ilock)*(IBLKSZ/5)+((jmkout-jlock)/5)
      if (lock.GT.MINLOCK) write(10,*) ilock,jlock/5,imkout,jmkout/5
              ilock=iblk+1
              jlock=0
              endif
 10   continue
      lock=(iout-ilock)*(IBLKSZ/5)+((jout-jlock)/5)
      if (lock.GT.MINLOCK) write(10,*) ilock,jlock/5,iout,jout/5
      return
      end
c
c
      subroutine table
c This subroutine creates the table of where the data is
c "good."
      parameter(IBLKSZ=10240,IBLKSZg=2048,NBLKS=2099)
      integer*2 buffer(0:IBLKSZ-1),b4(30),micro(NBLKS)
      integer j,ilock,jlock,lock,LOCKFLAG,filedescript
      integer DLY, NDLY, minlock,dev,mklimit
      integer slp,sllimit,msllimit
      common/buf/buffer
      common/lblk/LBLK
      common/fd/filedescript
      common/tab1/LOCKFLAG,ilock,jlock,LIMIT1low,LIMIT1up
      common/tab2/LIMIT4,MINLOCK,DLY,NDLY,b4
      common/tab3/dev,mklimit,micro
c
c set slp limit = sllimit
      sllimit=40
      msllimit=-40
```

```
      islpmax=10234
      do 20 j=1,IBLKSZ,5
      jgw=j-1
      j3=j+3
      if (LOCKFLAG.EQ.1) then
c                 data was "bad", check to see if it is now "good":
c                 (gravity wave channel not saturated,
c                  wire pushing not near the rails, and
c                  arm 2 light level low=second arm resonating)
         if (buffer(jgw).LT.2000 .AND. buffer(jgw).GT.-2000 .AND.
     &        buffer(j).GT.LIMIT1low .AND. buffer(j).LT.LIMIT1up .AND.
     &        buffer(j3).LT.LIMIT4) then
c
c           data is within dc limits, check slope.
c
c Calculate slp
      call db>dt(j3,slp)
c
       if(slp.lt.sllimit.and.slp.gt.msllimit) then
c
c data is good
                        ilock=LBLK
                        jlock=j+(5*DLY)
 33                     if(jlock.ge.IBLKSZ) then
                          jlock=jlock-IBLKSZ
                          ilock=ilock+1
                          goto 33
                        endif
                        LOCKFLAG=0
                     endif
         endif
      else
c            LOCKFLAG=0, data was good, make sure it still is:
         if (buffer(jgw).GE.2000 .OR. buffer(jgw).LE.-2000 .OR.
     &        buffer(j).LE.LIMIT1low.OR.buffer(j).GE.LIMIT1up.OR.
     &        buffer(j3).GE.LIMIT4) then
c data is now bad, output limits of good data
c
      call outgood(j)
c
                     else
c the data is within dc limits but it may be bad because slope
c of dc light too big
c
c Calculate slp
      call db>dt(j3,slp)
c if slp is bad call outgood, which will output limits of good data
       if(slp.ge.sllimit.or.slp.le.msllimit) call outgood(j)
                     endif
      endif
   20 continue
      return
      end
c
      subroutine db>dt(j3,slp)
c This routine looks for rapid changes in the DC light by
```

pre_table.f Page 9

```
c comparing the light level at one time with the light
c level .030 seconds earlier.
      parameter(IBLKSZ=10240,IBLKSZg=2048,NBLKS=2099)
      integer*2 buffer(0:IBLKSZ-1),b4(30),micro(NBLKS)
      integer filedescript
      integer j3,slp
      integer LIMIT4,MINLOCK,DLY,NDLY,dev,mklimit
      common/buf/buffer
      common/lblk/LBLK
      common/fd/filedescript
      common/tab2/LIMIT4,MINLOCK,DLY,NDLY,b4
      common/tab3/dev,mklimit,micro
c
      islpmax=10234
c Calculate slp
      if (LBLK.eq.0.AND.j3.le.149) then
         slp=0
         return
      endif
      if(j3.lt.149) then
         k=(j3+1)/5
         slp=buffer(j3)+buffer(j3+5)-b4(k)-b4(k+1)
      endif
      if(j3.eq.149)slp=buffer(j3)+buffer(j3+5)-b4(30)-buffer(4)
      if(j3.gt.149.and.j3.lt.islpmax) slp=buffer(j3)+buffer(j3+5)-
     &                    buffer(j3-150)-buffer(j3-145)
c
      return
      end
c
      subroutine mike
c this is an ac power meter for
c channel 2 of the tape(microphone and seismometer)
c unlike other vetos there is no explicit delay, either
c a block is good, in which case micro(blk)=1, or bad
c in which case micro(blk)=-1.
      parameter(IBLKSZ=10240,IBLKSZg=2048,NBLKS=2099)
      integer*2 buffer(0:IBLKSZ-1),b4(30),micro(NBLKS)
      integer j,ilock,jlock,lock,LOCKFLAG,filedescript
      integer DLY, NDLY, minlock
      integer dev,mklimit,sumx,sumxx,dev
      common/buf/buffer
      common/lblk/LBLK
      common/fd/filedescript
      common/tab1/LOCKFLAG,ilock,jlock,LIMIT1low,LIMIT1up
      common/tab2/LIMIT4,MINLOCK,DLY,NDLY,b4
      common/tab3/dev,mklimit,micro
c
c Navg should be a factor of 2048
      Navg=64
c set threshold
      mklimit=20000
      Nloops=IBLKSZg/Navg
c calculate standard dev over Navg points
c isample is sample number in buffer of that block
c corresponding to the micro & seismo sample I want.
```

pre_table.f Page 10

```
      isample=-3
      do 30 j=1,Nloops
      sumx=0
      sumxx=0
      do 40 k=1,Navg
      isample=isample+5
      sumx=sumx+buffer(isample)
      sumxx=sumxx+ (buffer(isample)*buffer(isample))
 40   continue
      dev=sumxx-((sumx*sumx)/Navg)
      if(dev.gt.mklimit) then
              micro(LBLK)=-1
              return
      endif
c
 30   continue
      micro(LBLK)=1
  1   continue
      return
      end
```

T45.tab:

LIMIT1low	LIMIT1up	LIMIT4	minlock	DLY	NDLY	Tape no.
-210	194	290	1000	1000	10000	45.0000
2	0	79	2047			
81	0	140	1516			
219	535	323	2047			
325	0	438	2047			
440	0	536	2047			
538	0	694	2047			
696	0	888	2047			
890	0	1361	2047			
1363	0	1466	2047			
1468	0	1833	1174			
1839	32	1940	277			
1945	1155	1968	1940			
5000	0	0	0			

FLAG

B.4 The Binary Star Filter

This filter is discussed in Sections 5.1 and 5.2.5. The program which filters the data for coalescing binaries is called *filtFbins.f*. The routines which are most important in doing the actual analysis are *FFTX* and *Xinterval*. Most of the rest of the program deals with manipulating the data so that only "good" data are analyzed. *FFTX* performs the actual FFT, *Xinterval* calculates which data should be used when resampling the data in even steps of χ.

```
c                       filtFbins.f
        parameter (IAPFINC=1,IAPCINC=2,IHFINC=4,IHCINC=8)
        parameter (IDIM=512,LOGLEN=9,IDIM2=257,JDIMt=100000)
        parameter (IBLKSZ=2048,IBLKSZg=2048,NBLKS=2099,numbins=99)
c IBLKSZ= the size of each block on the tape/5
c       = size of each block in the file.
c IBLKSZg= the number of gravity wave samples on
c each block of the tape.
c  NBLKS= the number of the last block=the number of blocks on the tape-1
c numbins=(number of bins output is divided into for output histograms)-1
c (1/scale)=size of each bin. Maximum size that is included in the
c histogram=(numbins+1)/scale.
c The routine FFTX in this program differs from the routine in other
c programs because multiplication by scale takes place
c in this routine, using the AP.
c In my thesis filter units refers to output of FFT times scale.
        real sigX(IDIM)
        real sigt(JDIMt)
        implicit double precision (d,t,X)
        integer nXloc(IDIM)
        integer*2 buffer(0:IBLKSZ-1)
        integer*4 bin(IDIM2,0:numbins)
c buffer has indices running from 0 to IBLKSZ-1
        integer i,fftsrc,coef,ffttmp,absscr,scloff
        integer*4 LBLK,filedescript,dly,ndly
        common/buf/buffer
        common/lblk/LBLK
        common/fd/filedescript
        common/Xint/nXloc
        common/ARAYS/ sigX
        common/OFFSTS/ fftsrc,coef,ffttmp,absscr,scloff
        common/datainput/ sigt
        common/bininfo/bin,scale,IBLKIN,JIN,icount,ithresh
c       prepare input and output files
        open(4,file="/usr/sheri/analysis/Tnumpre.dat",
     &  form="unformatted",access="direct",recl=2*IBLKSZ)
        open(9,file="filbin.dat",form="unformatted",
     &  access="direct",recl=4*IDIM2*(numbins+1))
        open(13,file="/usr/sheri/analysis/Tnum.tab")
        rewind(13)
        read(13,*) limit1low,limit1up,limit4,minlock,dly,ndly,tapeno
        print*, limit1low,limit1up,limit4,minlock,dly,ndly,tapeno
        print*,"idim,loglen,idim2,JDIMt =",IDIM,LOGLEN,IDIM2,JDIMt
c       SET INITIAL VALUES (in sec or Hz)
        tau=1.0
        t0=.89
        tfinal=tau-.003
        scale=5.0E-09
        ithresh=30
        dX=(X(tfinal,tau)-X(t0,tau))/IDIM
        df0=1./(IDIM*dX)
        nsample=10000
        dt0=.0005
        ndt0=dt0*nsample
        print*,"tau,t0,dX,df0,nsample,dt0,scale",tau,t0,dX,
     &  df0,nsample,dt0,scale
```

```
      print*,"i,sigX(i),IBIN,IBLKIN,JIN,icount"
c     PREPARE ARRAY PROCESSOR
      call apprep
c     SET BIN=HISTOGRAMS TO ZERO
      do 13 i=1,IDIM2
      do 12 j=1,numbins
      bin(i,j)=0
 12   continue
 13   continue
c     CALCULATE nXloc=location of dX*n in array sigt(n)
      call Xinterval(t0,tau,nsample,dX,tfinal)
      nfinal=nXloc(IDIM)
      JDmnf=JDIMt-nfinal
c Start reading in data
c LBLK=the number of the last block read in
c (they are numbered from 0 to 2099 (March/1987))
c JLIMIT=the smallest number of consecutive points the filter will analyze.
c subroutine block reads block LBLK+1 from disc and sets LBLK=LBLK+1
c since it reads from the disc and not from tape blocks which contain
c "bad" data need not be read, but can be skipped.
c IBLKIN,JIN,IBLKOUT,JOUT are the block and sample number
c lock was acquired and lost, 0<=IBLK*<NBLKS, 0<=J*<IBLKSZg
c NUMSAMP=# of gw samples in that stretch of data.
c icount=sample # after JIN--used to keep track of where in the input file
c you are.
      LBLK=-1
      JLIMIT=nfinal
 38   read(13,*) IBLKIN,JIN,IBLKOUT,JOUT
      icount=0
      if(IBLKIN.EQ.5000) goto 40
      NUMSAMP=(IBLKOUT-IBLKIN)*IBLKSZg + JOUT-JIN+1
      if (NUMSAMP.LT.JLIMIT) then
c skip these blocks entirely, they don't contain enough data
            goto 38
      endif
      if (NUMSAMP.le.JDIMt) then
            if(LBLK.lt.IBLKIN) then
c block number IBLKIN has not been read yet, so read it.
                  LBLK=IBLKIN-1
                  call block
            endif
            i1=IBLKOUT
            i2=JIN
            i3=JOUT
            i4=1
            i5=NUMSAMP
            call bufsigt(i1,i2,i3,i4,i5)
c bufsigt(i1,i2,i3,i4,i5) loads sigt(n) from n=i4 to n=i5 with the
c current contents of the buffer beginning at sample i2, and
c stops at block i1 with the sample i3,
c (sample i2 and i3 vary from 0 to IBLKSZg-1).
c
c next filter the data in sigt, since this stretch of
c 'good' data fits in sigt, sigt won't have to be shifted.
            jstep=0
            jlast=NUMSAMP-nfinal
```

```
c jlast = last n of sigt(n) which has enough data
c after it to apply the filter.
 43             if (jstep.gt.jlast) goto 38
                do 44 i=1,IDIM
 44             sigX(i)=sigt(nXloc(i)+jstep)
                call FFTX
                call bins
                jstep=jstep+ndt0
                icount=icount+ndt0
                goto 43
        endif
        if (NUMSAMP.gt.JDIMt) then
                if(LBLK.lt.IBLKIN) then
                        LBLK=IBLKIN-1
                        call block
                endif
                i1=LBLK + int((JDIMt+JIN)/IBLKSZg)-1
                i2=JIN
                i3=IBLKSZg-1
                i4=1
                i5=(IBLKSZg*(i1-LBLK)-JIN+IBLKSZg)
                call bufsigt(i1,i2,i3,i4,i5)
 49             jstep=0
                jlast=i5-nfinal
 47             if (jstep.gt.jlast) then
                        if (LBLK.eq.IBLKOUT) goto 38
                        call block
                        call shift(jstep,i5)
c subroutine shift(i1,i2) moves data from sigt(n) n=i1,i2
c to n=1,i2-i1+1.
c Next calculate proper limits for bufsigt
                        i2=0
                        i3=IBLKSZg-1
                        i4=i5-jstep+2
                        i1=LBLK + int((JDIMt-i4)/IBLKSZg)-1
                        if (i1.gt.IBLKOUT)then
                           i1=IBLKOUT
                           i3=JOUT
                        endif
                        i5=(IBLKSZg*(i1-LBLK)+i3+i4)
                        call bufsigt(i1,i2,i3,i4,i5)
                        goto 49
                        endif
                do 48 i=1,IDIM
 48             sigX(i)=sigt(nXloc(i)+jstep)
                call FFTX
                call bins
                jstep=jstep+ndt0
                icount=icount+ndt0
                goto 47
        endif
  40    continue
c OUTPUT BIN
        write(9,rec=1) bin
        print*,"5000 5000. 5000 5000 5000 5000"
        call mapfree()
```

```
        close(4)
        close(9)
        close(13)
        end


        subroutine block
c this routine does what cblock$ does, only it reads from
c file 4 rather then tape.  It reads in one block and increments
c LBLK.
c blocks are numbered from 0 to 2099, so block K is at rec=k+1
        parameter (IBLKSZ=2048,IBLKSZg=2048,NBLKS=2099)
        integer*2 buffer(0:IBLKSZ-1)
        integer*4 LBLK
c buffer has indices running from 0 to IBLKSZ-1
        common/buf/buffer
        common/lblk/LBLK
        LBLK=LBLK+1
        read(4,rec=LBLK+1) buffer
        return
        end

        subroutine apprep
c This routine prepares the array processor for FFTX
        parameter (IAPFINC=1,IAPCINC=2,IHFINC=4,IHCINC=8)
        parameter (IDIM=512,LOGLEN=9,IDIM2=257,numbins=99)
        real signal(IDIM)
        integer*4 bin(IDIM2,0:numbins)
        integer i,fftsrc,coef,ffttmp,abssrc,scloff
        common/ARAYS/ signal
        common/OFFSTS/ fftsrc,coef,ffttmp,abssrc,scloff
        common/bininfo/bin,scale,IBLKIN,JIN,icount,ithresh
        call mapinit(1)
c calculate where in AP memory vectors should be stored
        i = and(loglen,1)
        if (i .eq. 1)then
                fftsrc = 2*idim
                ffttmp=idim
        else
                fftsrc = idim
                ffttmp = 2*idim
        endif
        coef = 0
        abssrc=(2*idim)+3
        scloff=6*idim2
c generate coefficient table for fft
        call mapffttab(coef,loglen)
c load "scale" into AP
        call maplodfs(scale,scloff)
        return
        end


        subroutine FFTX
c This routine takes FFT, takes the absolute value, and
c multiplies by scale. The scaling factor facilitates
```

```
c creating the histograms.
        parameter (IAPFINC=1,IAPCINC=2,IHFINC=4,IHCINC=8)
        parameter (IDIM=512,LOGLEN=9,IDIM2=257,numbins=99)
        real signal(IDIM)
        integer fftsrc,coef,ffttmp,abssrc,scloff
        common/ARAYS/ signal
        common/OFFSTS/ fftsrc,coef,ffttmp,abssrc,scloff
        call maplodfv(signal,IHFINC,fftsrc,IAPFINC,idim)
        call mapsync(-1)
        call maprfftnc(fftsrc,IAPFINC,coef,IAPCINC,ffttmp,IAPFINC,idim)
c take abs value of fft
        call mapnrmsqcfv(idim,IAPCINC,abssrc,IAPFINC,idim2)
c divide by scaling factor
        call mapmulfsv(scloff,abssrc,IAPFINC,idim,IAPFINC,idim2)
c shift data from AP to CPU
        call mapstrfv(idim,IAPFINC,signal,IHFINC,idim2)
        call mapbwaitrbe()
        return(0)
        end

        subroutine Xinterval(t0,tau,nsample,dX,tfinal)
c This subroutine calculates which points from sigt should
c be loaded into sigX, to swith "time" coordinate from
c t to X.
        parameter (Npower=9,NX=512)
        integer nXloc(NX)
        implicit double precision (d,t,X)
        common/Xint/ nXloc
        n=1
        nXloc(1)=n
        Xn=X(t0,tau)
c loop thru all tn<tfinal
 20             Xn=Xn+dX
                n=n+1
                tn=tofX(Xn,tau)
                Xloc=((tn-t0)*nsample)+1.
                nXloc(n)=nint(Xloc)
        if(tn.lt.tfinal.AND.n.lt.NX) go to 20
        return
        end
c X(t,tau)
        function X(t,tau)
        implicit double precision (d,t,X)
        X=-1.6*tau*((1-t/tau)**(.625))
        return
        end
c tofX(X,tau)
        function tofX(X,tau)
        implicit double precision (d,t,X)
        tofX=tau*(1.-((-.625*X/tau)**1.6))
        return
        end
c shift(i1,i2)
c This subroutine moves data from sigt(n) n=i1,i2
c to n=1,i2-i1+1.
        subroutine shift(i1,i2)
```

```
      parameter(JDIMt=100000,IBLKSZ=2048,IBLKSZg=2048)
      real sigt(JDIMt)
      integer*2 buffer(0:IBLKSZ-1)
      integer*4 LBLK,filedescript
      common/buf/buffer
      common/lblk/LBLK
      common/fd/filedescript
      common/datainput/sigt
      m=i1
      i=1
 15   sigt(i)=sigt(m)
      i=i+1
      m=m+1
      if(m.le.i2) goto 15
      return
      end
c subroutine bufsigt
c This routine moves good data from the buffer to sigt.
      subroutine bufsigt(i1,i2,i3,i4,i5)
      parameter(JDIMt=100000,IBLKSZ=2048,IBLKSZg=2048)
      real sigt(JDIMt)
      integer*2 buffer(0:IBLKSZ-1)
      integer*4 LBLK,filedescript
      common/buf/buffer
      common/fd/filedescript
      common/lblk/LBLK
      common/datainput/sigt
      j1=i2
 5    if(LBLK.eq.i1)jf=i3
      if(LBLK.lt.i1)jf=IBLKSZg-1
      if(LBLK.gt.i1) print*, "Error is reading in too many blocks"
      do 10 j=j1,jf
c this statement is entirely dependent on the tape/file format!!!
      sigt(i4)=buffer(j)
      i4=i4+1
 10   continue
      if(LBLK.eq.i1) then
        if(i4.ne.i5+1) print*,"error in bufsigt,i4,i5,LBLK:  ",i4,i5,LBLK
        return
      endif
      call block
      j1=0
      goto 5
      end
c
c subroutine bins
c This routine creates histograms of output, if something is
c too large for any of the histograms bins it prints a flag.
c It also prints out any points over a lower threshold=ithresh.
c
c scale=step size between bins
c numbins = number of bins data broken into
c (maximum point binned is numbins*scale)
      subroutine bins
      parameter (IAPFINC=1,IAPCINC=2,IHFINC=4,IHCINC=8)
      parameter (IDIM=512,LOGLEN=9,IDIM2=257,JDIMt=100000)
```

filtFbins.f Page 7

```
      parameter (IBLKSZ=2048,IBLKSZg=2048,NBLKS=2099,numbins=99)
      real sigX(IDIM)
      integer*4 bin(IDIM2,0:numbins)
      common/ARAYS/ sigX
      common/bininfo/bin,scale,IBLKIN,JIN,icount,ithresh
      do 10 i=1,IDIM2
      IBIN=nint(sigX(i))
      if(IBIN.gt.numbins) then
           print*,i,sigX(i),IBIN,IBLKIN,JIN,icount,"!!!!!"
        else
             bin(i,IBIN)=bin(i,IBIN)+1
             if(IBIN.gt.ithresh)print*,i,sigX(i),IBIN,IBLKIN,JIN,icount
        endif
10    continue
      return
      end
```

B.5 The Codes used to Reduce the Results

As mentioned in Section 5.2.5, the threshold in *filtFbins.f* was set very low, and one section of the data could trigger many channels. The program *readlog.f* reads the output of *filtFbins.f* and assigns to each section of the data which was over the threshold of *filtFbins.f* the one event which was the best fit to a binary star coalescence. The program *thrshevent.f* then reads through the output of *readlog.f* and prints out only those events over a fairly high threshold. These are the events which were reported in Chapter 6.

```
c                       readlog.f
c this program ignores channels 1-19 and 201-257 because they're
c uncalibrated in terms of strain.
        integer block,dead,deltai,icount,icntmx,ichan,imx
        integer isig,jin,jmx,IBLKSZg
        real sigX,sigmx
        real*8 time
c       prepare input and output files
        open(9,file="Tnum.log")
        open(10,file="Tnum.event")
        rewind(9)
        rewind(10)
c initialize stuff to zero
        dead=2140
c dead=the dead time, this routine will label
c only the largest point in the dead time as
c an event.
c dead=2140=2*(the length of the binary star filter)
        IBLKSZg=2048
        sample=10000.
        ichlow=20
        ichhigh=200
        imx=0
        sigmx=0
        iblkmx=0
        jmx=0
        icntmx=0
c read in ichan, sigX(ichan), and compare it with Jmax(ichan)
        write(10,*) "ichan,sigX,block,nsmp,time"
 20     read(9,*) ichan,sigX,isig,iblkin,jin,icount
c check for EOF, this is marked by flag:ichan=5000
        if (ichan.eq.5000) goto 40
        if (ichan.lt.ichlow.OR.ichan.gt.ichhigh) goto 20
        deltai=(IBLKSZg*(iblkin-iblkmx))+(jin+icount-jmx-icntmx)
        if(deltai.lt.dead) then
                if(sigmx.lt.sigX) then
                        imx=ichan
                        sigmx=sigX
                        iblkmx=iblkin
                        jmx=jin
                        icntmx=icount
                        endif
                else
c deltai>dead implies no longer within deadtime, output sigmx,
c then reset sigmx to current event
                time=((iblkmx*IBLKSZg)+jmx+icntmx)/sample
                block=iblkmx+int((jmx+icntmx)/IBLKSZg)
                nsmp=(time*sample)-(block*IBLKSZg)
                if(time.ne.0) write(10,*) imx,sigmx,block,nsmp,time
                imx=ichan
                sigmx=sigX
                iblkmx=iblkin
                jmx=jin
                icntmx=icount
                endif
        goto 20
 40     time=((iblkmx*IBLKSZg)+jmx+icntmx)/sample
        block=iblkmx+int((jmx+icntmx)/IBLKSZg)
        nsmp=(time*sample)-(block*IBLKSZg)
        if(time.ne.0) write(10,*) imx,sigmx,block,nsmp,time
        write(10,*) 5000,5000.,5000,5000,5000.
        close(9)
        close(10)
        end
```

```
c                thrshevent.f
c This program simply reads Tnum.event and outputs
c anything over a given threshold.
        integer block,ichan
        real sigX,thresh
        real*8 time
c       prepare input and output files
        open(10,file="Tnum.event")
        rewind(10)
c initialize stuff to zero
        thresh=60.
        print*,"threshold=",thresh
        print*,"ichan,sigX,block,nsmp,time"
c check for EOF, this is marked by flag:ichan=5000
 20     read(10,*) ichan,sigX,block,nsmp,time
        if (ichan.eq.5000) goto 40
        if(sigX.ge.thresh) print*,ichan,sigX,block,nsmp,time
        goto 20
 40     continue
        close(10)
        end
```

B.6 Automation

Once the limits have been chosen, the short routine *doitall* will run all of the above programs. Simply type in *"doitall XX"* where *XX* is the number of the tape being analyzed. The file *tapeXXlimits.dat* contains information on the thresholds chosen, *tape45limits.dat* is given below.

```
deassign
assign 1600
pre_table <tape$1limits.dat
deassign
filtFbins > T$1.log
mv filbin.dat filbin$1.dat
mv Tnum.tab T$1.tab
mv Tnumpre.dat T$1pre.dat
ft 7 100000 T$1.log >Tnum.log
readlog
rm Tnum.log
thrshevent >T$1.thresh
mv Tnum.event T$1.event
```

LIMIT1low	LIMIT1up	LIMIT4	minlock	DLY	NDLY	tape no.
-210	194	290	1000	1000	10000	45

tape45limits.dat

B.7 The Code for Detection of "Bumps"

The program *bumps.f* calculates the slope of the light level using a least square method. The slope is calculated every 25msec. The characteristic duration of each bump was approximately 100msec; calculating the slope every 25msec prevents one from missing a bump.

```
c                          bump.f
c
        parameter (IBLKSZ=10240,IBLKSZg=2048,NBLKS=2099,Iavgsz=256)
c IBLKSZ=total number of data points in 1 block, there are IBLKSZ/5 gw
c points in a block (assuming there are 5 channels of data recorded).
c NBLKS=number of blocks on tape minus one.
c Iavgsz=number of points used to find slope.
c IBLKSZg/Iavgsz must be an integer.
        integer*2 buffer(0:IBLKSZ-1),dclight(Iavgsz)
        integer iblock,iavg,n,nbuffer,offset,fd,CHlight
        integer IBLKIN,IBLKOUT,JIN,JOUT,dly,ndly,tapeno
        integer*4 LBLK,filedescript
        real alpha,bmpthrshp,bmpthrshn
        common/buf/buffer
        common/lblk/LBLK
        common/fd/filedescript
        common/sloperout/dclight,alpha
c open tape
        call copen$
        open(13,file="/usr/sheri/analysis/Tnum.tab")
        rewind(13)
        read(13,*) limit1low,limit1up,limit4,minlock,dly,ndly,tapeno
        print*, limit1low,limit1up,limit4,minlock,dly,ndly,tapeno
c SET INITIAL VALUES (in sec or Hz)
        CHlight=4
        LBLK=-1
        numslps=IBLKSZg/Iavgsz
        bmpthrshp=.05
        bmpthrshn=-.05
```

```
        print*, "bmpthrshp,bmpthrshn=",bmpthrshp,bmpthrshn
        print*, "BLOCK, SAMPLE(here to +",Iavgsz,"),  bumpslope"
        read(13,*) IBLKIN,JIN,IBLKOUT,JOUT
        if (IBLKIN.eq.5000) goto 40
        do 21 iblock=0,NBLKS
        call cblock$
        do 23 iavg=1,numslps
        offset=(iavg-1)*Iavgsz
        nbuffer=(offset*5) +CHlight
        do 22 n=1,Iavgsz
        dclight(n)=buffer(nbuffer)
        nbuffer=nbuffer+5
 22     continue
        call slope
        if(alpha.gt.bmpthrshp.OR.alpha.lt.bmpthrshn) then
c check if data was "good"
 24             if(LBLK.gt.IBLKOUT) then
                        read(13,*) IBLKIN,JIN,IBLKOUT,JOUT
                        if (IBLKIN.eq.5000) goto 40
                        goto 24
                        endif
                if(LBLK.ge.IBLKIN.and.LBLK.le.IBLKOUT)  then
c data may have been good (I don't bother to check JIN or JOUT)
                        print*,LBLK,offset,alpha
                        endif
                endif
 23     continue
 21     continue
 40     close(13)
        call cclose$
        end
c
        subroutine slope
c
c calculate slope of points in array dclight(n) vs n
c by least squares method
        parameter (IBLKSZ=10240,IBLKSZg=2048,NBLKS=2099,Iavgsz=256)
        integer*2 dclight(Iavgsz)
        real alpha,beta,denom,sumxx,sumx,sumy,sumxy
        common/sloperout/dclight,alpha
c first set sums to zero
        sumx=0
        sumxy=0
        sumxx=0
        sumy=0
        do 10 j=1,Iavgsz
        y=real(dclight(j))
        sumx=sumx+j
        sumxy=sumxy+(j*y)
        sumxx=sumxx+(j*j)
        sumy=sumy+y
  10    continue
c calculate slope of y=alpha*x + beta
        denom=(sumxx*Iavgsz)-(sumx*sumx)
        beta=((sumxx*sumy)-(sumx*sumxy))/denom
        alpha=((Iavgsz*sumxy)-(sumx*sumy))/denom
        return
        end
```

Appendix C

More information

Tape	Starting Time	Ending Time
	Universal Time (dd:hh:mm:ss)	
44	68:00:59:10	68:01:06:20
45	68:01:09:30	68:01:16:31
46	68:01:19:30	68:01:26:41
47	68:01:29:10	68:01:36:21
48	68:01:40:10	68:01:47:20
49	68:01:50:30	68:01:57:41
50	68:02:02:30	68:02:09:41

Table C.1: The time at which these data were collected.

Date (Universal Time)	Detector		
	Caltech	Glasgow	MIT
Feb 27 (058)	check	—	—
Feb 28 (059)	check	—	—
March 5 (064)	20:00-21:00	20:00-21:00	—
March 8 (067)	14:00-16:30	—	14:30-16:30
March 9 (068)*	0:00-2:30	0:00-2:30	0:00-2:30
March 11 (070)	6:00-9:00	7:30-10:30	6:00-9:00

* Data analyzed, (March 8, 1988, Pacific Standard Time)

Table C.2: The times at which Caltech, Glasgow and MIT were collecting data.

Figure C.1: The raw data for the events listed in Table 6.3.

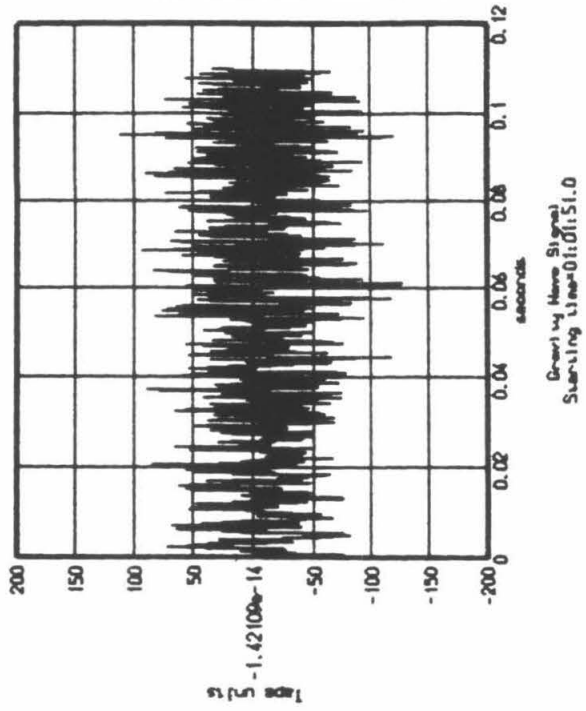

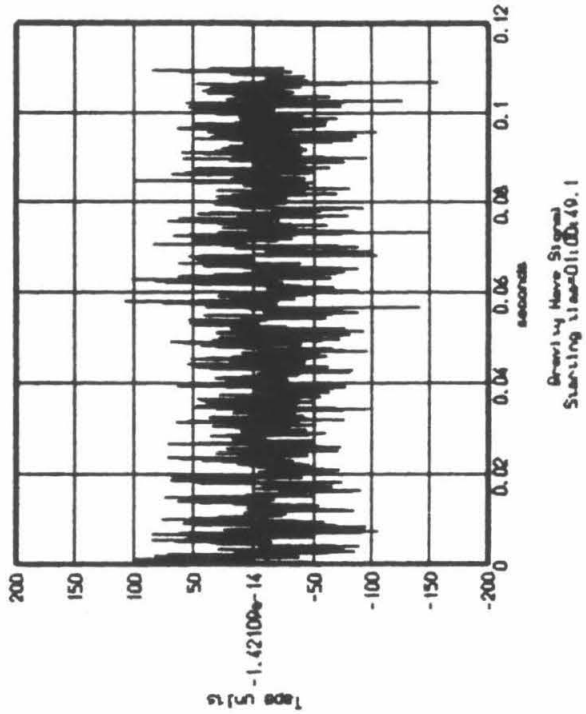

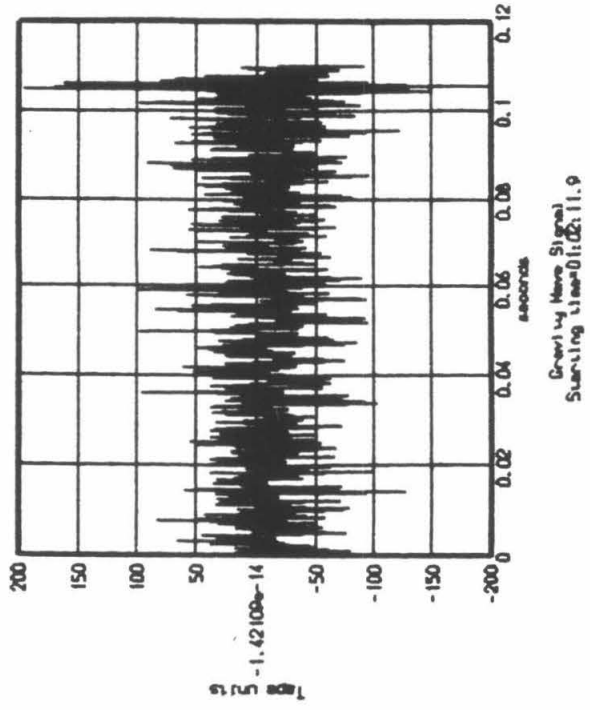
200
150
100
50
-50
-100
-150
-200
0
0.02
0.04
0.06
0.08
0.1
0.12
seconds
Gravity Wave Signal
Starting time=01:01:51.4
Time Series -1.42109e-14

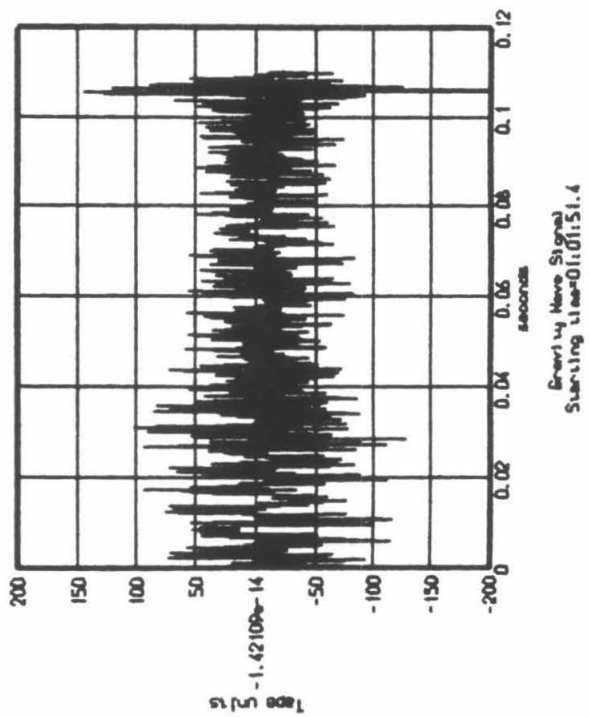
200
150
100
50
-50
-100
-150
-200
0
0.02
0.04
0.06
0.08
0.1
0.12
seconds
Gravity Wave Signal
Starting time=01:02:11.9
Time Series -1.42109e-14

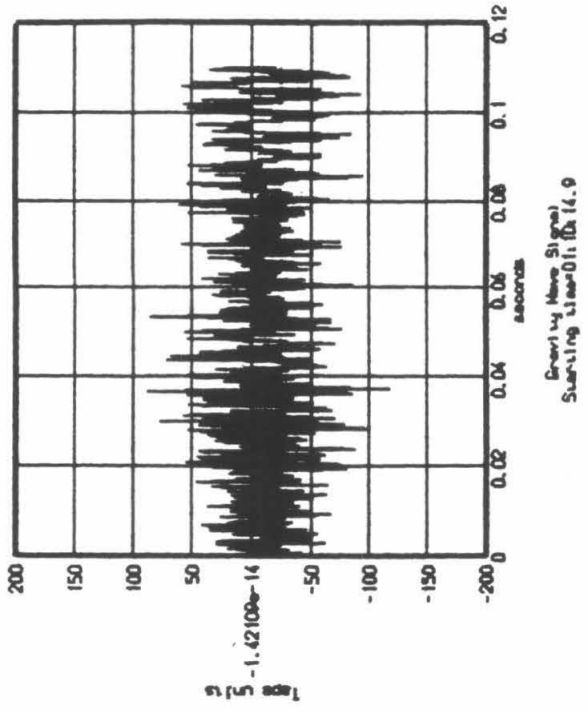
200
150
100
50
-50
-100
-150
-200
0
0.02
0.04
0.06
0.08
0.1
0.12
seconds
Drawing Wave Signal
Starting time=01:02:13.4
Time Shift -1.42108e-14

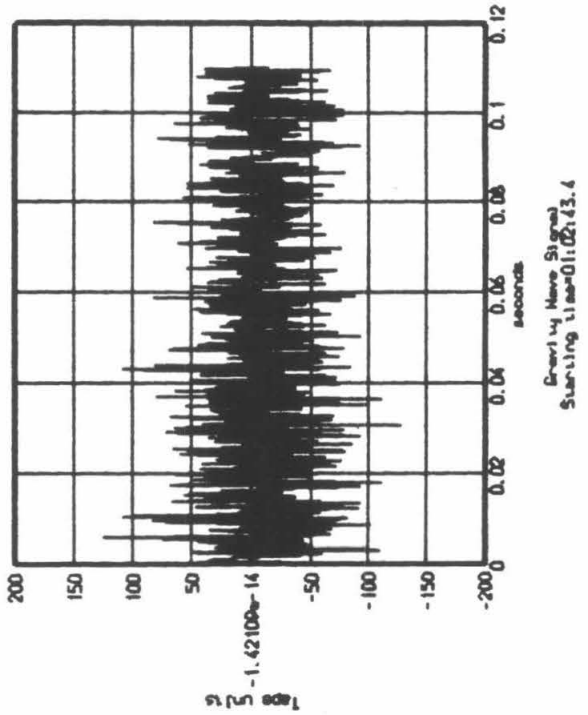
200
150
100
50
-50
-100
-150
-200
0
0.02
0.04
0.06
0.08
0.1
0.12
seconds
Drawing Wave Signal
Starting time=01:02:14.9
Time Shift -1.42108e-14

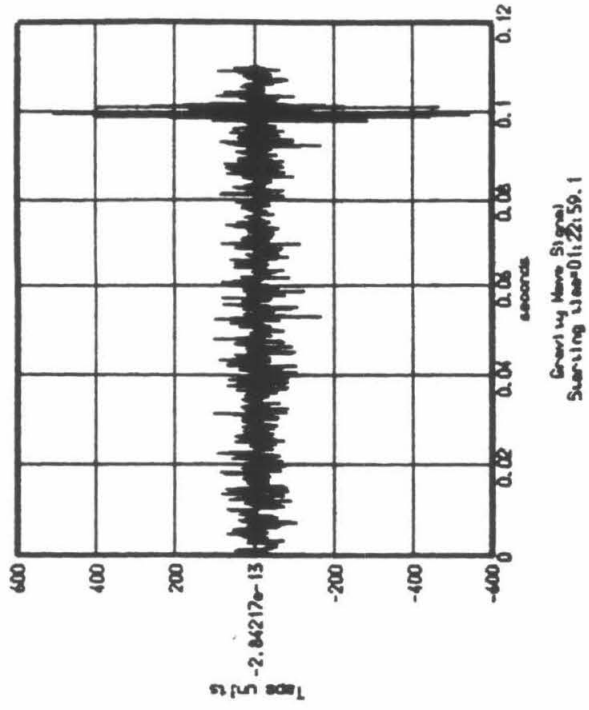
Gravity Wave Signal
Starting time=01:22:59.1
seconds
0
0.02
0.04
0.06
0.08
0.1
0.12
600
400
200
-200
-400
-600
Tape Sig
-2.84217e-13

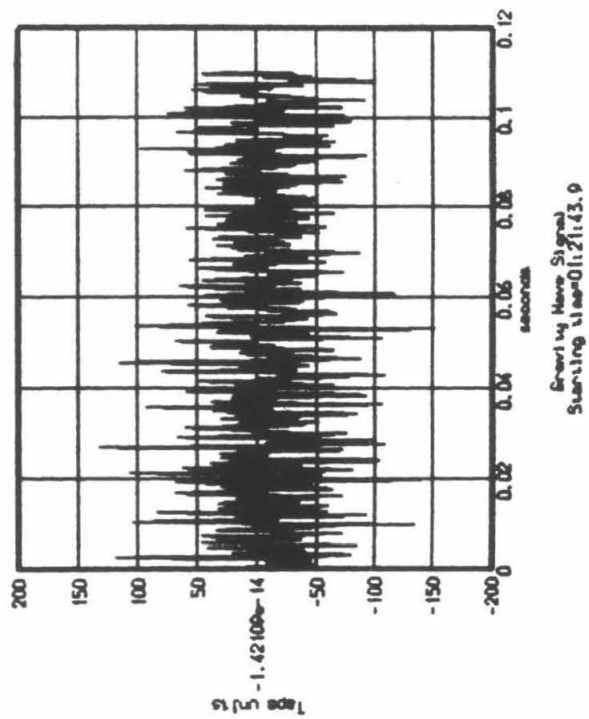
Gravity Wave Signal
Starting time=01:21:43.9
seconds
0
0.02
0.04
0.06
0.08
0.1
0.12
200
150
100
50
-50
-100
-150
-200
Tape Sig
-1.42108e-14

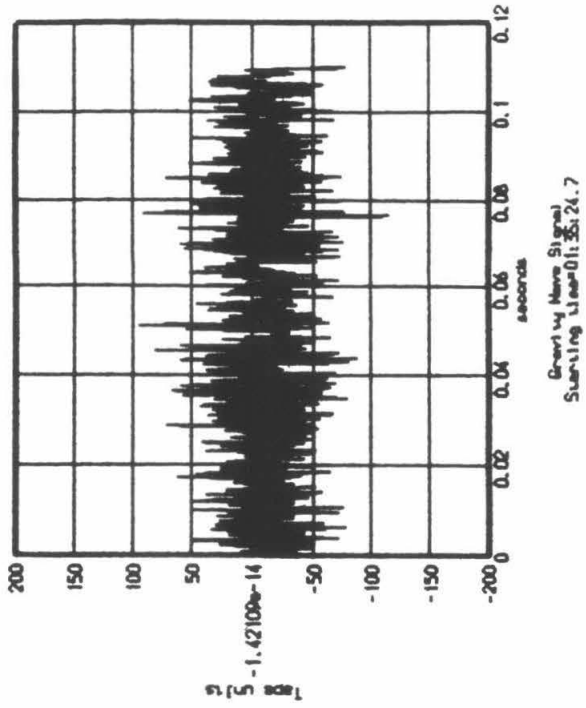
Tape Units
200
150
100
50
-50
-100
-150
-200
-1.42108e-14
0
0.02
0.04
0.06
0.08
0.1
0.12
seconds
Gravity Wave Signal
Starting time=01:35:24.7

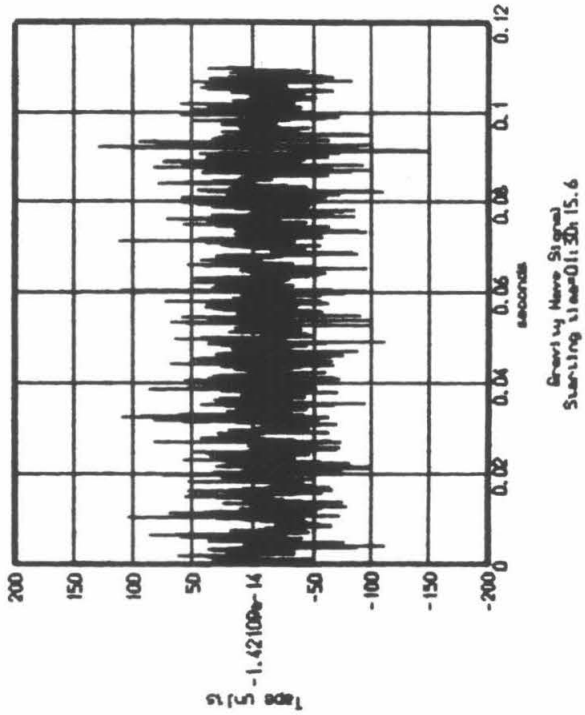
Tape Units
200
150
100
50
-50
-100
-150
-200
-1.42108e-14
0
0.02
0.04
0.06
0.08
0.1
0.12
seconds
Gravity Wave Signal
Starting time=01:30:15.6

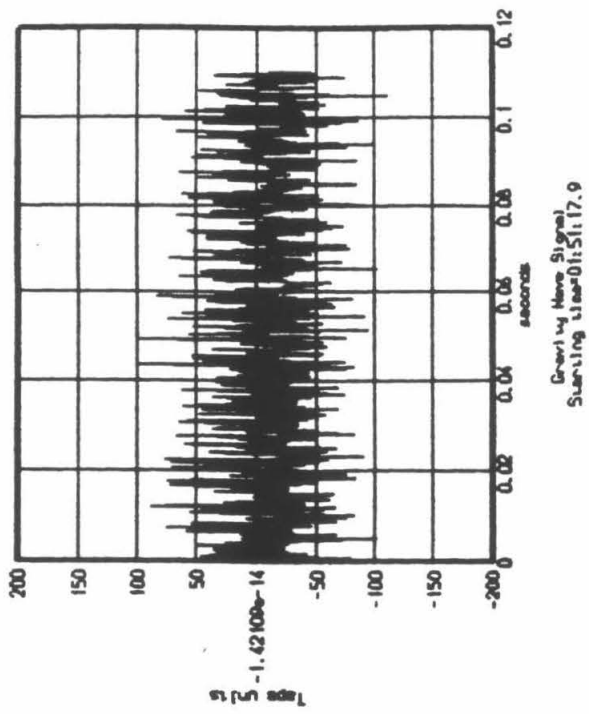
200
150
100
50
-50
-100
-150
-200
0
0.02
0.04
0.06
0.08
0.1
0.12
seconds
Gravity Wave Signal
Starting time=01:51:17.9
Time Delta -1.42108e-14

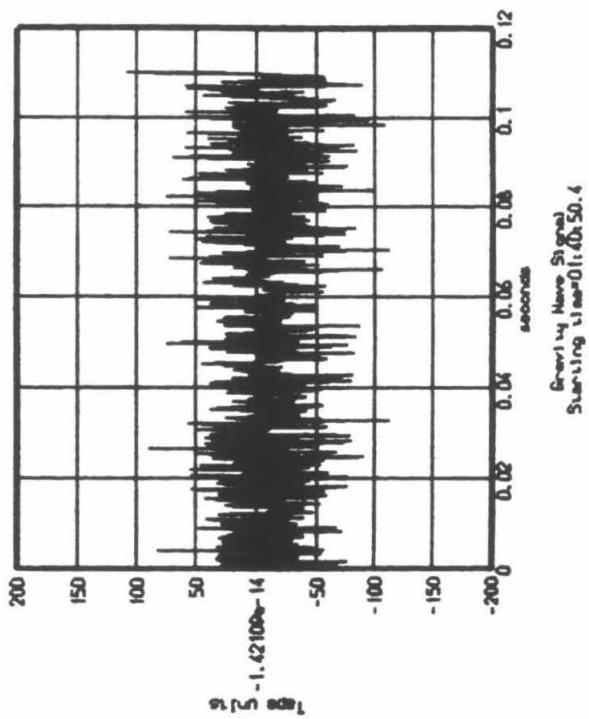
200
150
100
50
-50
-100
-150
-200
0
0.02
0.04
0.06
0.08
0.1
0.12
seconds
Gravity Wave Signal
Starting time=01:40:50.4
Time Delta -1.42108e-14

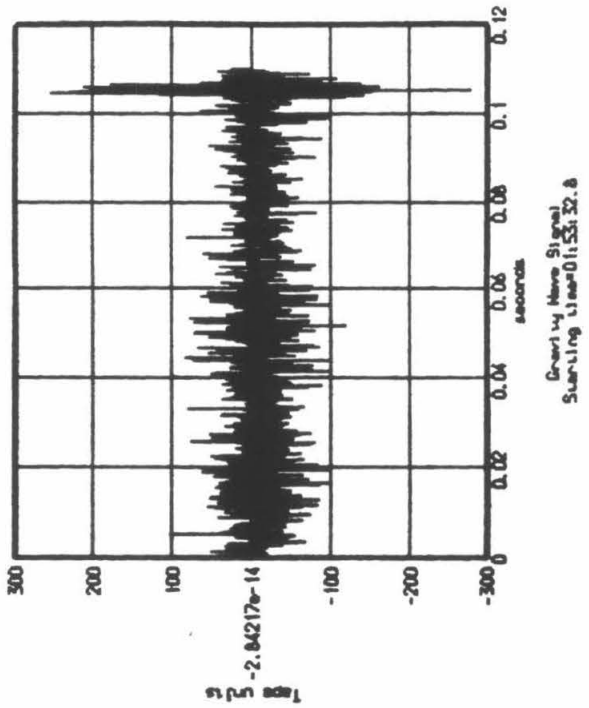
300
200
100
-100
-200
-300
0
0.02
0.04
0.06
0.08
0.1
0.12
seconds
-2.84217e-14

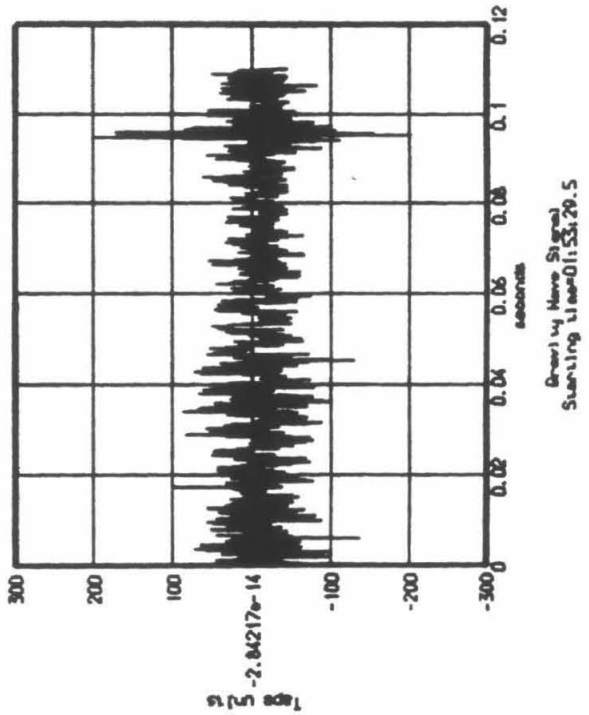
300
200
100
-100
-200
-300
0
0.02
0.04
0.06
0.08
0.1
0.12
seconds
-2.84217e-14

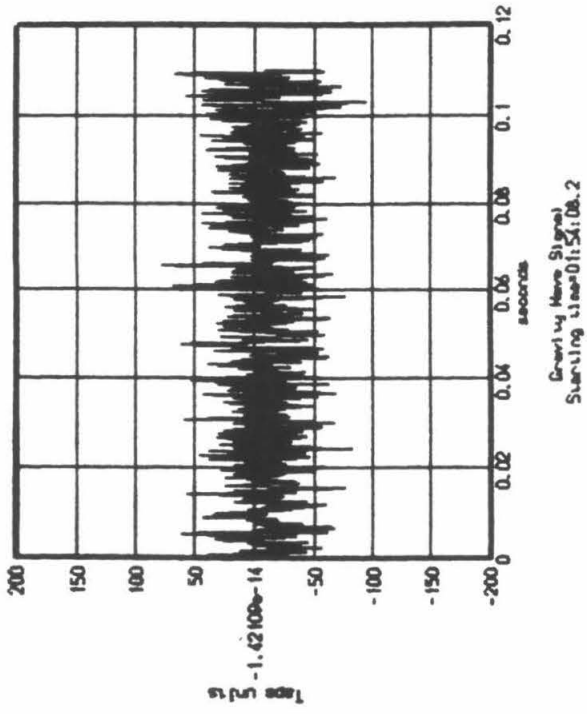
200
150
100
50
-50
-100
-150
-200
0
0.02
0.04
0.06
0.08
0.1
0.12
seconds
Gravity Wave Signal
Starting time=01:54:08.2
Time (s)
-1.42108e-14

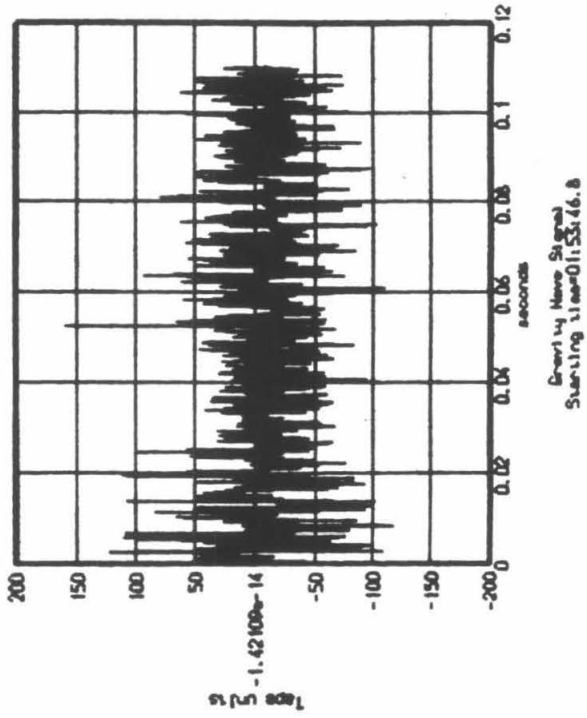
200
150
100
50
-50
-100
-150
-200
0
0.02
0.04
0.06
0.08
0.1
0.12
seconds
Gravity Wave Signal
Starting time=01:53:46.8
Time (s)
-1.42108e-14

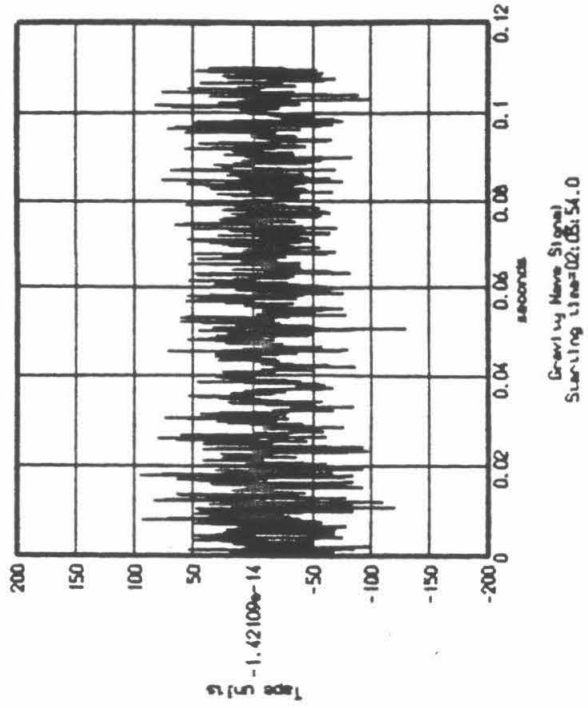
200
150
100
50
-50
-100
-150
-200
0
0.02
0.04
0.06
0.08
0.1
0.12
seconds
Gravity Wave Signal
Starting time=02:08:54.0
Time Shift -1.42109e-14

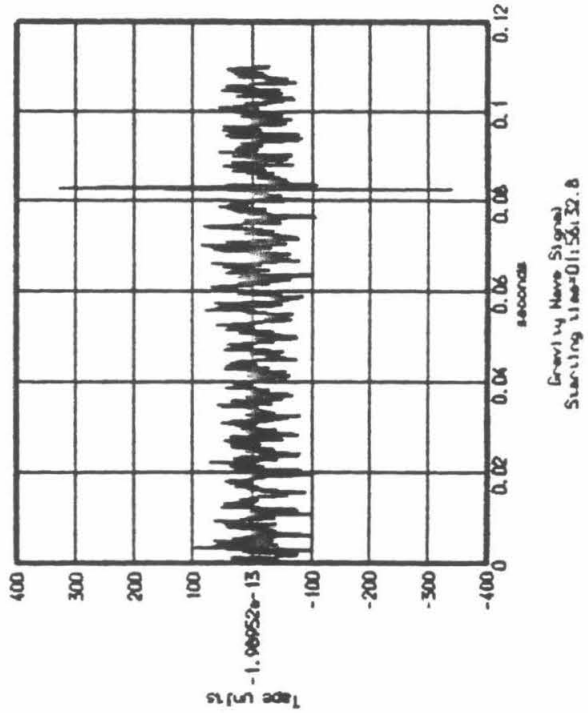
400
300
200
100
-100
-200
-300
-400
0
0.02
0.04
0.06
0.08
0.1
0.12
seconds
Gravity Wave Signal
Starting time=01:56:32.8
Time Shift -1.98952e-13

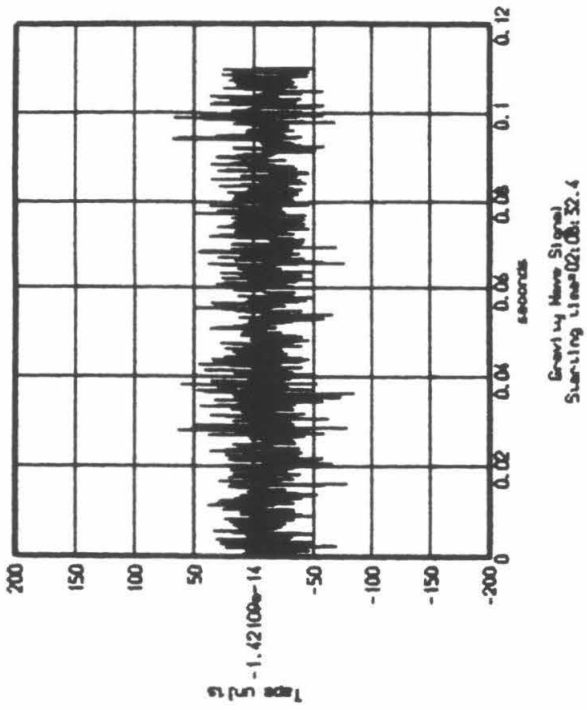
200
150
100
50
-50
-100
-150
-200
0
0.02
0.04
0.06
0.08
0.1
0.12
seconds
Gravity Wave Signal
Starting time=02:08:32.4
Tape Unit -1.42100e-14

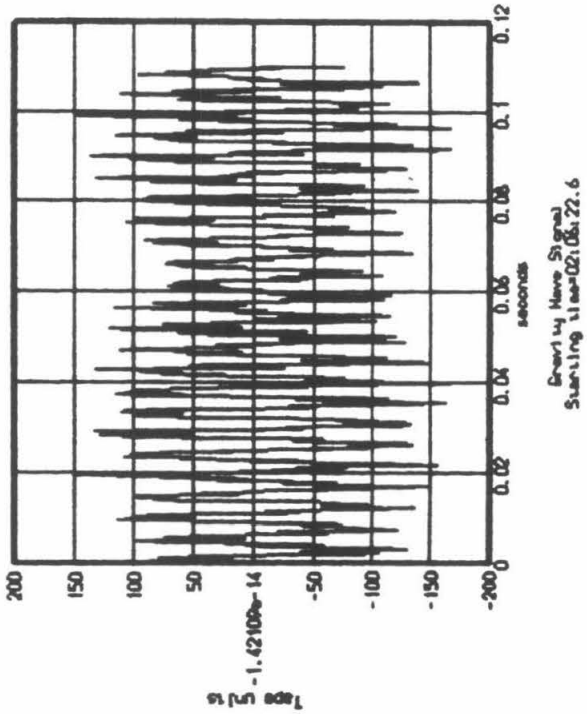
200
150
100
50
-50
-100
-150
-200
0
0.02
0.04
0.06
0.08
0.1
0.12
seconds
Gravity Wave Signal
Starting time=02:08:22.6
Tape Unit -1.42100e-14

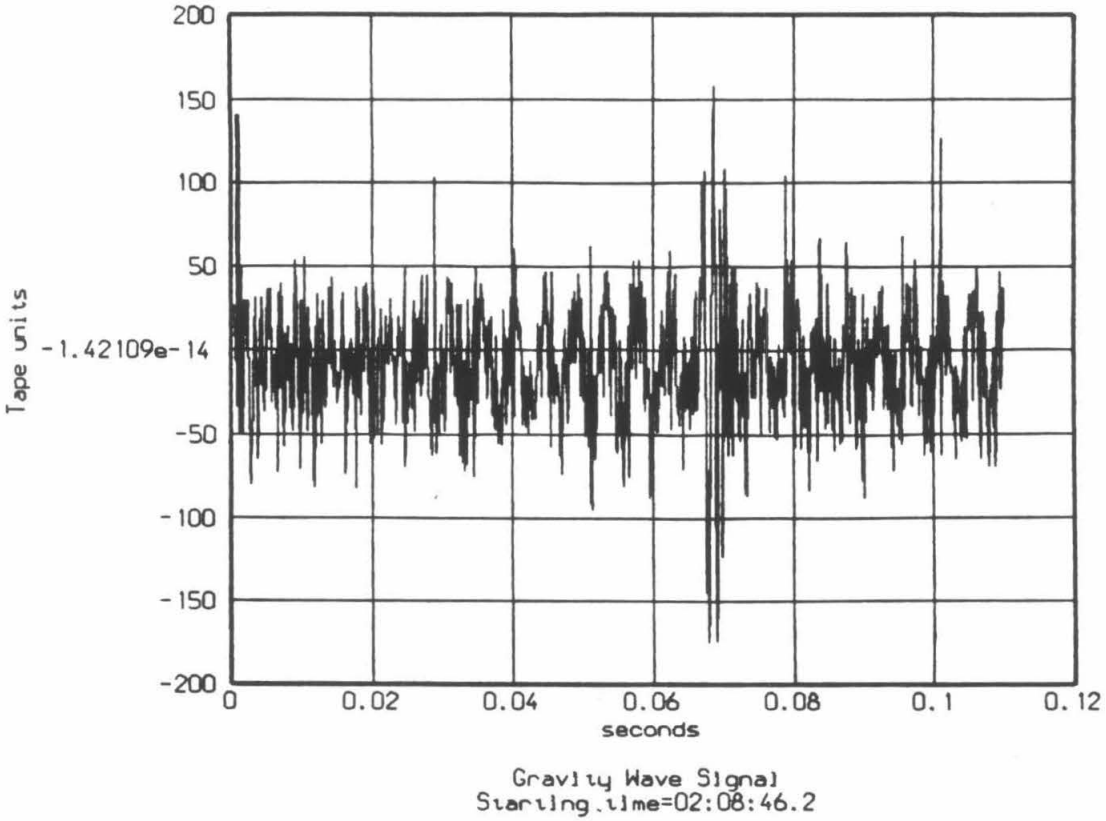
200
150
100
50
-1.42109e-14
-50
-100
-150
-200
Tape units
0
0.02
0.04
0.06
0.08
0.1
0.12
seconds
Gravity Wave Signal
Starting time=02:08:46.2

Figure C.2: Close-ups of the spikes in the data.

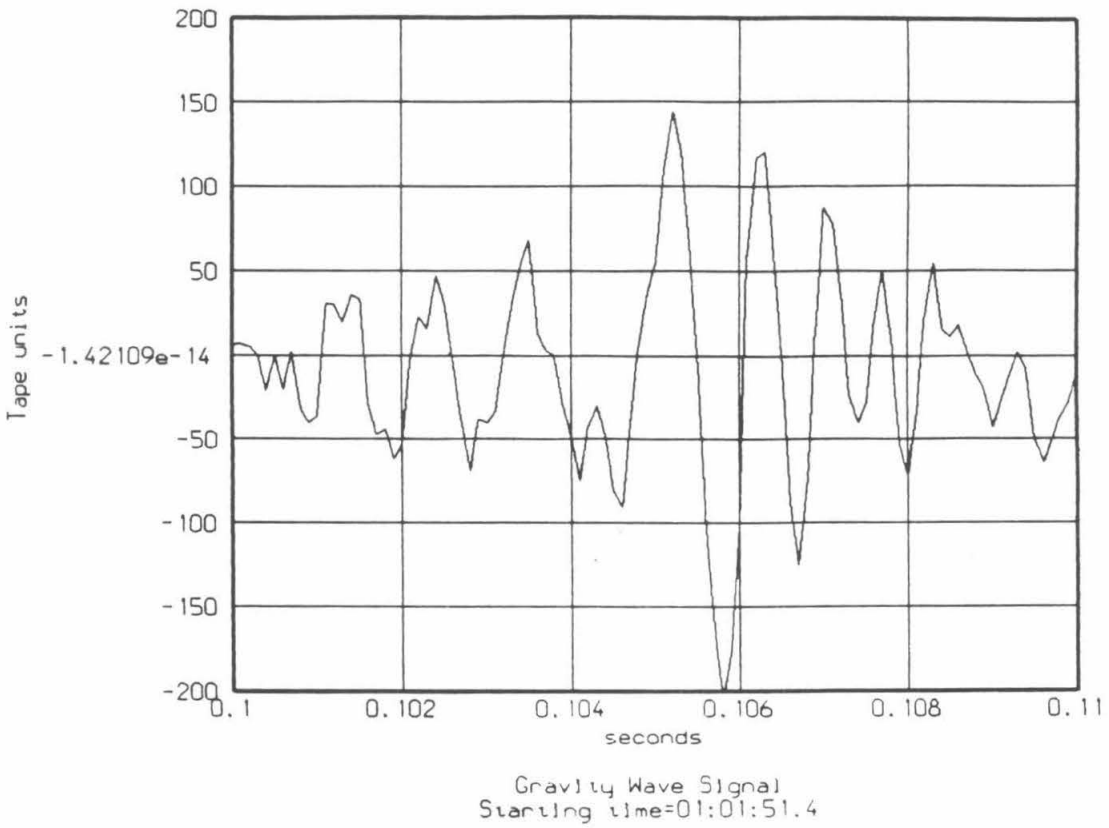

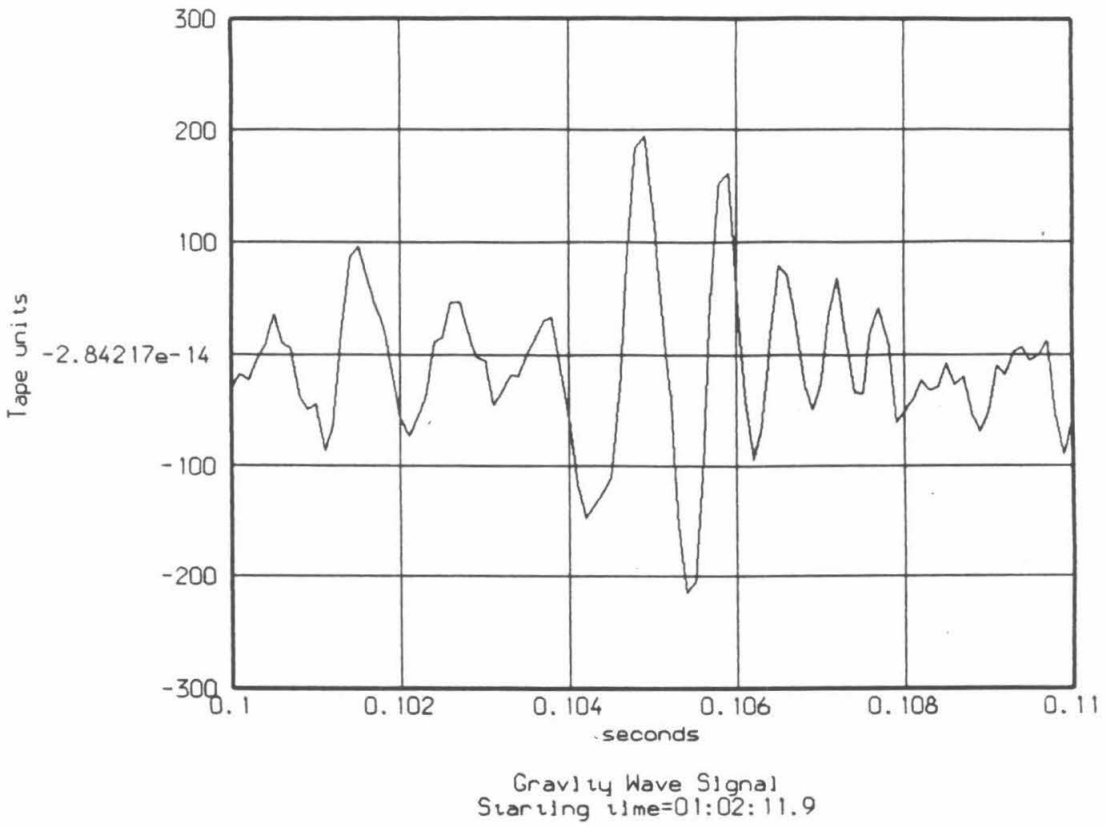
300
200
100
-2.84217e-14
-100
-200
-300
Tape units
0.1
0.102
0.104
0.106
0.108
0.11
seconds
Gravity Wave Signal
Starting time=01:02:11.9

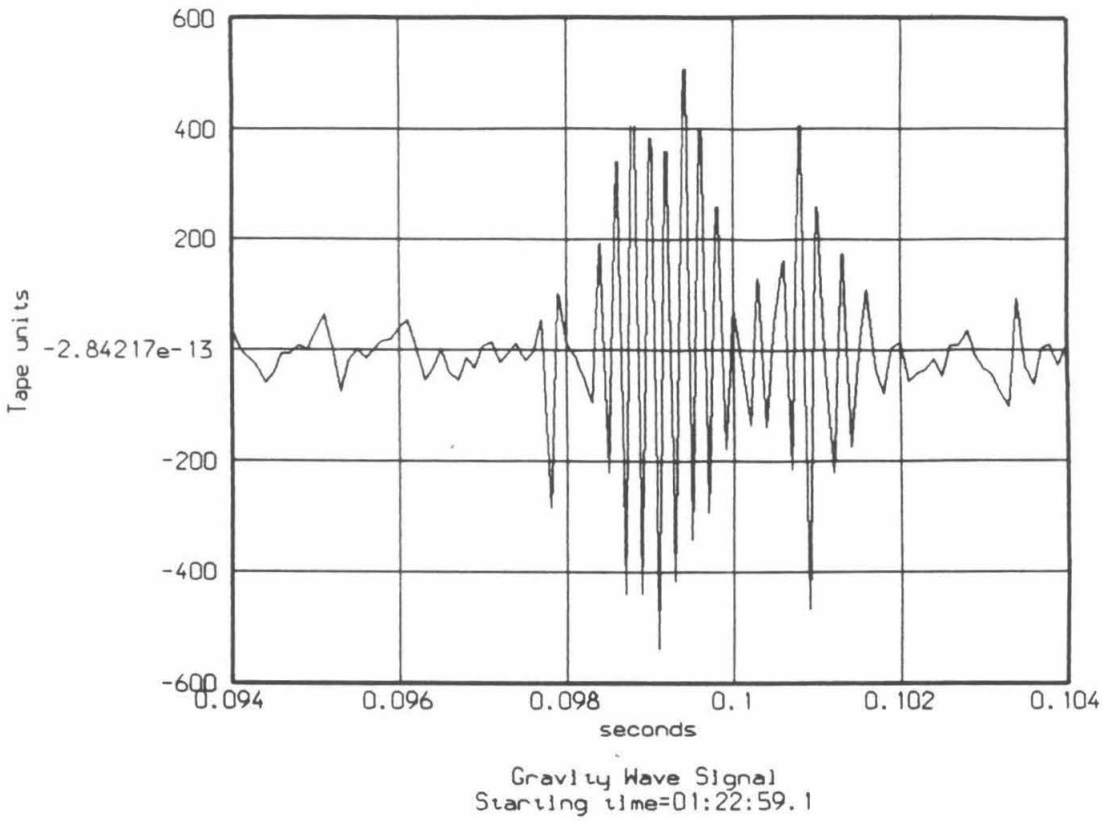
600
400
200
-2.84217e-13
-200
-400
-600
Tape units
0.094
0.096
0.098
0.1
0.102
0.104
seconds
Gravity Wave Signal
Starting time=01:22:59.1

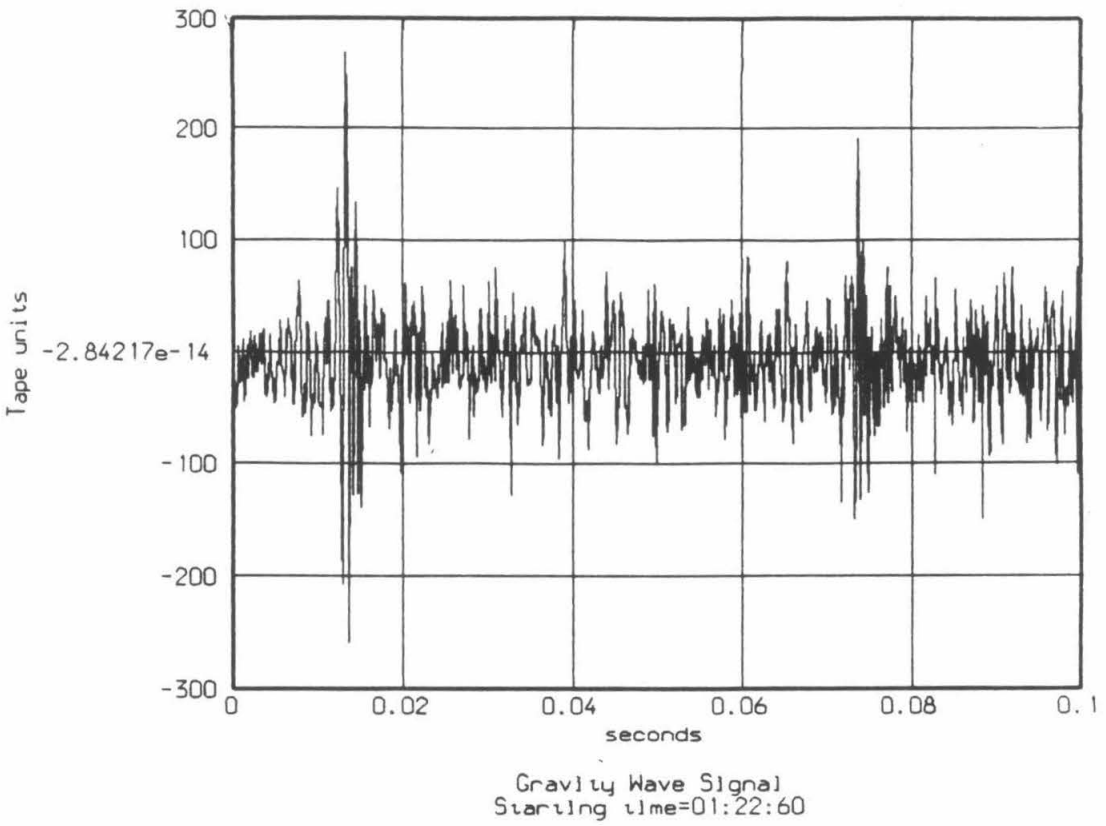
300
200
100
-2.84217e-14
-100
-200
-300
Tape units
0
0.02
0.04
0.06
0.08
0.1
seconds
Gravity Wave Signal
Starting time=01:22:60

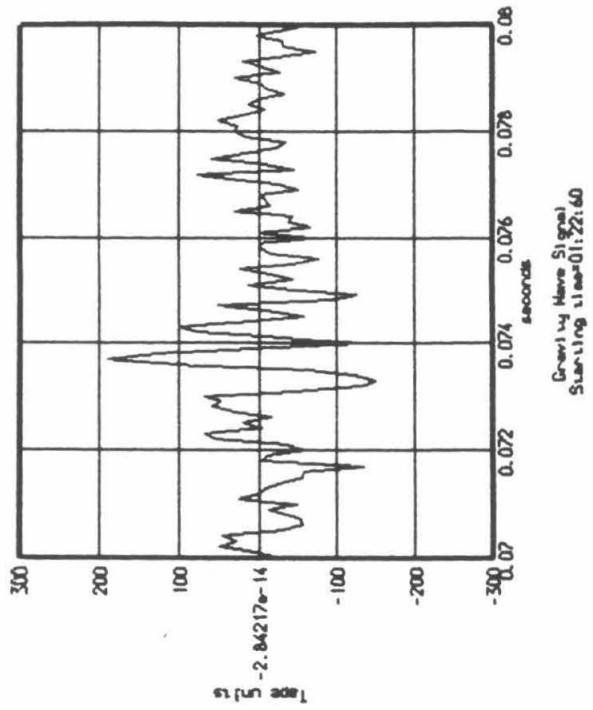
300
200
100
-100
-200
-300
0.07
0.072
0.074
0.076
0.078
0.08
seconds
Gravity Wave Signal
Starting time=01:22:60
Tape Units -2.84217e-14

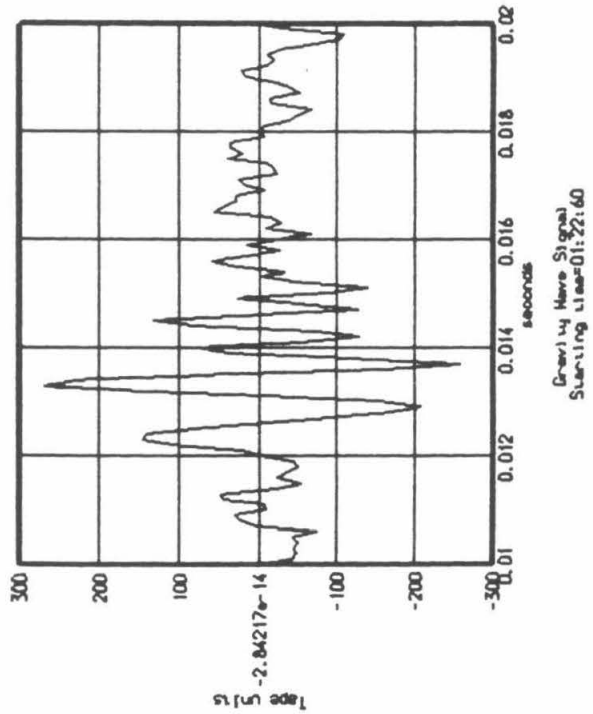
300
200
100
-100
-200
-300
0.01
0.012
0.014
0.016
0.018
0.02
seconds
Gravity Wave Signal
Starting time=01:22:60
Tape Units -2.84217e-14

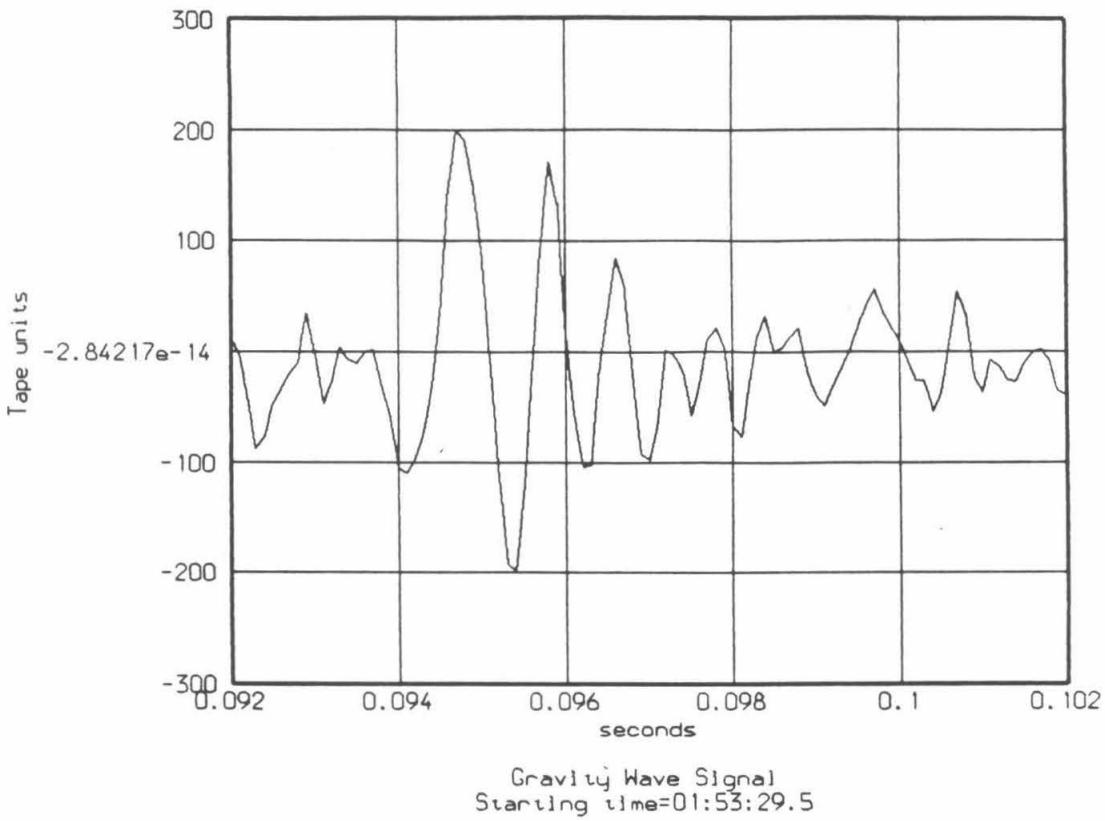
300
200
100
-2.84217e-14
-100
-200
-300
Tape units
0.092
0.094
0.096
0.098
0.1
0.102
seconds
Gravity Wave Signal
Starting time=01:53:29.5

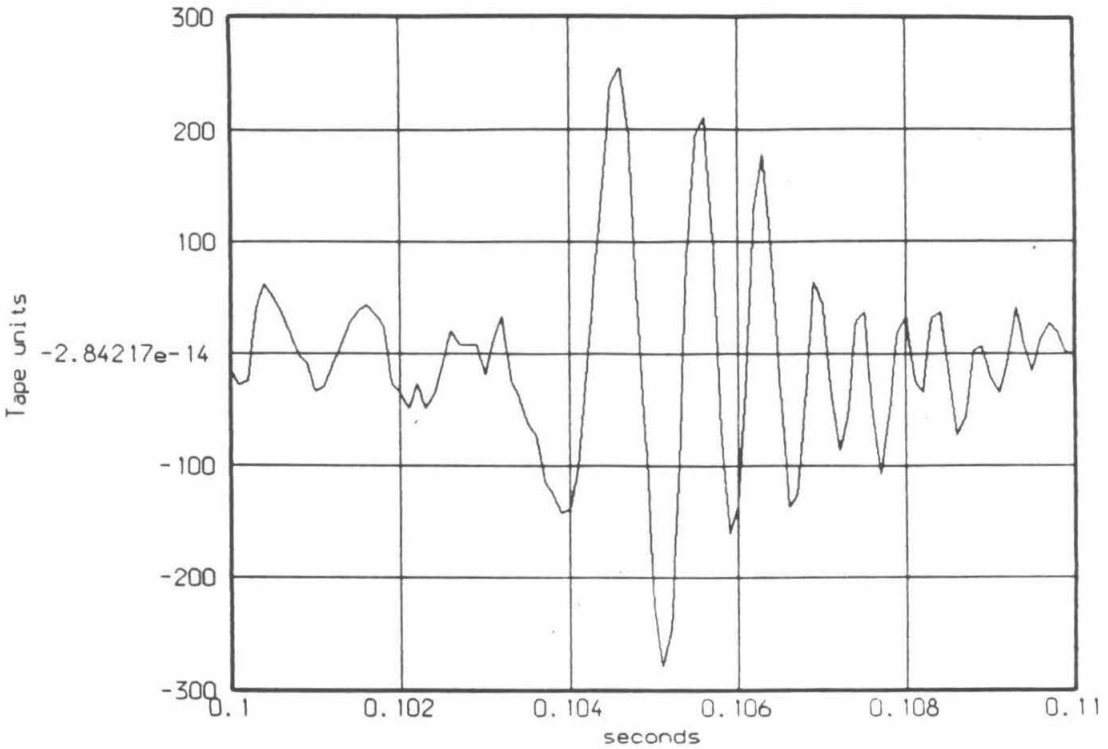
300
200
100
-2.84217e-14
-100
-200
-300
Tape units
0.1
0.102
0.104
0.106
0.108
0.11
seconds
Gravity Wave Signal
Starting time=01:53:32.8

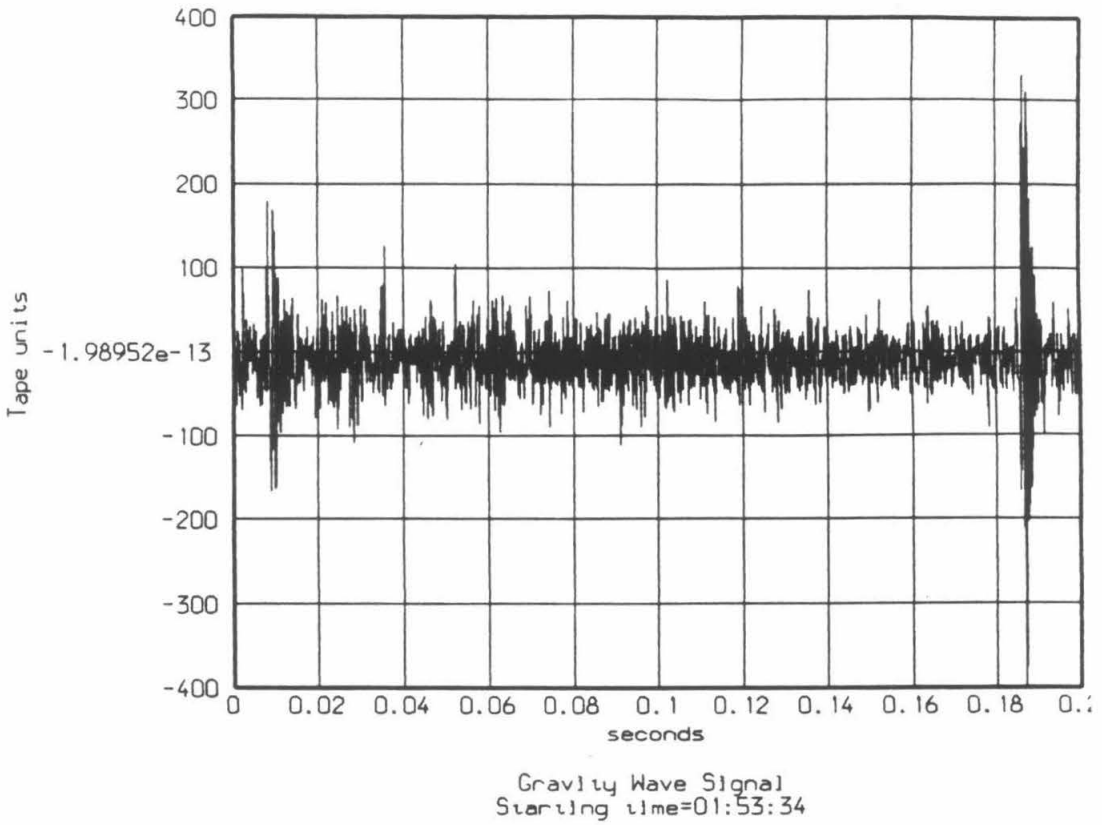
400
300
200
100
-1.98952e-13
-100
-200
-300
-400
Tape units
0
0.02
0.04
0.06
0.08
0.1
0.12
0.14
0.16
0.18
seconds
Gravity Wave Signal
Starting time=01:53:34

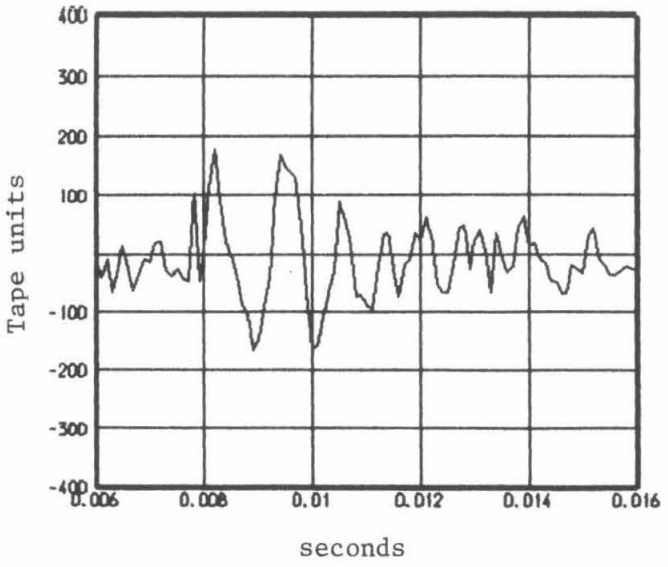

Gravity Wave Signal
Starting time=01:53:34

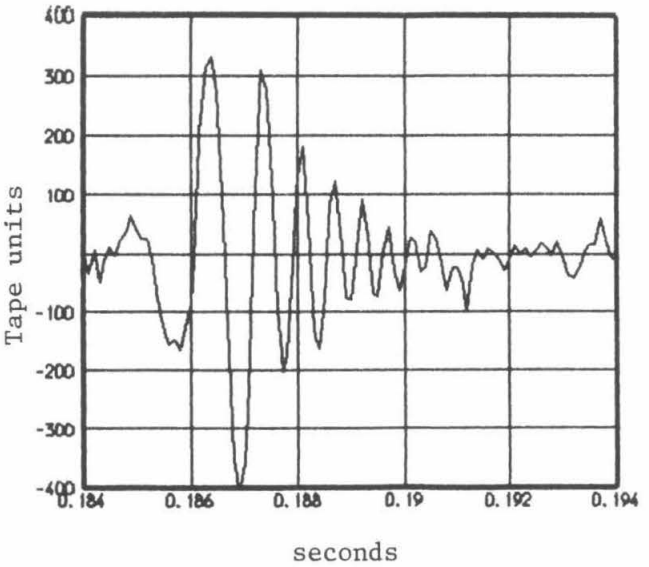

Gravity Wave Signal
Starting time=01:53:34

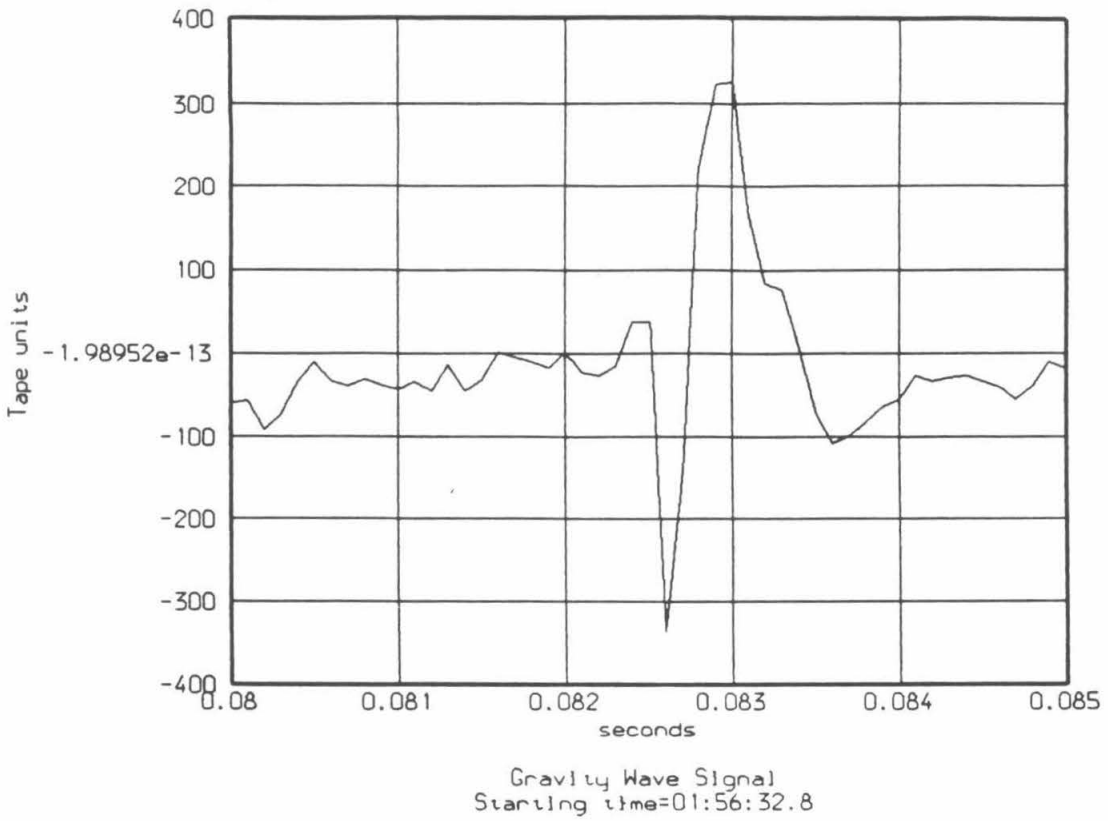
400
300
200
100
-1.98952e-13
-100
-200
-300
-400
Tape units
0.08
0.081
0.082
0.083
0.084
0.085
seconds
Gravity Wave Signal
Starting time=01:56:32.8

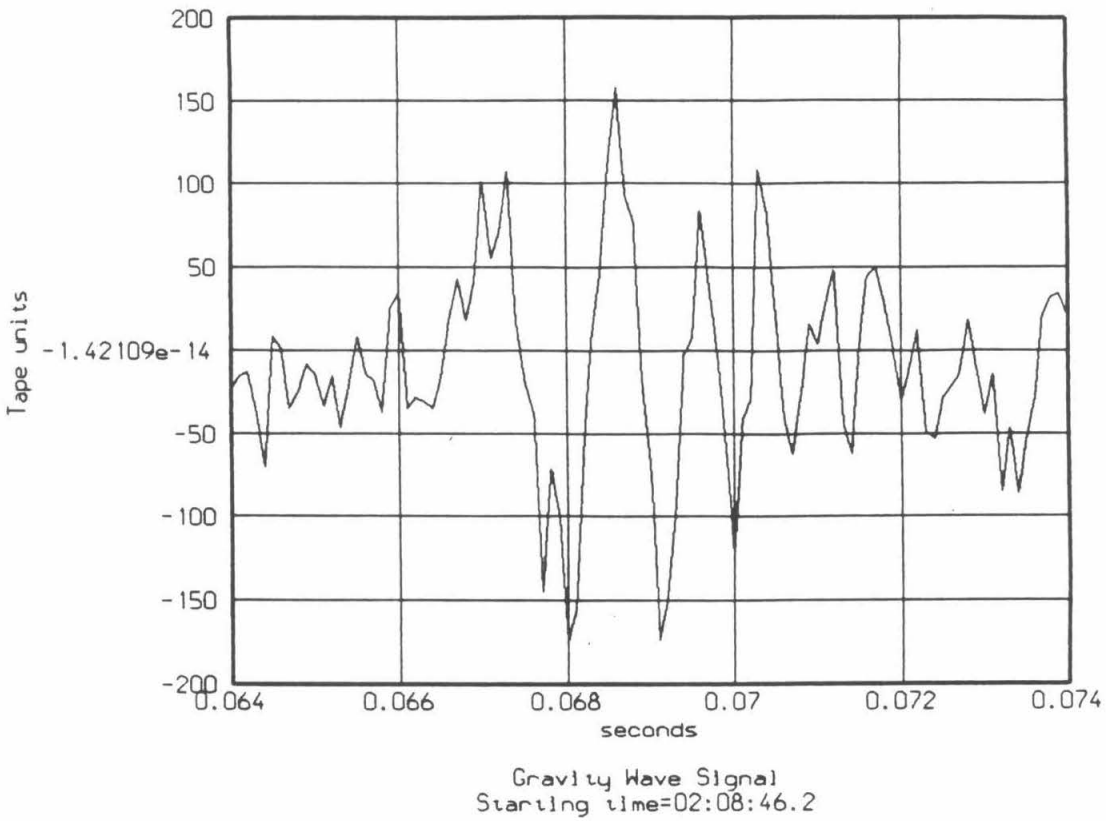
200
150
100
50
-1.42109e-14
-50
-100
-150
-200
Tape units
0.064
0.066
0.068
0.07
0.072
0.074
seconds
Gravity Wave Signal
Starting time=02:08:46.2

Figure C.3: The auxiliary signals recorded during the largest spike.*

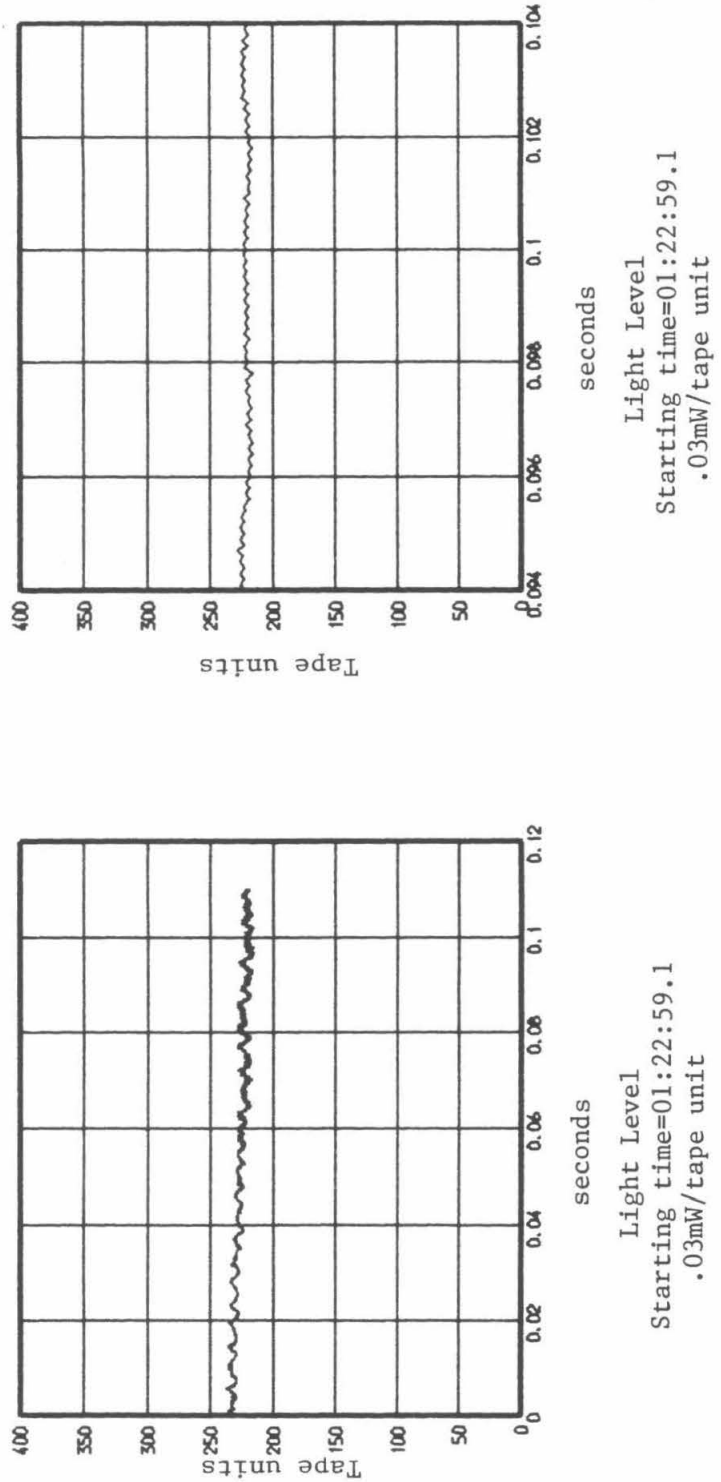

* See pages 145 and 155 for the gravity wave signal.

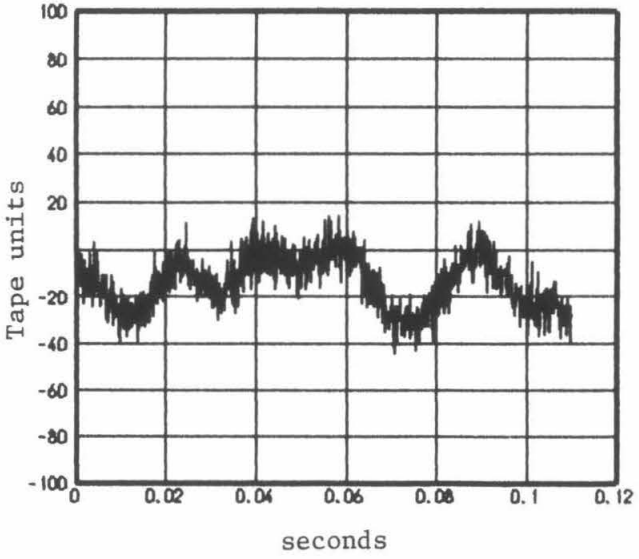

Seismometer and Microphone
Starting time=01:22:59.1

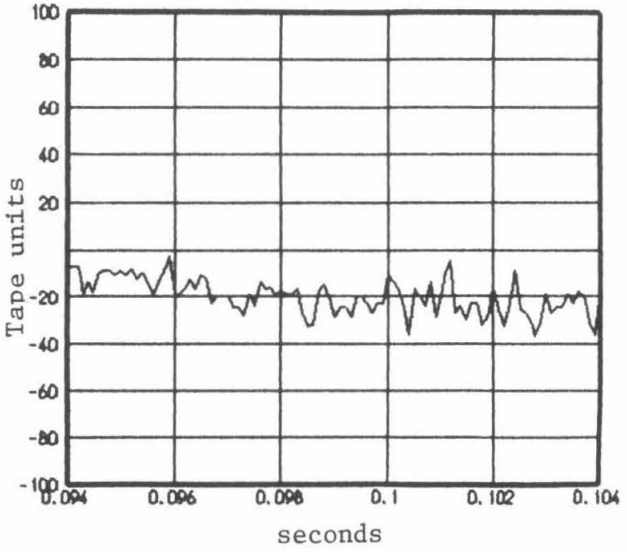

Seismometer and Microphone
Starting time=01:22:59.1

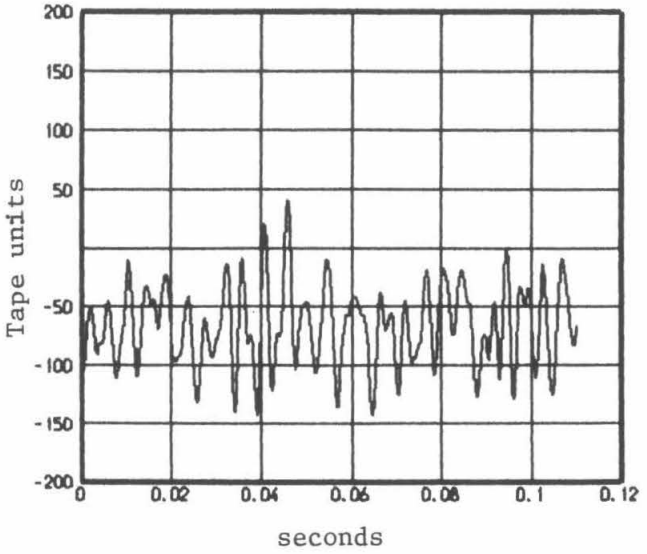

Low frequency feedback to the
First Cavity
Starting time=01:22:59.1

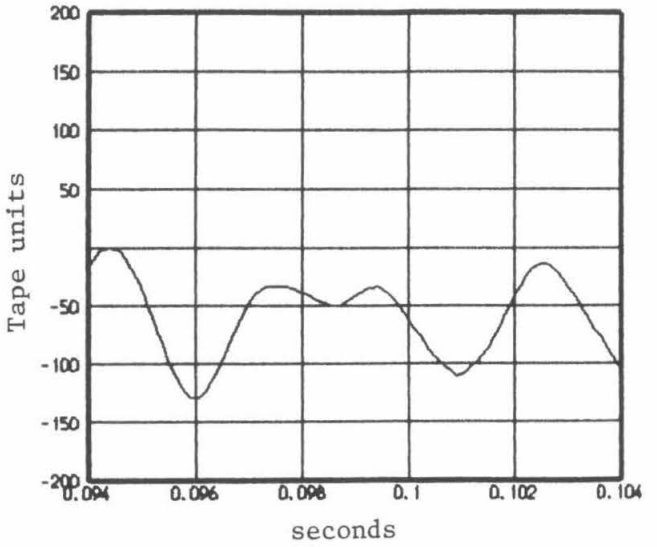

Low frequency feedback to the
First Cavity
Starting time=01:22:59.1

Bibliography

[1] J.H. Taylor and J.M. Weisberg, *The Astrophysical Journal* **253**, 908–920, (1982).

[2] J. Weber, *Physical Review* **22**, D1302, (1969).

[3] S.P. Boughn, W.M. Fairbank, R.P.Giffard, J.M. Hollenhorst, E.R. Mapoles, M.S. McAshan, P.F. Michelson, H.J. Paik, and R.C. Taber, *The Astrophysical Journal* **261**, L19-L22, (1982).

[4] G.E. Moss, L.R. Miller, and R.L. Forward, *Applied Optics* **10**, 2495, (1971).

[5] A proposal to NSF: *Caltech/MIT Project for a Laser Interferometer Gravitational Wave Observatory*, unpublished, (1987).

[6] M. Hereld, "A Search for Gravitational Radiation from PSR 1937+214," Caltech Ph.D. Thesis, (1984).

[7] J. Livas, "Upper Limits for Gravitational Radiation from Some Astrophysical Sources," MIT Ph.D. Thesis, (1987).

[8] D. Dewey, "A Search for Astronomical Gravitational Radiation with an Interferometric Broadband Antenna," MIT Ph.D. Thesis, (1986).

[9] K.S. Thorne, "Gravitational Radiation" in *300 Years of Gravitation*, eds. S.W. Hawking and W. Israel, Cambridge University Press, (1987).

[10] B. F. Schutz, *Nature (London)* **323**, 310, (1986).

[11] C.W. Misner, K.S. Thorne, and J.A. Wheeler, *Gravitation*, W.H. Freeman and Company, San Francisco, (1973).

[12] S. Weinberg, *Gravitation and Cosmology: Principles and Applications of the General Theory of Relativity*, Wiley, New York, (1972).

[13] M.E. Zucker, "Experiments with a 40 Meter Interferometric Gravitational Wave Antenna," Caltech Ph.D. Thesis, (1988).

[14] R.L. Forward, and D. Berman, *Physical Review Letters* **18**, 1071, (1967).

[15] P.C. Peters, and J. Mathews, *Physical Review* **131**, 435, (1963).

[16] P.C. Peters, *Physical Review* **136**, B1224, (1964).

[17] S.L. Smith, *Physical Review* **36** D2901, (1987).

[18] J.P.A. Clark and D.M. Eardley, *Astrophysical Journal* **215**, 311 (1977).

[19] J.P.A. Clark, E.P.J. van den Heuvel, and W. Sutantyo, *Astonomy and Astrophysics* **72**, 120, (1974).

[20] J.R. Bond and B.J. Carr, *Monthly Notices of the Royal Astronomical Society* **207**, 585, (1984).

[21] M. Zimmerman and K.S. Thorne, in *Essays in General Relativity*, ed. F. J. Tipler, p. 139, Academic Press, New York, (1980).

[22] R.W.P. Drever, J.L. Hall, F.V. Kowalski, J. Hough, G.M. Ford, A.J. Munley, and H. Ward, *Applied Physics* **31**, B97-105, (1983).

[23] R.W.P. Drever, "Interferometric Detectors for Gravitational Radiation," *Gravitational Radiation*, NATO Advanced Physics Institute, Les Houches, eds. N. Deruelle and T. Piran, North Holland Publishing, (1983).

[24] R. Weiss, Internal report, unpublished, "Noise Sources in the LIGO," (1988,unpublished).

[25] S.E. Whitcomb, Caltech internal report, "Shot Noise in the Caltech Gravitational Wave Detector—the Mid-1984 Configuration," (1984,unpublished).

[26] G. Gutt, Caltech internal report, "Seismic Noise in the Caltech Detector," (1986,unpublished).

[27] C.M. Caves, in *Quantum Measurement and Chaos*, eds. E.R. Pike and S. Sarkar, p. 195, Plenum, New York, (1987).

[28] R. Spero, Caltech internal report, "Optimum Modulation Index," (1986,unpublished).

[29] C.M. Caves, *Physical Review* **23**, D1693, (1981).

[30] M. Xiao, L.-A. Wu, and H.J. Kimble, *Physical Review Letters* **59**, 278-281, (1987).

[31] A. Bostick, in preparation.

[32] A. Rudiger, R. Schilling, L. Schnupp, W. Winkler, H. Billing, and K. Maischberger, *Opt. Acta* **28**, 641, (1981).

[33] J. Clapp, Caltech internal report, "Geometrical Fluctuations in a Fabry-Perot Interferometer," (unpublished).

[34] D.Z. Anderson, J.C. Frisch, and C.S. Masser, *Applied Optics* **23**, 1238, (1984).

[35] D.Z. Anderson, *Applied Optics* **23**, 2944, (1984).

[36] L.A. Wainstein and V.D. Zubakov, *Extraction of Signals from Noise*, Dover, New York, (1970), p. 86ff.

[37] H.D. Helms, *IEEE Transactions on Audio and Electroacoustics* **15**, 85-90, (1967).

[38] R.L. Burden, J.D. Faires, A.C. Reynolds, *Numerical Analysis* Prindle, Weber and Schmidt, Boston, (1981).

[39] E. Amaldi, *et al.*, "First Gravity Wave Coincidence Experiment Between Three Cyrogenic Resonant-Mass Detectors: Louisiana-Rome-Stanford," in preparation.

[40] M.E. Zucker, private communication.

[41] M. Born, and E. Wolf, *Principles of Modern Optics*, Pergamon, New York, (1980).